

AN ABSTRACT OF THE THESIS OF

Clifford Neal Dahm

(Name)

for the

Master of Arts

(Degree)

in Oceanography

(Major)

presented on

April 29, 1974

(Date)

Title: A STUDY OF NUTRIENT DYNAMICS IN THE ATLANTIC

OCEAN

*Redacted for Privacy*

Abstract approved: \_\_\_\_\_

P. Kilho Park

During the GEOSECS cruise of the R/V KNORR, July 1972-April 1973, a very complete and high quality nutrient data set was acquired for the Atlantic Ocean. One hundred and twenty-one hydrographic stations were occupied throughout the Atlantic providing an internally consistent picture of the nutrient dynamics for this ocean.

The dynamic and biological controls on the nutrient distribution were viewed by means of horizontal distribution patterns, vertical profiling, and statistical modeling of relationships between oxygen, potential temperature, salinity, and nutrients. The general conclusions are summarized as follows:

1. The nutrient concentrations in the Atlantic exhibit the interplay at all depths of nutrient rich waters of South Atlantic origin with nutrient poor waters of the North Atlantic. This interrelationship of the two water sources manifests itself in numerous extrema (maxima and minima) in the water column.

2. For intermediate and deep waters, the strong predominance of lateral transport over processes of vertical dissipation are apparent in the Atlantic. Identifiable water types with only small variations of potential temperature ( $\theta$ ), salinity (S), and preformed nutrients can be characterized thousands of miles from their region of origin.

3. Silicate distribution in the Atlantic exhibits very marked gradients between waters of South and North Atlantic origin. Variations of up to  $100 \mu\text{m}/\text{kg}$  occur where salinity differences are less than  $0.3\text{‰}$ . Great potential exists for the use of silicate as a water mass tracer for Antarctic Intermediate Water (AAIW), North Atlantic Deep Water (NADW), and Antarctic Bottom Water (AABW).

4. The deep and bottom water nutrient distribution can be explained purely from hydrodynamic considerations. Nutrients, dissolved oxygen ( $\text{O}_2$ ), and apparent oxygen utilization (AOU) behave like conservative parameters. The rates of oxidation in deep water are slow relative to the physical processes of mixing and advection.

5. The total organic carbon (TOC) is relatively invariant below a few hundred meters. Significant variation at the cores of NADW, AAIW, and at the ocean bottom is indistinguishable at the present analytical capability. This supports the observation of very low rates of oxidation in the abyssal waters of the Atlantic.

6. The use of statistical models of  $O_2$  as a function of  $\theta$  or  $S$  and a nutrient are consistent with  $\theta$ - $S$  diagrams in distinguishing the influence of various water types. In addition, a subsurface water type is seen in temperate and equatorial regions which is due to biochemical activity. This water type corresponds to the portion of the water column where rapid oxidation of organic carbon ceases. It is characterized by a low preformed nutrient concentration but a relatively high oxidative nutrient portion.

7. Statistical modeling for a series of stations in the Drake Passage shows the extent of biological depletion across the Passage and points out the influence of an oxygen rich bottom water in the southern reaches of the Drake Passage. This is bottom water from the South Scotia Sea observed by other authors.

8. An apparent breakdown of Redfield's ratio for the  $\Delta O_2 : \Delta PO_4$  and the  $\Delta O_2 : \Delta NO_3$  in the bottom waters of the Atlantic is seen. My analysis indicates that the variation is due not to an inconsistency in the Redfield ratio but to the very low rates of oxidation at great depths. Nearly all the variation in the oxygen content of the deep water at an equatorial station and a station in the Drake Passage can be explained by the use of a conservative variable such as  $\theta$  or  $S$ . Significant oxidation larger than the analytical errors of the GEO-SECS methods cannot be seen for the stations considered at present.

A Study of Nutrient Dynamics in the Atlantic Ocean

by

Clifford Neal Dahm

A THESIS

submitted to


Oregon State University

in partial fulfillment of  
the requirements for the  
degree of

Master of Arts


June 1974

APPROVED:

  
*Redacted for Privacy*

---

Professor of Oceanography  
in Charge of Major

  
*Redacted for Privacy*

---

Dean of School of Oceanography

*Redacted for Privacy*

---

Dean of Graduate School

Date thesis is presented April 29, 1974

Typed by Suelynn Williams for Clifford Neal Dahm

## ACKNOWLEDGMENTS

One of my colleagues has suggested that this section of his thesis state that I acknowledge no one as I did the whole damn thing myself. Thankfully, I can make no claim to such a statement.

It has been a sometimes hectic but extremely rewarding and enjoyable experience working for my major professor, Dr. P. Kilho Park. I have learned a good deal of oceanography from him and just as important I grew richer as a human being. I look forward to further rewarding experiences in the future.

Secondly, I must thank Suelynn Williams who has wrought more last minute miracles than I care to remember. Without her help this thesis would not be a reality at this time. Also, my appreciation to Marilyn Guin whose last minute assistance on some of the graphics was most helpful.

This work was supported by the National Science Foundation grants GX-28167 and GA-12113.

## TABLE OF CONTENTS

|  | <u>Page</u> |
|--|-------------|
| I. INTRODUCTION  | 1           |
| II. OBSERVATIONS AND METHODS   | 9           |
| III. SELECTED HORIZONTAL DISTRIBUTIONS<br>OF GEOSECS DATA  | 11          |
| A. Surface   | 11          |
| B. $\sigma_{\theta} = 27.34$   | 18          |
| C. $\sigma_{\theta} = 27.82$   | 24          |
| D. Bottom  | 35          |
| IV. GRAPHICAL PRESENTATION OF NUTRIENT<br>AND HYDROGRAPHIC DATA IN THE WESTERN<br>BASINS OF THE ATLANTIC OCEAN | 44          |
| V. NUTRIENT-OXYGEN RELATIONSHIPS IN THE<br>ATLANTIC USING MULTIPLE LINEAR REGRESSION<br>ANALYSIS               | 61          |
| VI. CONCLUDING REMARKS   | 93          |
| BIBLIOGRAPHY   | 94          |

## LIST OF TABLES

| <u>Table</u> |   | <u>Page</u> |
|--------------|---|-------------|
| III-1        | Intersection depth and total organic carbon concentration for a best two line fit of $\theta$ -TOC data.  | 42          |
| IV-1         | Water type characterization in the Drake Passage for salinity, potential temperature, and silicate.   | 54          |
| V-1          | Characterization of water masses at station 49 by $\theta$ , S, $\text{PO}_4(\text{p})$ , and $\text{NO}_3(\text{p})$ .   | 74          |
| V-2          | Regression equations of $\text{O}_2$ on $\text{PO}_4$ and $\theta^\circ\text{C}$ and on $\text{NO}_3$ and $\theta^\circ\text{C}$ at station 49.   | 78          |
| V-3          | Characteristic S, $\theta$ , $\text{PO}_4(\text{p})$ , and $\text{NO}_3(\text{p})$ for the water types present in the Drake Passage.  | 82          |
| V-4          | Regression equations of $\text{O}_2$ on $\text{PO}_4$ and $\theta^\circ\text{C}$ , $\text{NO}_3$ and $\theta^\circ\text{C}$ , $\text{PO}_4$ and S, and $\text{NO}_3$ and S for station 78 in the Drake Passage. | 89          |



## LIST OF FIGURES

| <u>Figure</u> |  | <u>Page</u> |
|---------------|--|-------------|
| III-1         | Selected GEOSECS stations used to view horizontal nutrient and hydrographic distributions in the Atlantic Ocean. | 12          |
| III-2         | Potential temperature near the sea surface.  | 12          |
| III-3         | Salinity near the sea surface.   | 13          |
| III-4         | Dissolved oxygen near the sea surface.   | 13          |
| III-5         | Phosphate near the sea surface.  | 15          |
| III-6         | Nitrate near the sea surface.  | 15          |
| III-7         | Silicate near the sea surface.   | 16          |
| III-8         | AOU near the sea surface.  | 16          |
| III-9         | Preformed nitrate near the sea surface.  | 17          |
| III-10        | Preformed phosphate near the sea surface.  | 17          |
| III-11        | TOC in the surface waters of the Atlantic.   | 19          |
| III-12        | Depths corresponding to the 27.34 potential density surface ( $\sigma_{\theta}$ ) at the selected stations.      | 19          |
| III-13        | Potential temperature at $\sigma_{\theta} = 27.34$ .   | 20          |
| III-14        | Salinity at $\sigma_{\theta} = 27.34$ .  | 20          |
| III-15        | Dissolved oxygen at $\sigma_{\theta} = 27.34$ .  | 22          |
| III-16        | Phosphate at $\sigma_{\theta} = 27.34$ .   | 22          |
| III-17        | Nitrate at $\sigma_{\theta} = 27.34$ .   | 23          |
| III-18        | Silicate at $\sigma_{\theta} = 27.34$ .  | 23          |

LIST OF FIGURES CONTINUED

| <u>Figure</u> |   | <u>Page</u> |
|---------------|---|-------------|
| III-19        | AOU at $\sigma_{\theta} = 27.34$ .  | 25          |
| III-20        | TOC at $\sigma_{\theta} = 27.34$ .  | 25          |
| III-21        | Preformed phosphate at $\sigma_{\theta} = 27.34$ .  | 26          |
| III-22        | Preformed nitrate at $\sigma_{\theta} = 27.34$ .  | 26          |
| III-23        | Depths corresponding to the 27.82 potential density surface for the selected Atlantic stations. | 27          |
| III-24        | Potential temperature for the 27.82 potential density surface.                                  | 27          |
| III-25        | Salinity for the 27.82 potential density surface.   | 29          |
| III-26        | Dissolved oxygen for the 27.82 potential density surface.                                       | 29          |
| III-27        | Phosphate for the 27.82 potential density surface.  | 30          |
| III-28        | Nitrate for the 27.82 potential density surface.  | 30          |
| III-29        | Silicate for the 27.82 potential density surface.   | 31          |
| III-30        | AOU for the 27.82 potential density surface.  | 31          |
| III-31        | Preformed phosphate for the 27.82 potential density surface.                                    | 32          |
| III-32        | Preformed nitrate for the 27.82 potential density surface.                                      | 32          |
| III-33        | TOC for the 27.82 potential density surface.  | 34          |
| III-34        | Depth at the ocean bottom for the selected GEOSECS stations.                                    | 34          |
| III-35        | Potential temperature near the ocean bottom for the selected GEOSECS stations.                  | 36          |

## LIST OF FIGURES CONTINUED

| <u>Figure</u> |   | <u>Page</u> |
|---------------|---|-------------|
| III-36        | Salinity near the ocean bottom for the selected GEOSECS stations.         | 36          |
| III-37        | Dissolved oxygen near the ocean bottom in the Atlantic.                   | 37          |
| III-38        | Phosphate near the ocean bottom in the Atlantic.                          | 37          |
| III-39        | Nitrate near the ocean bottom in the Atlantic.                            | 38          |
| III-40        | Silicate near the ocean bottom in the Atlantic.                           | 38          |
| III-41        | AOU near the ocean bottom in the Atlantic.                                | 40          |
| III-42        | Preformed phosphate near the ocean bottom in the Atlantic.                | 40          |
| III-43        | Preformed nitrate near the ocean bottom in the Atlantic.                  | 41          |
| III-44        | TOC near the ocean bottom in the Atlantic.                                | 41          |
| IV-1          | The cruise track for GEOSECS in the western basins of the Atlantic Ocean. | 44          |
| IV-2          | The potential temperature profile for the western Atlantic.               | 45          |
| IV-3          | Salinity distribution in the western Atlantic.                            | 45          |
| IV-4          | $\sigma_4$ distribution in the western Atlantic.                          | 47          |
| IV-5          | Dissolved oxygen distribution in the western Atlantic.                    | 47          |
| IV-6          | Phosphate in the western Atlantic.  | 49          |
| IV-7          | Nitrate in the western Atlantic.  | 49          |

LIST OF FIGURES CONTINUED

| <u>Figure</u> |  | <u>Page</u> |
|---------------|--|-------------|
| IV-8          | Silicate in the western Atlantic.  | 51          |
| IV-9          | Silicate versus depth profiles for stations 76-78 in the Drake Passage with the cores of the various water masses lettered.                                  | 53          |
| IV-10         | Depth to $\sigma_{\theta}$ relationship in the western Atlantic.   | 56          |
| IV-11         | Oxygen to $\sigma_{\theta}$ relationship in the western Atlantic.  | 56          |
| IV-12         | AOU to $\sigma_{\theta}$ relationship in the western Atlantic.   | 57          |
| IV-13         | Silicate to $\sigma_{\theta}$ relationship in the western Atlantic.  | 57          |
| IV-14         | Phosphate to $\sigma_{\theta}$ relationship in the western Atlantic.   | 58          |
| IV-15         | Preformed phosphate to $\sigma_{\theta}$ relationship in the western Atlantic.   | 58          |
| IV-16         | Nitrate to $\sigma_{\theta}$ relationship in the western Atlantic.   | 59          |
| IV-17         | Preformed nitrate to $\sigma_{\theta}$ relationship in the western Atlantic.   | 59          |
| V-1           | GEOSECS station 49 location in the South Atlantic.   | 63          |
| V-2           | GEOSECS station locations across the Drake Passage.  | 64          |
| V-3           | $(O_{2(100\%)} - a_1 \cdot PO_{4(p)})$ versus $\theta^{\circ}C$ diagram (a) and $O_{2\ res}$ versus $\theta^{\circ}C$ diagram (b) of a hypothetical station. | 67          |
| V-4           | Oxygen residuals versus potential temperature at station 49. $PO_4$ is the nutrient parameter.   | 70          |
| V-5           | Oxygen residuals versus potential temperature at station 49. $NO_3$ is the nutrient parameter.   | 70          |

## LIST OF FIGURES CONTINUED

| <u>Figure</u> |  | <u>Page</u> |
|---------------|--|-------------|
| V-6           | $\theta$ -S diagram for station 49.  | 72          |
| V-7           | Expanded $\theta$ -S diagram for $\theta = 0-5^{\circ}\text{C}$ and $S = 34.5-35.0\text{‰}$ region of station 49.  | 72          |
| V-8           | $\theta$ - $\text{PO}_{4(\text{p})}$ diagram at station 49.  | 73          |
| V-9           | $\theta$ - $\text{NO}_{3(\text{p})}$ diagram at station 49.  | 73          |
| V-10          | TOC as a function of $\theta$ with the best fit two phase regression and intersection point.   | 76          |
| V-11          | Preformed nutrients versus depth at station 49.  | 80          |
| V-12          | Oxygen residuals versus salinity from the regression model using S and $\text{PO}_{4}$ or $\text{NO}_{3}$ as independent variables for stations 76-78 in the Drake Passage.          | 83          |
| V-13          | $\theta$ -S diagrams for stations 76-78 in the Drake Passage.  | 84          |
| V-14          | Best fit lines of the $\text{O}_{2 \text{ res}}$ versus S data for stations 76-78 in Drake Passage after a combined regression model using $\text{PO}_{4}$ as the nutrient variable. | 86          |

# A STUDY OF NUTRIENT DYNAMICS IN THE ATLANTIC OCEAN

## I. INTRODUCTION

The GEOSECS (Geochemical Ocean Sections Study) in the Atlantic Ocean has amassed an enormous amount of excellent quality hydrographic and chemical data. Utilizing a cooperative effort between oceanographic institutions throughout the United States and the world, an intensive survey of the chemistry of the Atlantic has been carried out from July 1972 to April 1973. As a part of this effort, Oregon State University provided the expertise for the nutrient (phosphate, nitrate and nitrite, and silicate) and organic carbon analyses. As a result, a thorough and high quality nutrient data library has been acquired for this ocean.

With the use of this data, the dynamics of many of the physical and biological processes active in the Atlantic Ocean can be viewed more accurately. Drawing from some of the classic papers on the nutrient dynamics of the Atlantic Ocean, with the benefit of high quality data such as provided by GEOSECS, a further understanding of this ocean can be gained.

The study of the nutrient chemistry and the controlling dynamics for nutrient distribution in the Atlantic has had many contributors. Redfield (1942) utilized phosphate and oxygen to explore the movement of water masses throughout the Atlantic. Montgomery

(1938) established that isentropic mixing approximates a minimum energy requirement for water flow in the oceans. Redfield (1942) and Richards and Redfield (1955) combined the use of isentropic surfaces with nutrient chemistry to examine advection and mixing in various parts of the Atlantic. Riley (1951) included similar presentations of the characteristic distribution of nutrients, in addition to numerous additional mathematical studies on dissolved oxygen ( $O_2$ ) and nutrients, in his very complete picture of the Atlantic Ocean.

Redfield (1934 and 1942) also noted in two classic papers that the ratio of nitrogen to phosphorus in the ocean is very similar to that found in healthy phytoplankton populations. In addition, the inorganic nutrient phosphate ( $PO_4$ ) appears to consist of two portions -- one a biochemically derived segment termed oxidative phosphate ( $PO_{4(ox)}$ ) and a residual or preformed inorganic phosphate ( $PO_{4(p)}$ ) entirely independent in origin of decomposition and oxidation occurring after the water left the sea surface. The chemistry of nitrogen compounds is somewhat more complex (Harvey, 1955), but similar arguments divide the nitrate ( $NO_3$ ) in deep and intermediate water into a preformed and oxidative portion ( $NO_{3(ox)}$  and  $NO_{3(p)}$ ) (Park, 1967). Preformed nutrients have been demonstrated to be conservative (Pytkowicz and Kester, 1966), but have remained a relatively unused resource for examining the dynamics of the ocean, owing largely to insufficient precision and accuracy in the necessary

analytical techniques.

In recent years, the potential value of preformed nutrients and the associated concept of apparent oxygen utilization (AOU) from biochemical oxidation has emerged for use in studying oceanic circulation due to better quality nutrient data becoming available. Park (1967) observed the  $\text{NO}_{3(p)}:\text{PO}_{4(p)}$  ratio in waters off Oregon and suggested that water masses may be traceable to their source through this relationship. Redfield, Ketchum and Richards (1963) reviewed the state of knowledge on biological influences on seawater chemistry and discussed the variation in preformed phosphate levels for deep water masses in the Atlantic. In addition, incorporating the data of Redfield (1942), Fleming (1941) and other workers, the authors present a  $\Delta\text{O}:\Delta\text{C}:\Delta\text{N}:\Delta\text{P}$  ratio of -276:106:16:1 which is the generally accepted ratio, termed the Redfield ratio, used in the calculation of preformed nutrients and AOU. Pytkowicz (1968), Pytkowicz and Kester (1966), Alvarez-Borrego and Park (1973), Sugiura (1965), and Alvarez-Borrego and Park (1971) applied Redfield's ratio for use in studying the physical dynamics of water mass movement and interaction using AOU and  $\text{PO}_{4(p)}$  in the Pacific Ocean. In the Atlantic, the concepts of preformed nutrients and AOU have been less extensively applied. The GEOSECS data with its overall coverage and accuracy is excellent for this type of analysis.

The use of dissolved oxygen ( $\text{O}_2$ ) to study physical and



biological processes for the Atlantic Ocean is well documented. Riley (1951) presented  $O_2$  distributions throughout the Atlantic and used  $O_2$  versus sigma-t ( $\sigma_t$ ) plots to discuss the spreading on isentropic surfaces of the various Atlantic water masses from their sources of origin. Seiwel (1937), Skopintsev (1965) and Bubnov (1966) viewed the  $O_2$  minimum in the Atlantic. From their work, it is seen that the region of lowest  $O_2$  concentration in the Atlantic occurs in the eastern tropical Atlantic along the coast of Africa. From there these low  $O_2$  levels mix north, south, and west. The region of lowest  $O_2$  concentration corresponds to an area of high productivity (Hart and Currie, 1960). Richards and Redfield (1955) used  $O_2$ - $\sigma_t$  correlations in the North Atlantic to identify waters originating from such regions as the Caribbean Sea. Oceanographic studies of the Atlantic by Taft (1963), Arons and Stommel (1967), and Duedall and Coote (1972) considered circulation patterns in various parts of the Atlantic Ocean as seen by the  $O_2$  distribution. Richards (1957) presented a good descriptive paper on  $O_2$  that summarizes much of the  $O_2$  distribution for the Atlantic.

The silicate chemistry of the oceans of the world has generally been neglected until recently due to a sparsity of accurate and precise data. Richards (1958) suggested a  $\Delta N:\Delta Si$  ratio of about 1:1 in the equatorial Atlantic and pointed out the existence of silicate maxima and minima layers. Metcalf (1969) called for a deeper look into

the silicate chemistry in the oceans as its value as a tracer of water masses appears high, especially in the Atlantic Ocean. The depletion of silicate in the North Atlantic water masses and the enrichment in waters of Antarctic origin is clearly evident. Spencer (1972) amplified the potential value of silicate as a tracer in the North Atlantic by showing the quasiconservative nature of silicate during the mixing of North Atlantic Deep Water and Antarctic Bottom Water. Little in situ solution or dissolution from the bottom is seen at a GEOSECS test station when examining salinity-silicate diagrams. Viewing the entire Atlantic Ocean silicate profile shows great potential for analyzing abyssal circulation in the Atlantic.

An additional nutrient parameter measured by GEOSECS in the Atlantic is total organic carbon (TOC). Much research has been centered recently around the organic carbon levels in the oceans. Riley (1970) indicated that 98% of the organic matter in the oceans is in the dissolved form so that TOC measurements in the Atlantic correspond closely to many reported dissolved organic carbon (DOC) measurements by other workers. Duursma (1961 and 1965), Menzel (1964), and Skopintsev (1960) suggested that DOC may be valuable in distinguishing the origins of water types and for mixing studies. Later work in the Atlantic by Menzel and Ryther (1968) and Menzel (1970) showed that at the level of accuracy of the analysis, DOC is invariant, approximately 35-40  $\mu\text{M}/\text{kg}$ , below the upper 200-400

meters. Craig (1971) challenged this concept of complete biochemical oxidation in the upper few hundred meters on the basis of in situ  $O_2$  consumption in deep waters, but by far the largest bulk of the biochemical cycle from production to decomposition and solubilization occurs in the upper few hundred meters. As will be shown, GEOSECS organic carbon measurement substantiates this hypothesis.

Alvarez-Borrego (1973) presented a statistical model based on the Redfield ratio which provides a means of identifying water-type influences. Alvarez-Borrego et al. (1972), Alvarez-Borrego (1973), and Dahm et al. (1973) have shown applications of multiple linear regression models of  $O_2$  against a conservative variable such as temperature or salinity and a nutrient variable of  $PO_4$  or  $NO_3$  to trace water masses and to test Redfield's ratio. Plotting the variations of the observed field data from those predicted from the model develops a clear pattern of the water types present. The use of a technique which views relatively small variations between water types is well suited to the GEOSECS data as the errors in analytical measurement have been greatly reduced.

Realizing the valuable work already done in the Atlantic with past nutrient data, a reanalysis utilizing the complete and accurate GEOSECS nutrient data with these proven techniques presents a coherent picture of nutrient dynamics in the Atlantic. Three methods

are considered in this thesis to portray the GEOSECS nutrient data.

1. Approximately thirty stations were chosen throughout the Atlantic to provide a uniform view of the entire ocean. Four levels were examined for depth (Z), salinity (S), potential temperature ( $\theta$ ),  $O_2$ ,  $NO_3$ ,  $PO_4$ , silicate, AOU,  $NO_3(p)$ ,  $PO_4(p)$ , and TOC. The levels selected include the surface, the bottom,  $\sigma_\theta$  of 27.34 and  $\sigma_\theta$  of 27.82, where  $\sigma_\theta$  is the water density related to one atmosphere pressure and potential temperature. Antarctic Intermediate Water corresponds to  $\sigma_\theta$  of 27.34 while the Upper North Atlantic Deep Water with possible Mediterranean influence approximates the  $\sigma_\theta$  surface of 27.82. From these diagrams, nutrient levels and physical processes of mixing and advection can be viewed along an isentropic surface or at the surface or bottom of the Atlantic Ocean.

2. The western basins of the Atlantic Ocean were thoroughly covered by a north-south transect from 75°N to 60°S. The precise GEOSECS nutrient and  $O_2$  data provides an excellent visual view of the interacting processes determining the concentration of  $O_2$  and nutrients in the western basins of the Atlantic when plotted against latitude. Additional plots of  $\theta$ , S, and  $\sigma_4$  (potential density relative to a depth of 4 kilometers rather than the surface) are also shown as an additional aid in viewing Atlantic circulation patterns. Diagrams are constructed of  $\sigma_\theta$  versus such parameters as Z,  $O_2$ , AOU, silicate,  $PO_4$ ,  $NO_3$ ,  $PO_4(p)$ , and  $NO_3(p)$  in the fashion of Redfield

(1942). This provides a close look at the isentropic movements of the water masses in the Atlantic. In these diagrams, silicate is especially graphic in portraying the movement and interaction of the water masses of the Atlantic.

3. Multiple linear regression modeling is applied to an equatorial GEOSECS station and three GEOSECS stations in the Drake Passage to express the dependent variable  $O_2$  as a function of either  $\theta$  or  $S$  and either  $PO_4$  or  $NO_3$ . Plotting the residuals from the model versus  $\theta$  or  $S$  identifies the water types present at the station. The model also provides a means to check the Redfield ratio for  $\Delta O_2:\Delta PO_4$  and  $\Delta O_2:\Delta NO_3$  in the various regions of the water column influenced by the different water types present. The equatorial station is used to demonstrate the technique where a number of different water types display an influence. Then a more intensive study is made for the stations in the Drake Passage to help view circulation patterns and the biochemical activity apparent in this region below the southern tip of South America and the Antarctic continent.

## II. OBSERVATIONS AND METHODS

From July 18, 1972 to April 1, 1973, as part of GEOSECS, the R/V KNORR of the Woods Hole Oceanographic Institution carried out a detailed survey of the Atlantic Ocean for more than 40 physical and chemical parameters. The goal of the GEOSECS program is to obtain coordinated chemical and radiochemical data in each major ocean at a level of sophistication higher than any previous work.

The nutrient data for the Atlantic GEOSECS program was collected with a modified AutoAnalyzer-II system. Description of the methods, chemistries, and intercalibration tests were presented by Atlas et al. (1971), Hager et al. (1972), and Callaway et al. (1971). Analyses are run immediately after sampling. Precision of better than  $\pm 1\%$  was attained for the Atlantic data.

Oxygen is measured by the Carpenter modification of the Winkler titration (Carpenter, 1965). Precision has been shown to be better than  $\pm .5$  percent. All nutrient and oxygen data are expressed in  $\mu\text{M}/\text{kg}$ .

The total organic carbon analysis is a slightly modified version of the wet oxidation technique of Menzel and Vaccaro (1964). Accuracy is estimated at  $\pm 10 \mu\text{M}/\text{kg}$  with a precision at the 95 percent confidence interval of  $\pm 4 \mu\text{M}/\text{kg}$ .

Preformed nutrients and AOU were calculated from the -

Redfield ratio (Redfield, Ketchum, and Richards, 1963). The saturation value for dissolved oxygen ( $O_2'$ ) was found using the polynomial of Gilbert, Pawley, and Park (1968). All calculated values are also expressed in units of  $\mu\text{M}/\text{kg}$ .

### III. SELECTED HORIZONTAL DISTRIBUTIONS OF GEOSECS DATA

An initial perspective of the distribution of nutrients and the controlling hydrodynamics can be obtained from isolating certain depths or potential densities and plotting various parameters. Approximately thirty of the deeper and more heavily sampled GEOSECS stations were chosen so as to give an overall view of the Atlantic Ocean. The station numbers are given in Figure III-1. The two depths and two potential density surfaces studied are the surface, the bottom and the  $\sigma_{\theta}$  layers of 27.34 and 27.82. The  $\sigma_{\theta}$  surface of 27.34 was chosen as it corresponds in the South Atlantic to Antarctic Intermediate Water while the  $\sigma_{\theta}$  surface of 27.82 follows North Atlantic Deep Water and the influence of Mediterranean water.

#### A. Surface

Surface conditions for the temperate and polar regions were determined during the northern and southern summers. Surface temperatures extend from below 1°C in the south and below 2.5°C in the north to a value over 29°C near the equator in the eastern Atlantic (Fig. III-2). Surface salinity shows a maximum around 30°N in the North Atlantic and near 15°S in the South Atlantic (Fig. III-3). The distribution mirrors that shown by Von Arx (1962). The dissolved oxygen content exhibits that surface temperature controls



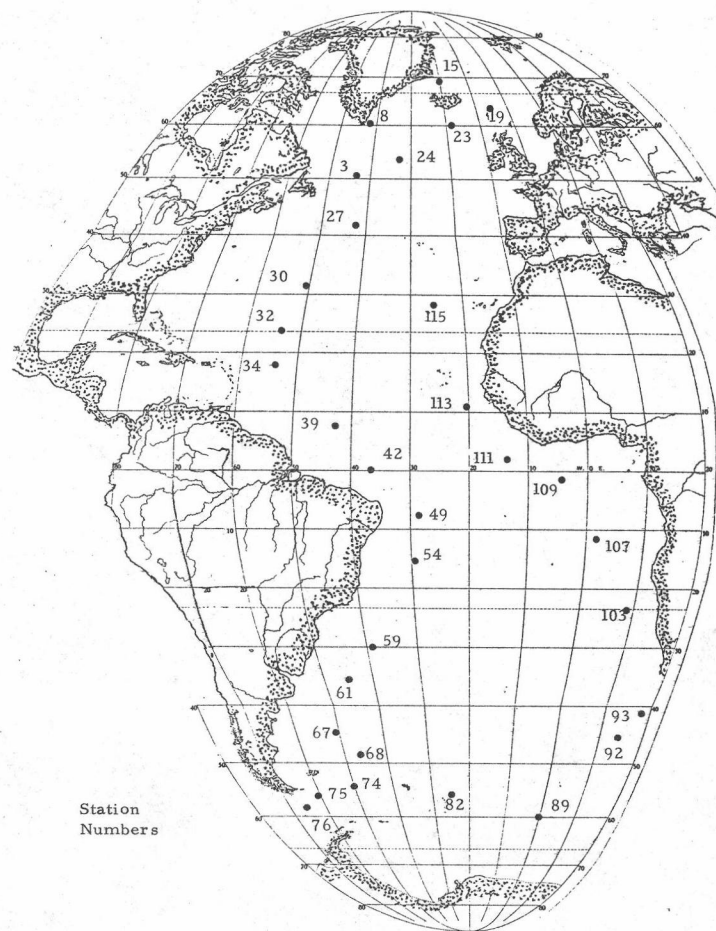


Figure III-1. Selected GEOSECS stations used to view horizontal nutrient and hydrographic distributions in the Atlantic Ocean.

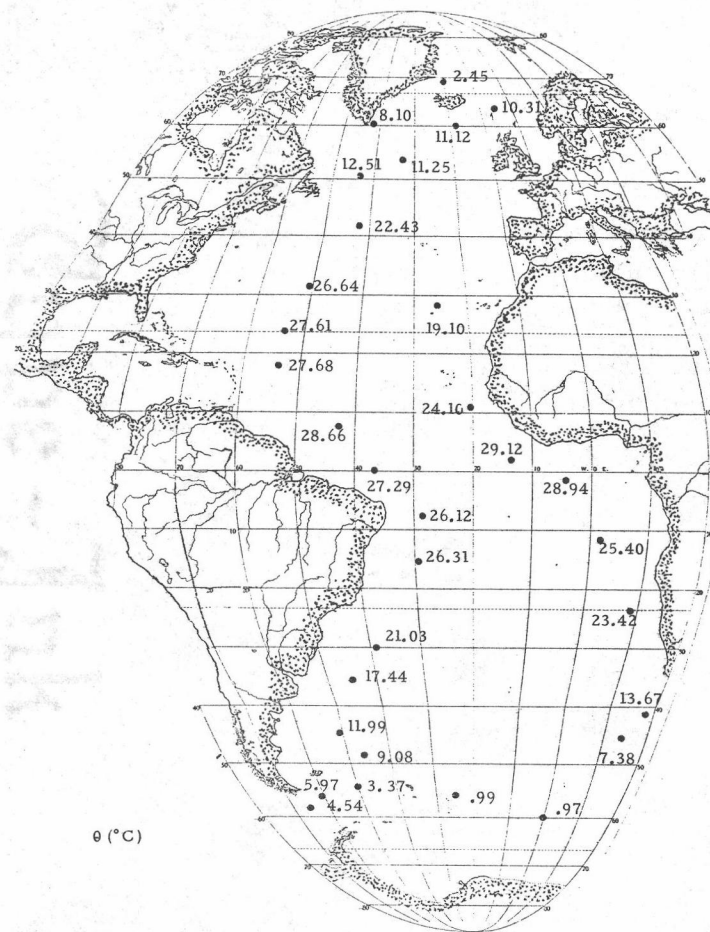


Figure III-2. Potential temperature near the sea surface.

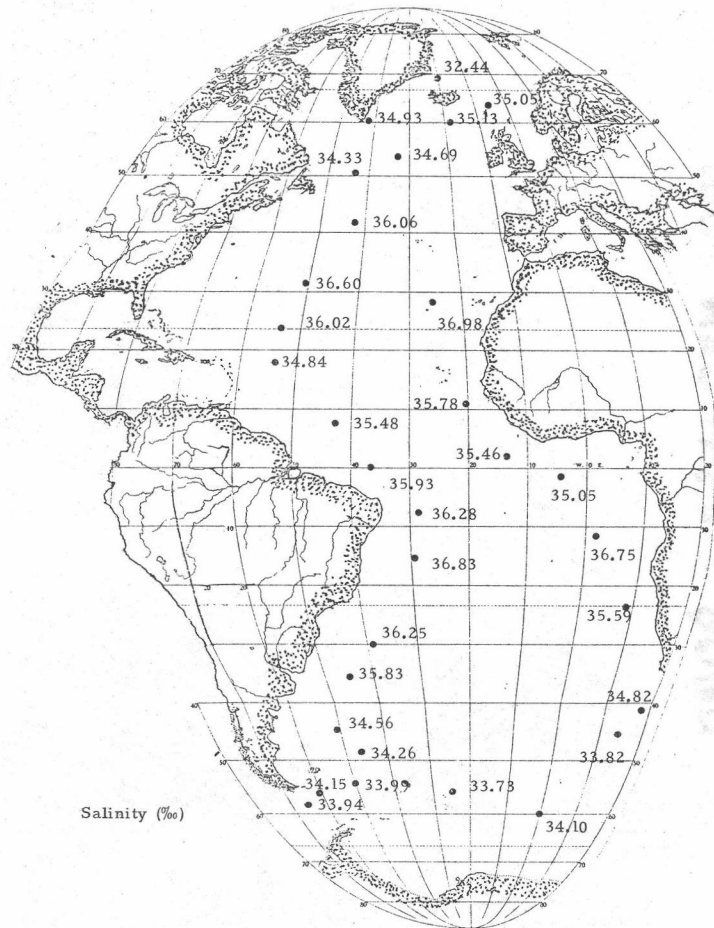


Figure III-3. Salinity near the sea surface.

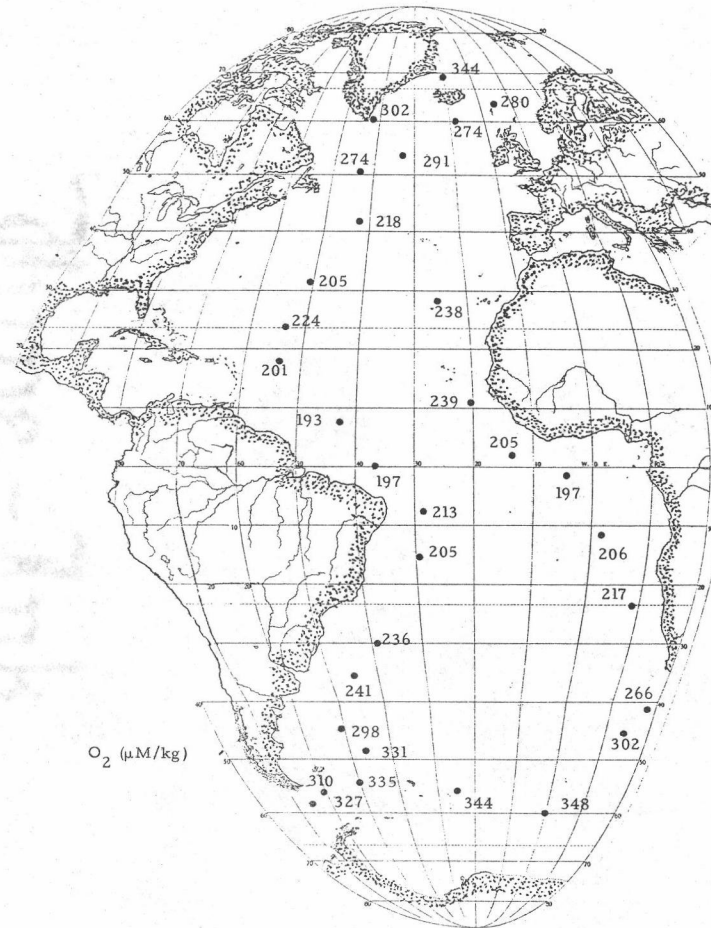


Figure III-4. Dissolved oxygen near the sea surface.

it mainly and salinity to a lesser extent (Fig. III-4), for increased temperature results in lower dissolved oxygen levels.

The nutrient distributions point out the relatively depleted condition in the far North Atlantic compared to the Southern Ocean (Fig. III-5 to III-7). Summer levels of  $\text{PO}_4$  and  $\text{NO}_3$  in the surface water of the Southern Ocean are over three times as high as in the most nutrient rich regions of the North Atlantic. Silicate is even more marked with differences of a factor of ten or more apparent.

The limiting nutrient in most of the temperate and equatorial region appears to be  $\text{NO}_3$ . Undetectable levels of  $\text{NO}_3$  are seen along much of the eastern Central Atlantic. Silicate and phosphate have also been highly reduced by biological productivity throughout the majority of the Atlantic. In the region of the Drake Passage, the very low levels of silicate relative to high  $\text{PO}_4$  and  $\text{NO}_3$  values may cause it to become limiting. This is due to the large silicate demand of the predominate diatom populations in this region.

The AOU,  $\text{PO}_{4(p)}$ , and  $\text{NO}_{3(p)}$  (Figs. III-8 to III-10) also reflect the surface depletion of nutrients and the resulting generally negative AOU. Kester and Pytkowicz (1968) and Pytkowicz (1971) discuss the concept of AOU and point out that photosynthesis and rapid surface water warming can generate negative AOU values. As the GEOSECS data at the far northern and southern latitudes was taken during summer months for each hemisphere, much of the negative character may

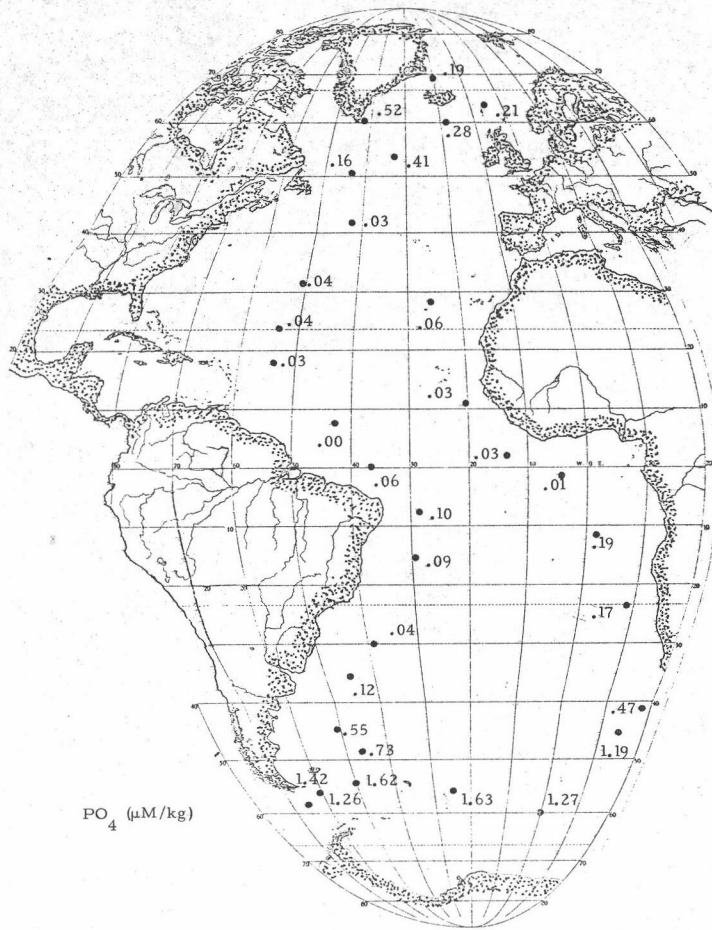


Figure III-5. Phosphate near the sea surface.

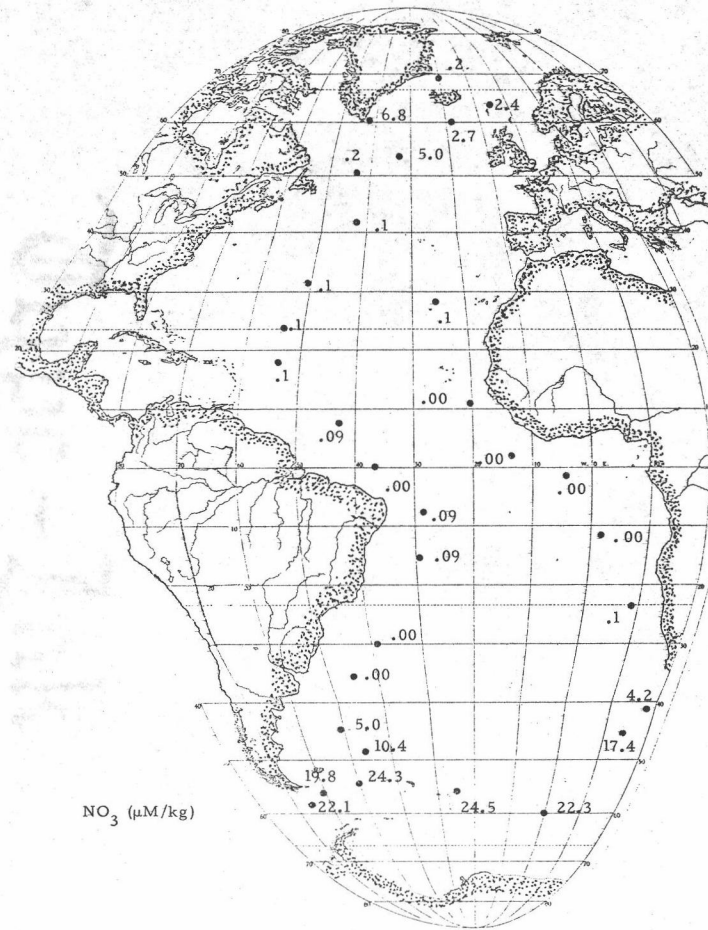


Figure III-6. Nitrate near the sea surface.

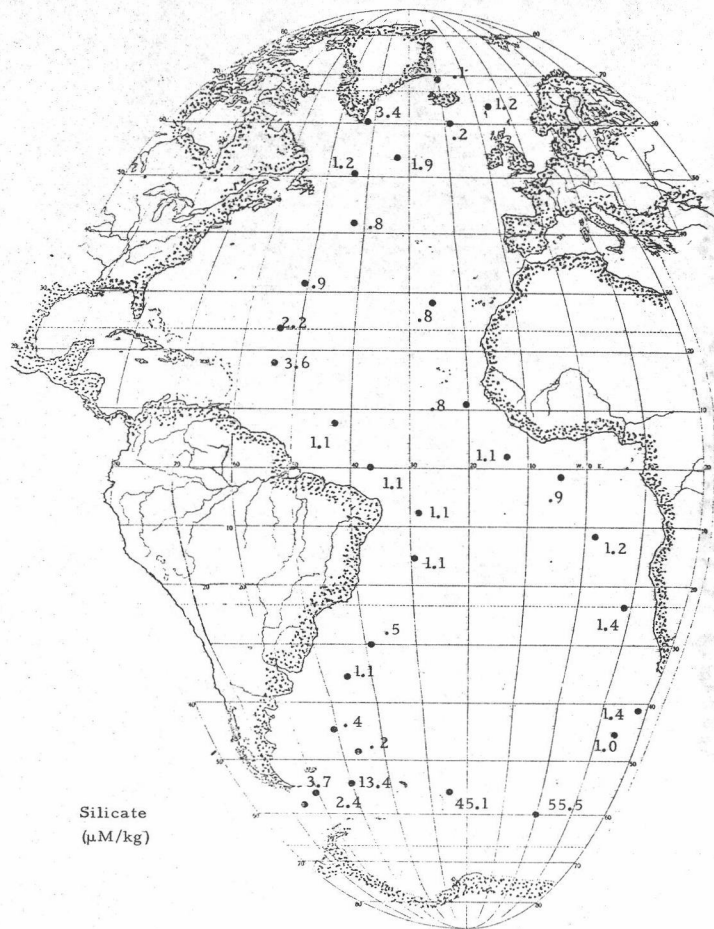


Figure III-7. Silicate near the sea surface.

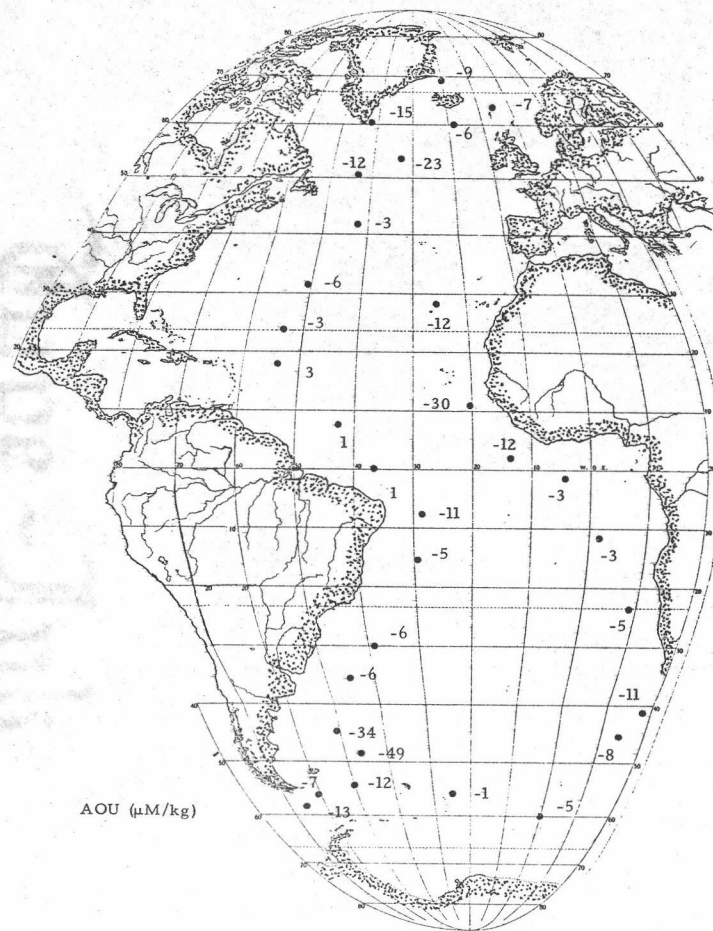


Figure III-8. AOU near the sea surface.

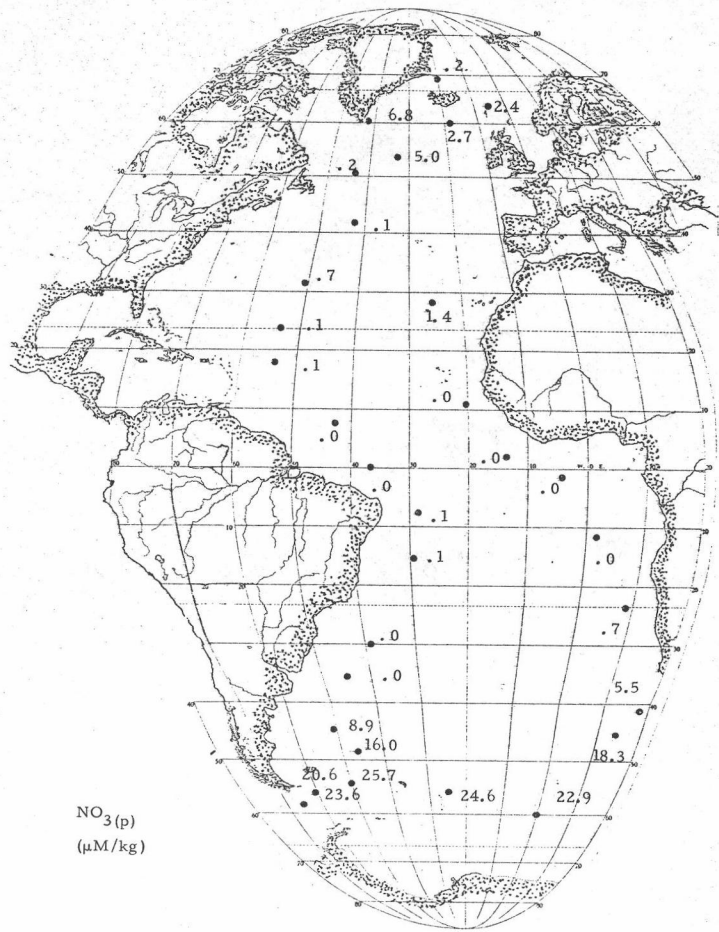


Figure III-9. Preformed nitrate near the sea surface.

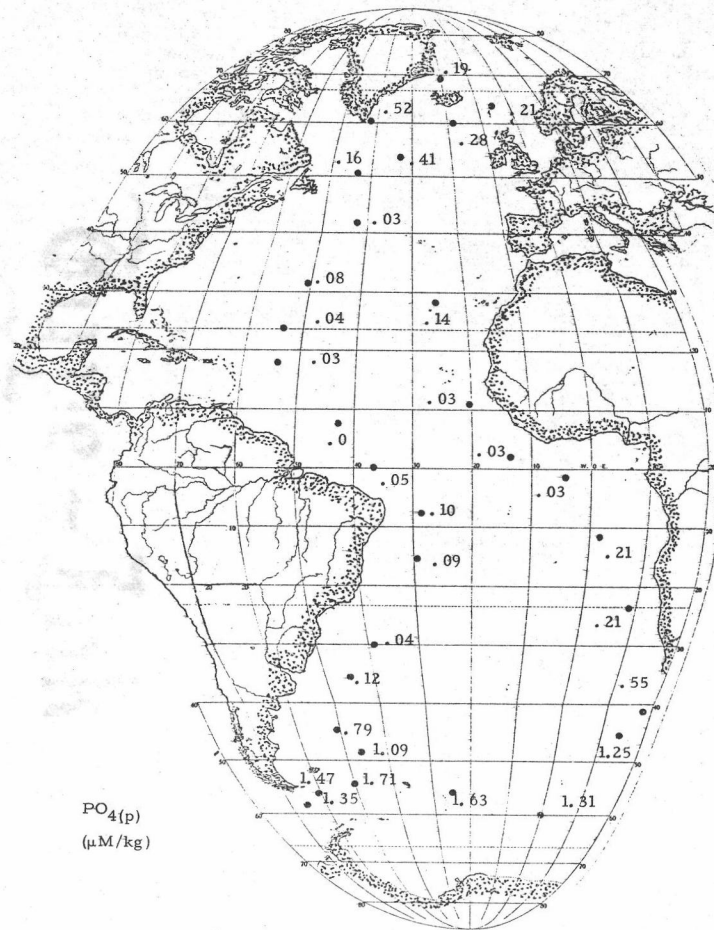


Figure III-10. Preformed phosphate near the sea surface.

be due to surface warming coupled with the biological primary productivity. The high negative AOU near the coast of Africa is more likely to correlate to high biological productivity. The preformed nutrient levels in the northern latitudes are somewhat lower than those of North Atlantic Deep Water, 0.80 to 12.0 for  $\text{PO}_4(\text{p})$  and  $\text{NO}_3(\text{p})$ , respectively, as some biological depletion has occurred. The high preformed nutrient levels in the southern latitudes are reflective of the extremely nutrient rich waters of this ocean.

The plot of TOC in the Atlantic at the surface (Fig. III-11) shows the highest levels in the eastern equatorial Atlantic. Stations below  $40^\circ\text{S}$  latitude are lower in surface organic carbon than areas nearer the equator.

B.  $\sigma_\theta = 27.34$

The depths corresponding to a  $\sigma_\theta$  of 27.34 vary from close to the surface in the higher latitudes to over 1200 meters near  $35^\circ\text{S}$  (Fig. III-12). The decrease in depth is steepest in the high latitudes where the intermediate water is formed. In the South Atlantic, a  $\sigma_\theta$  of 27.34 is at the core of AAIW.

The temperature and salinity regimes are indicative of the two sources for water of this density in the northern and southern latitudes of the Atlantic Ocean (Figs. III-13 and III-14). Generally high temperature and high salinity water are seen throughout the North

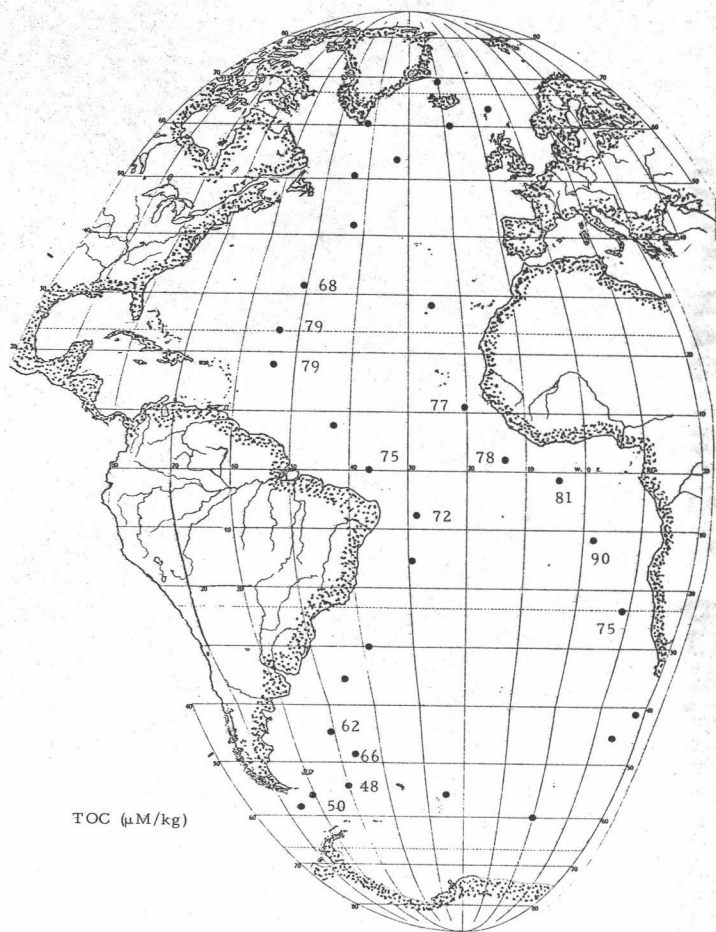


Figure III-11. TOC in the surface waters of the Atlantic.

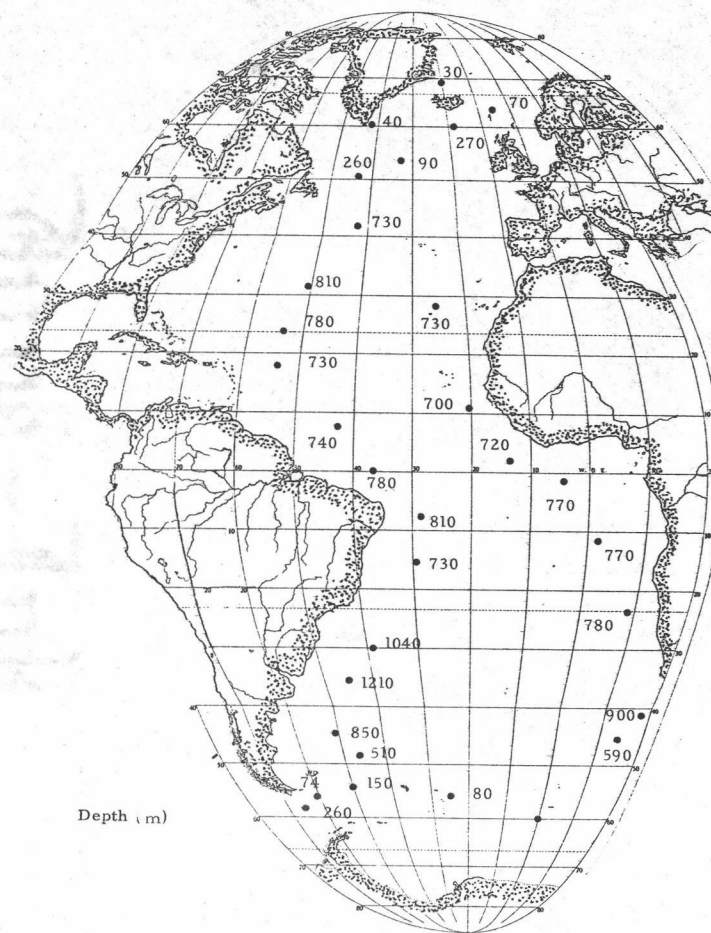


Figure III-12. Depths corresponding to the 27.34 potential density surface ( $\sigma_{\theta}$ ) at the selected stations.



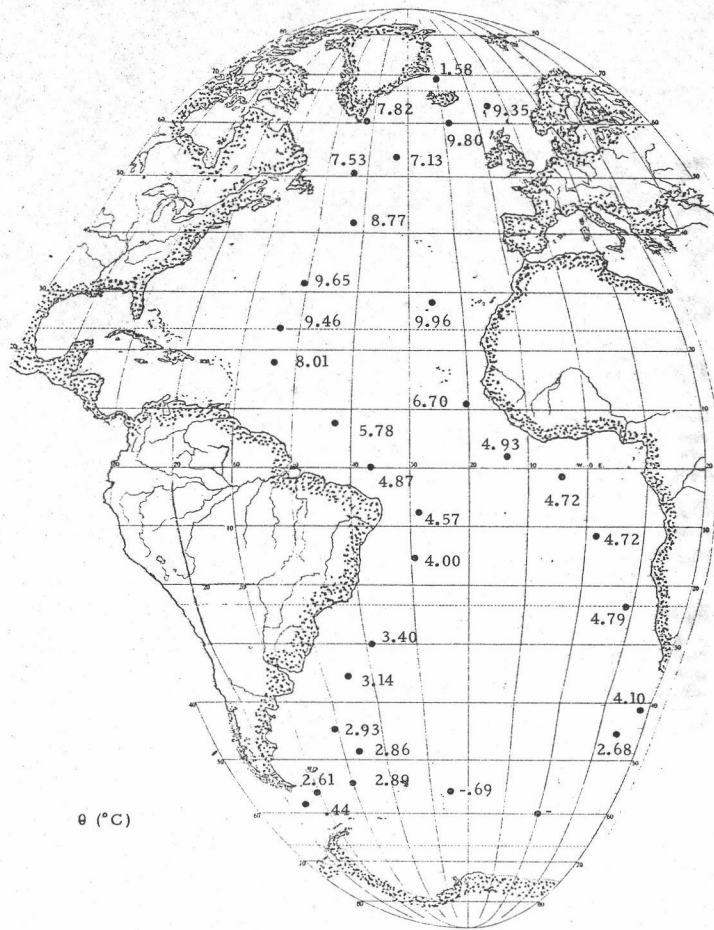


Figure III-13. Potential temperature at  $\sigma_\theta = 27.34$ .

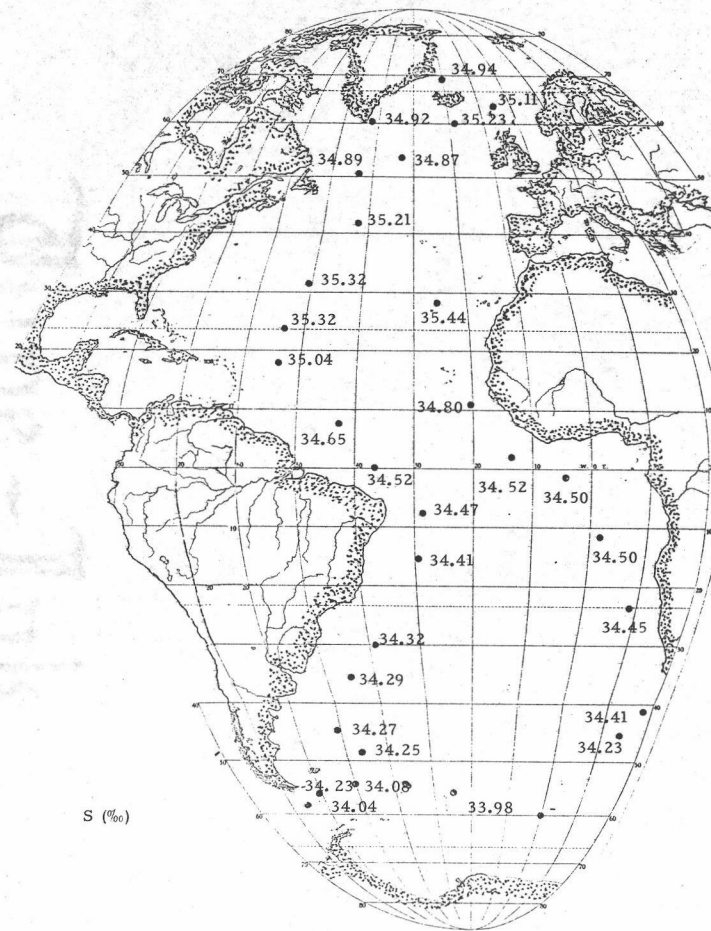


Figure III-14. Salinity at  $\sigma_\theta = 27.34$ .

Atlantic above 20°N while the South Atlantic presents low temperature and low salinity water. Gradual mixing is seen in the central Atlantic with the strongest mixing appearing between 10-20°N in the western basin.

The oxygen distribution is somewhat more complicated at this density surface (Fig. III-15). The localized effects of various intermediate waters and variable oceanic productivity and decomposition cause regional anomalies. But in general, the highly oxygenated water from the polar latitudes is attenuated by mixing and diffusion so that minimum values appear near the equator. The region of lowest oxygen is near the coast of central Africa near a recognized area of high productivity (Hart and Currie, 1960).

The nutrient profiles again demonstrate the poorness in nutrient abundance in the North Atlantic in comparison to the South Atlantic (Figs. III-16 to III-18). The  $\text{PO}_4$  and  $\text{NO}_3$  concentrations in the South Atlantic are double those of the North Atlantic while silicate levels vary by a factor of five. A region of considerable mixing at this density surface is again apparent in the western basin between 10-20° N. The  $\text{PO}_4$  and  $\text{NO}_3$  levels in the vicinity of the equator in the eastern Atlantic possess a slight maximum for the entire Atlantic at this isentropic surface. This may be related to the high productivity and decomposition in upwelling regions along coastal Africa which are then mixed by physical processes to deeper  $\sigma_\theta$  surfaces.

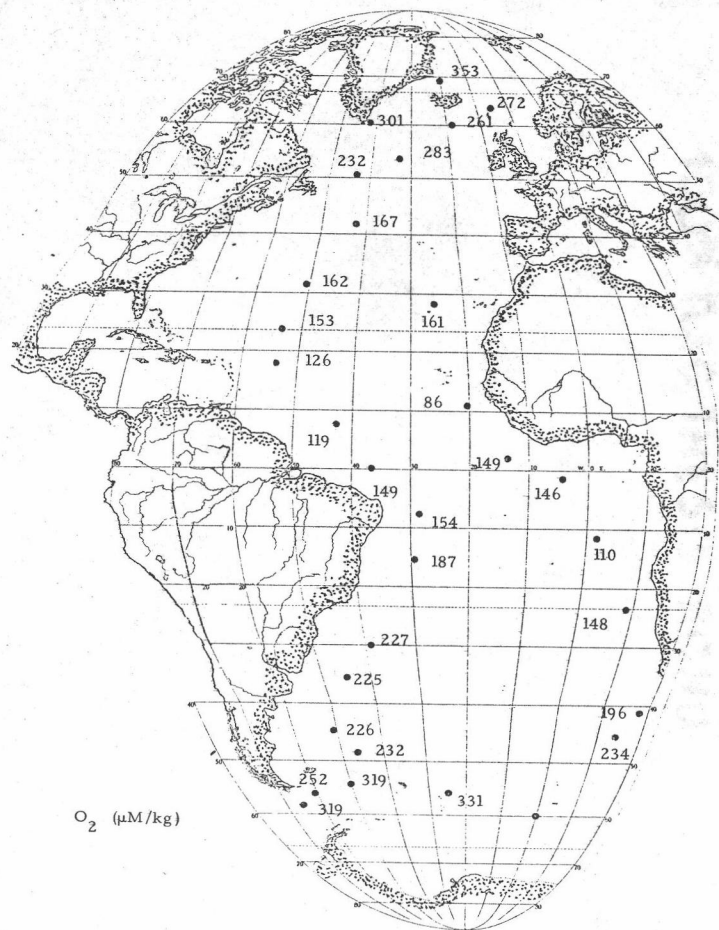


Figure III-15. Dissolved oxygen at  $\sigma_\theta = 27.34$ .

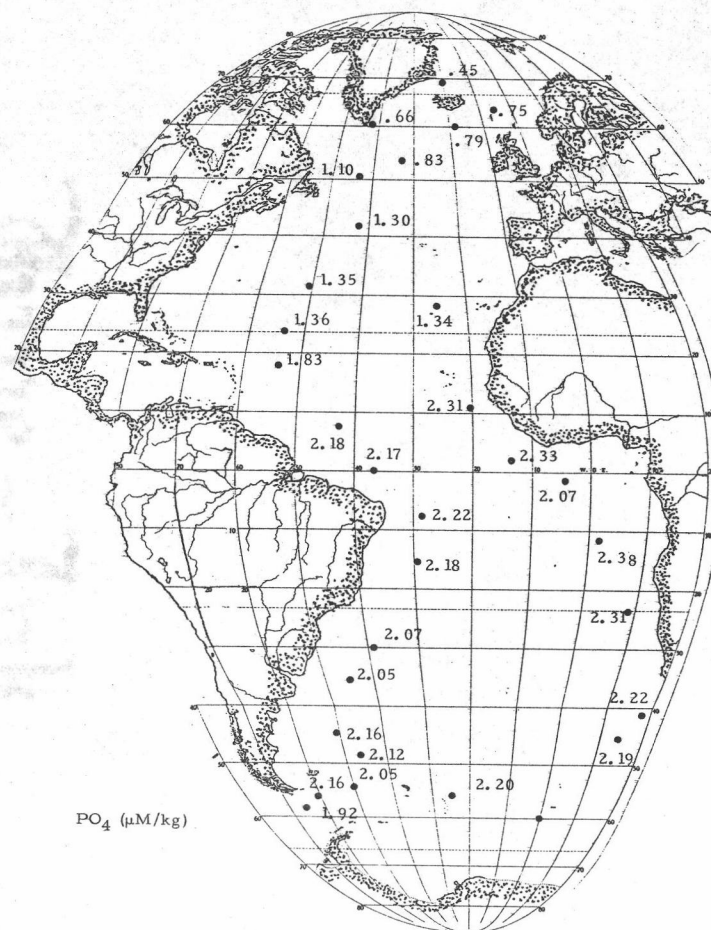


Figure III-16. Phosphate at  $\sigma_\theta = 27.34$ .

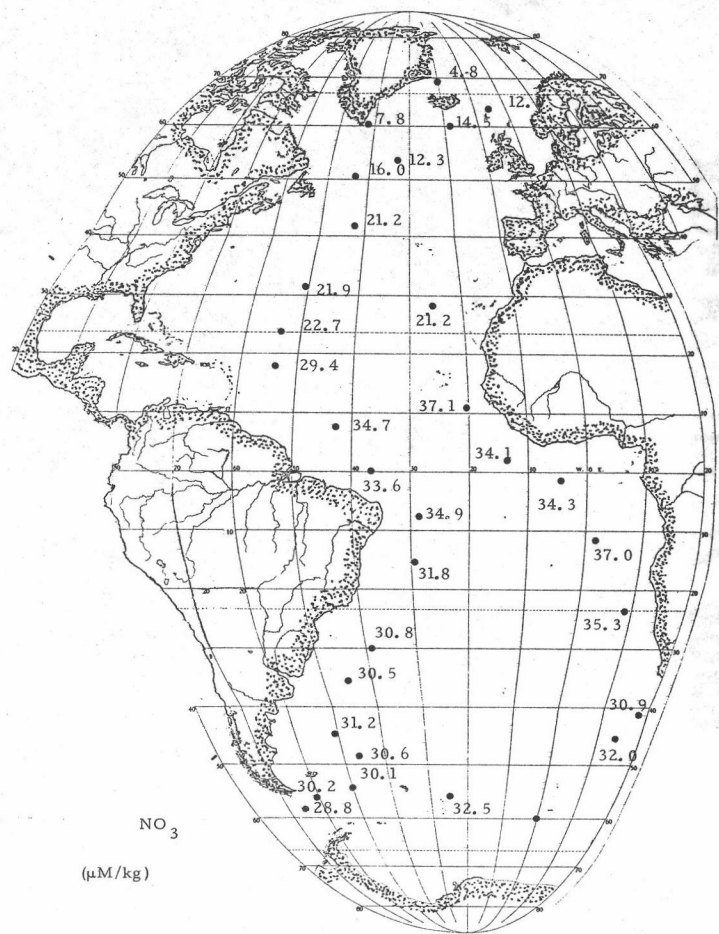


Figure III-17. Nitrate at  $\sigma_{\theta} = 27.34$ .

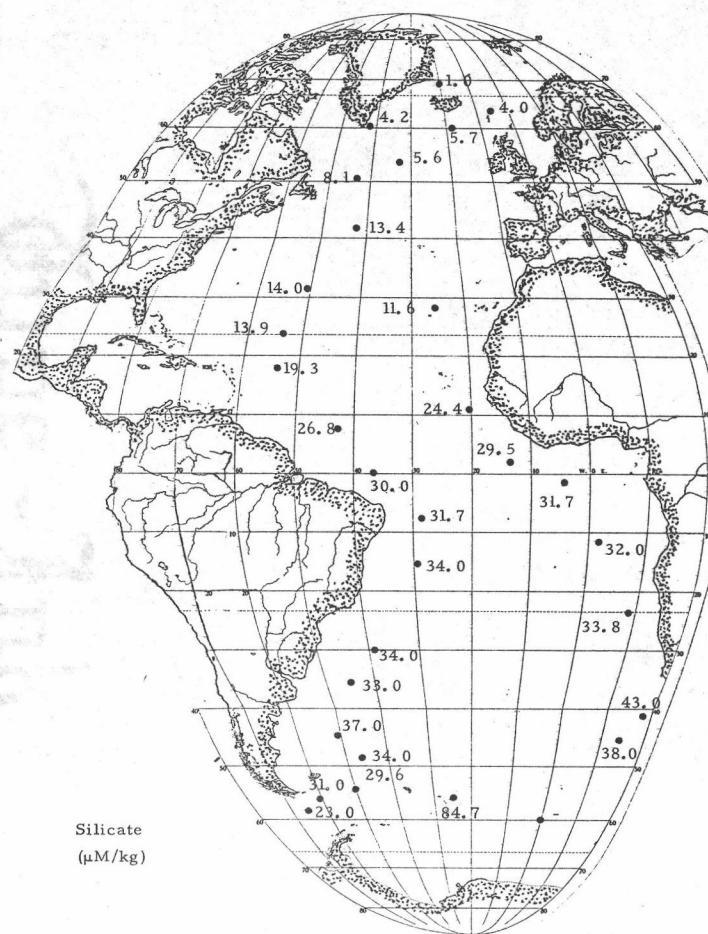


Figure III-18. Silicate at  $\sigma_{\theta} = 27.34$ .

The AOU at  $\sigma_\theta$  of 27.34 is lowest in source regions of the water masses (Fig. III-19). In the North Atlantic negative values appear where this density level approaches the sea surface. In the western basin there appears a gradual increase in AOU from the poles to the equator. As the levels of TOC are invariant at this density surface within the limits of the analysis (Fig. III-20), physical mixing processes with other more oxygen depleted waters are needed to explain the increase in AOU. Menzel and Ryther (1968) substantiate this argument by predicting  $O_2$  from considerations of salinity changes only for AAIW from 8°S to 35°S.

The conservative parameters,  $PO_{4(p)}$  and  $NO_{3(p)}$ , also are clear in dividing the Atlantic into a nutrient rich southern region and nutrient poor northern section with mixing towards the equator. The strong gradient in concentration between 10-20°N is again apparent (Figs. III-21 and III-22).

C.  $\sigma_\theta = 27.82$

With the exception of the stations in the most southern region of the Atlantic, the  $\sigma_\theta$  of 27.82 displays a strong influence of NADW with Mediterranean Water influence in large areas of the Central and North Atlantic. The depths for the  $\sigma_\theta$  surface range from near the surface at far northern stations to over 2400 meters in the Argentine Basin (Fig. III-23).

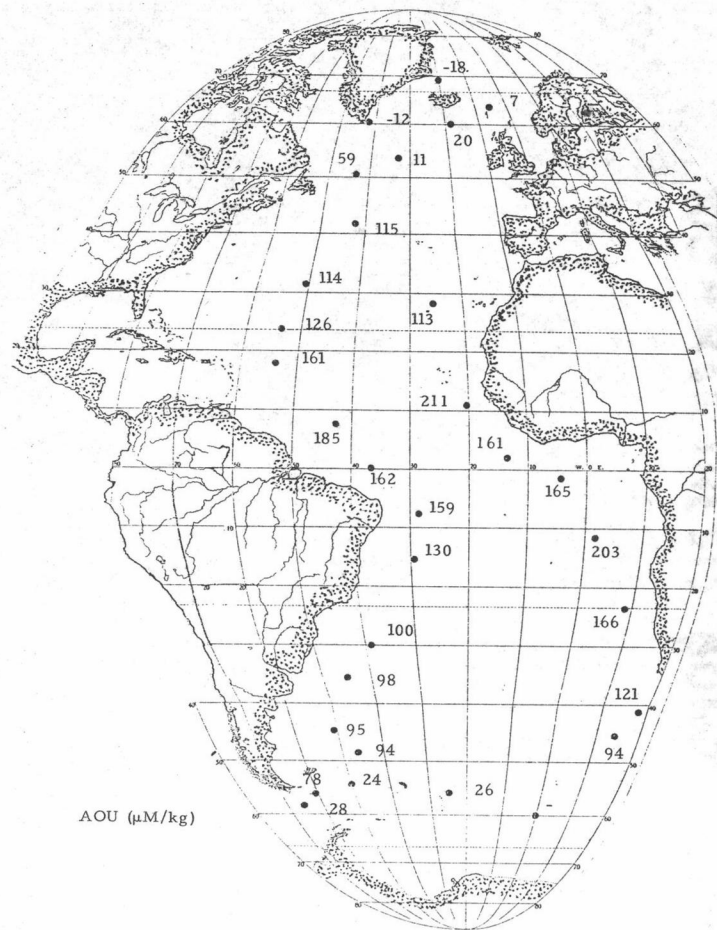


Figure III-19. AOU at  $\sigma_{\theta} = 27.34$ .

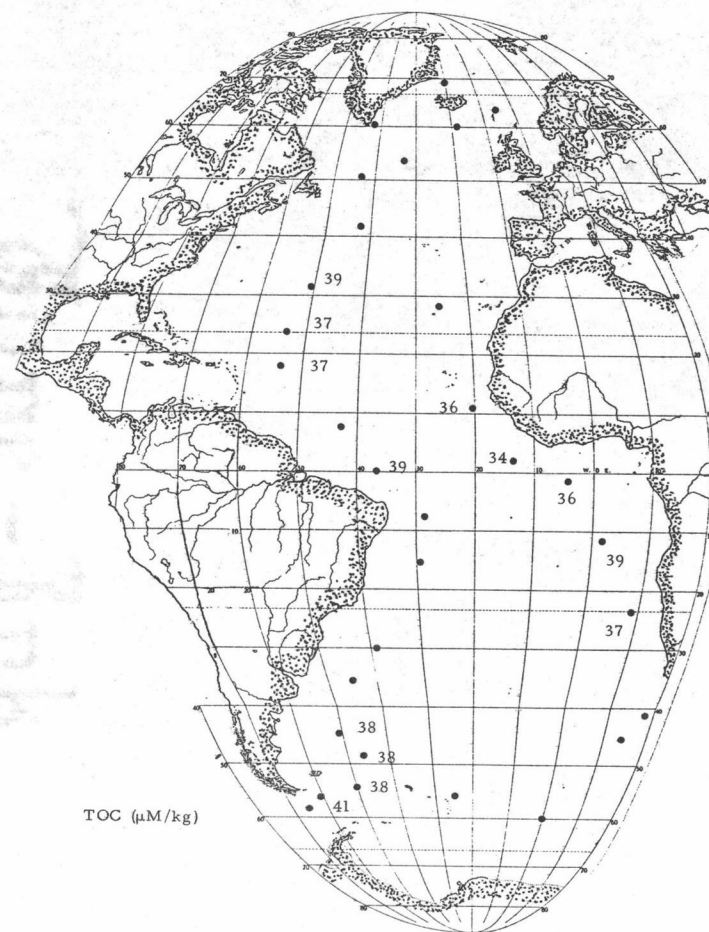


Figure III-20. TOC at  $\sigma_{\theta} = 27.34$ .

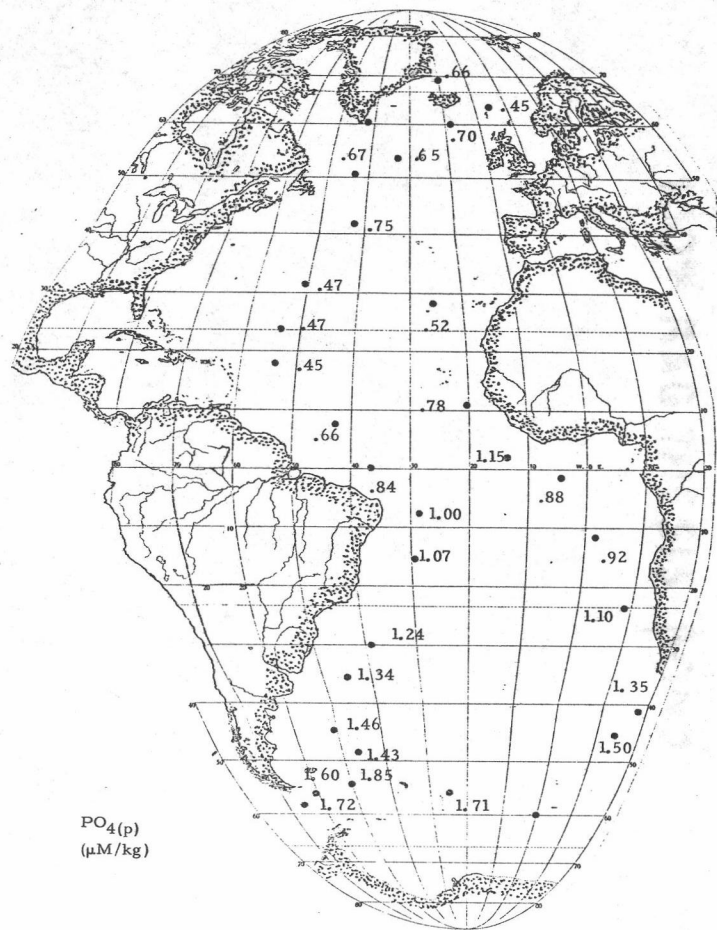


Figure III-21. Preformed phosphate at  $\sigma_{\theta} = 27.34$ .

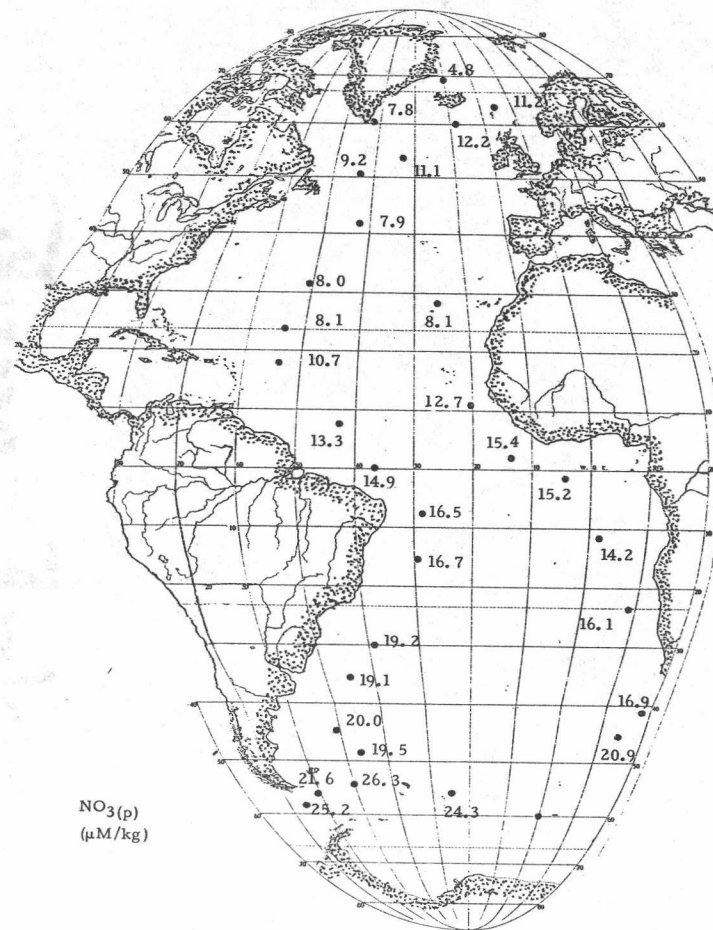


Figure III-22. Preformed nitrate at  $\sigma_{\theta} = 27.34$ .

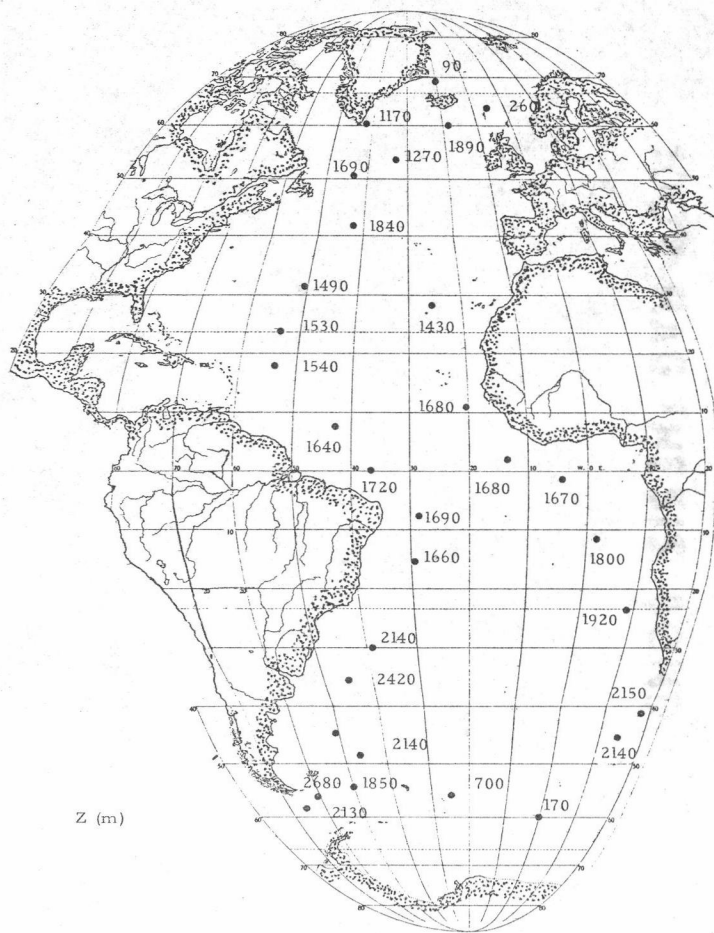


Figure III-23. Depths corresponding to the 27.82 potential density surface for the selected Atlantic stations.

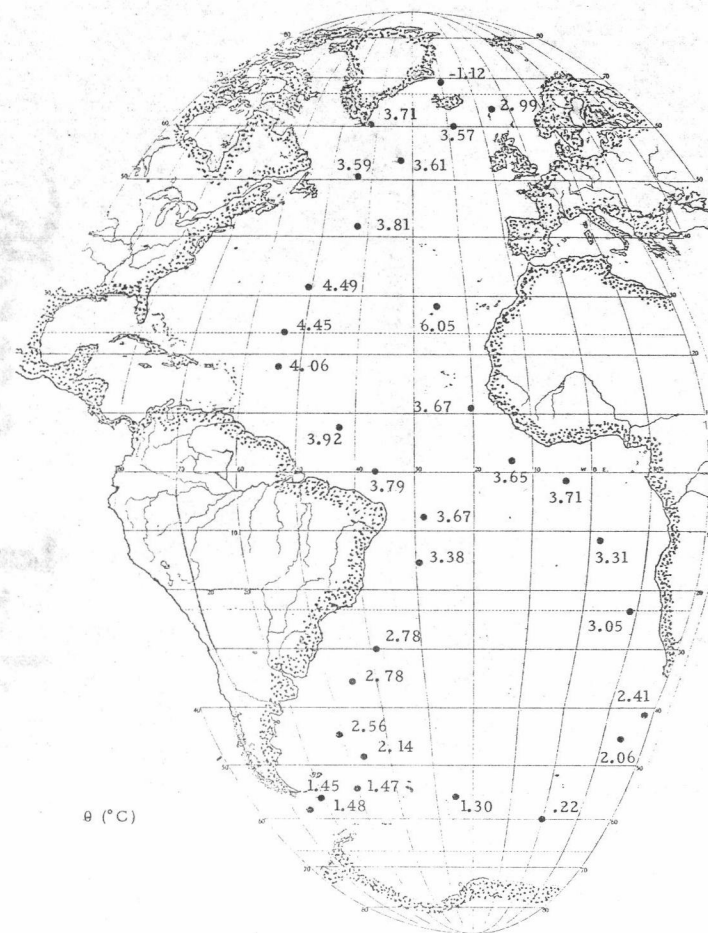


Figure III-24. Potential temperature for the 27.82 potential density surface.



The  $\theta$ , S, and  $O_2$  distributions (Fig. III-24 to III-26) show a northern water of less than  $4^\circ\text{C}$  and  $35\text{‰}$  moving southward. In the vicinity of  $30^\circ\text{N}$  a marked increase in temperature and salinity occurs. This is the influx of Mediterranean Water, high in salinity and temperature and low in oxygen, shown by Sverdrup, Johnson, and Fleming (1942). Influence of Mediterranean Water is seen to be stronger further to the south in the western basins than the eastern basins of the Atlantic as higher salinities and temperatures predominate further south. The influence of NADW is still strong near  $50^\circ\text{S}$  where salinities remain  $0.06\text{‰}$  higher,  $\theta$   $0.6^\circ\text{C}$  higher, and  $O_2$  levels slightly higher than Circumpolar Water of like density. Lateral transport clearly outweighs vertical dissipation at this density surface.

Perhaps a more graphic demonstration of the strong influence of NADW throughout much of the Atlantic is seen through the nutrient distribution, AOU,  $\text{PO}_{4(p)}$ , and  $\text{NO}_{3(p)}$  (Figs. III-27 and III-32). The  $\text{PO}_4$  and  $\text{NO}_3$  concentration remains below  $1.5$  and  $24 \mu\text{M/kg}$  as far as  $20^\circ\text{S}$ . Circumpolar Deep Water contains  $\text{PO}_4$  and  $\text{NO}_3$  levels of  $2.1$  and  $32 \mu\text{M/kg}$  at the same  $\sigma_\theta$  while the source waters for NADW are about  $1.1$  and  $17 \mu\text{M/kg}$ .

AOU,  $\text{PO}_{4(p)}$ , and  $\text{NO}_{3(p)}$  point out the influence of the Mediterranean Water in the central North Atlantic by the lowered  $\text{PO}_{4(p)}$ ,  $\text{NO}_{3(p)}$ , and increased AOU of this region. Also, substantially reduced preformed nutrients and AOU are present far to the south at

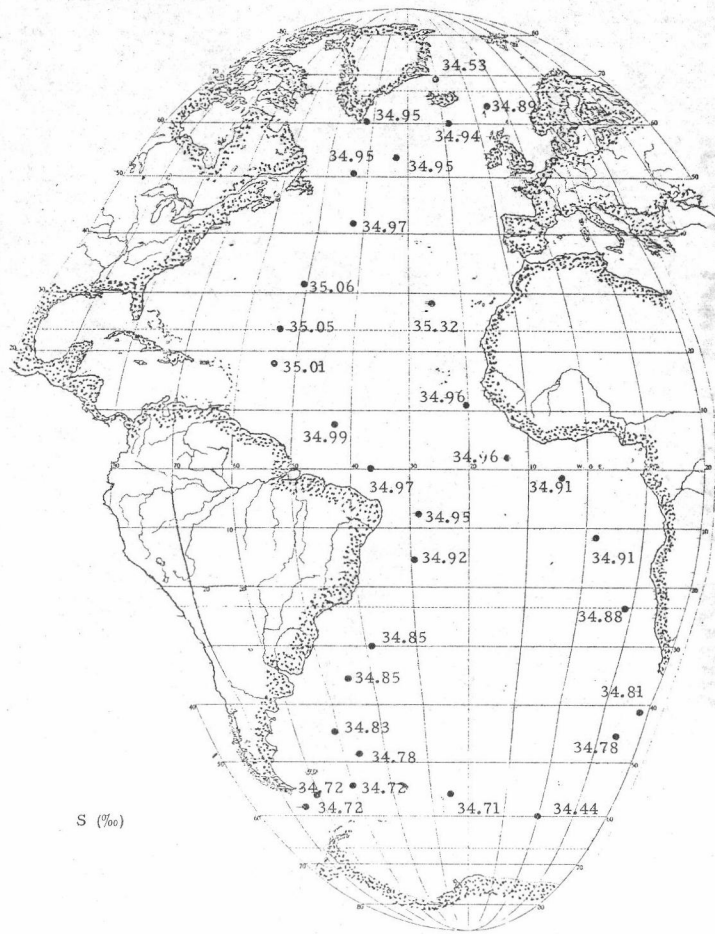


Figure III-25. Salinity for the 27.82 potential density surface.

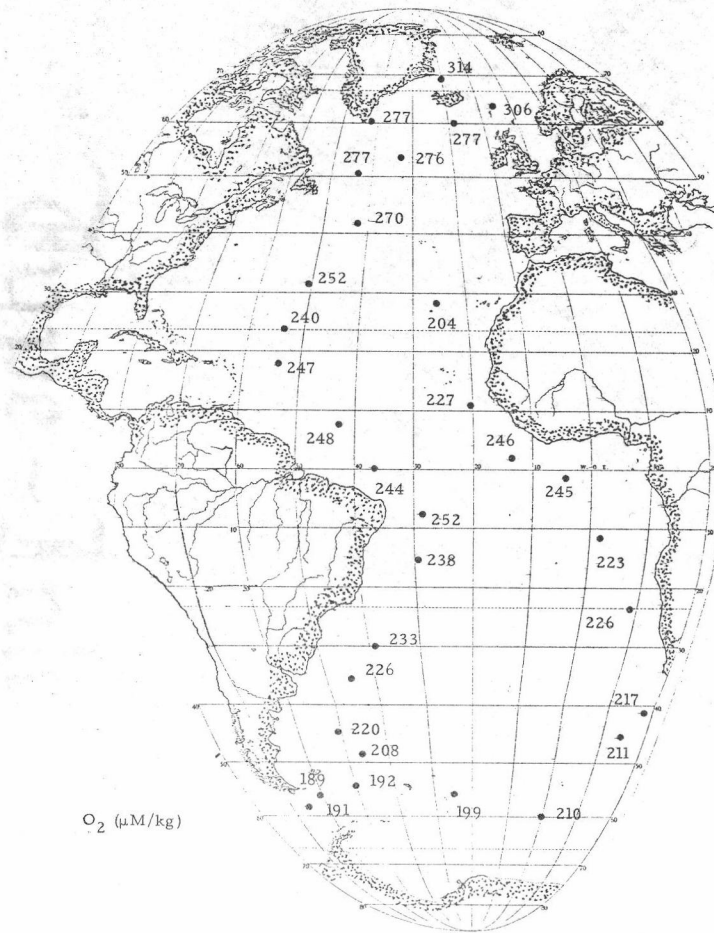


Figure III-26. Dissolved oxygen for the 27.82 potential density surface.

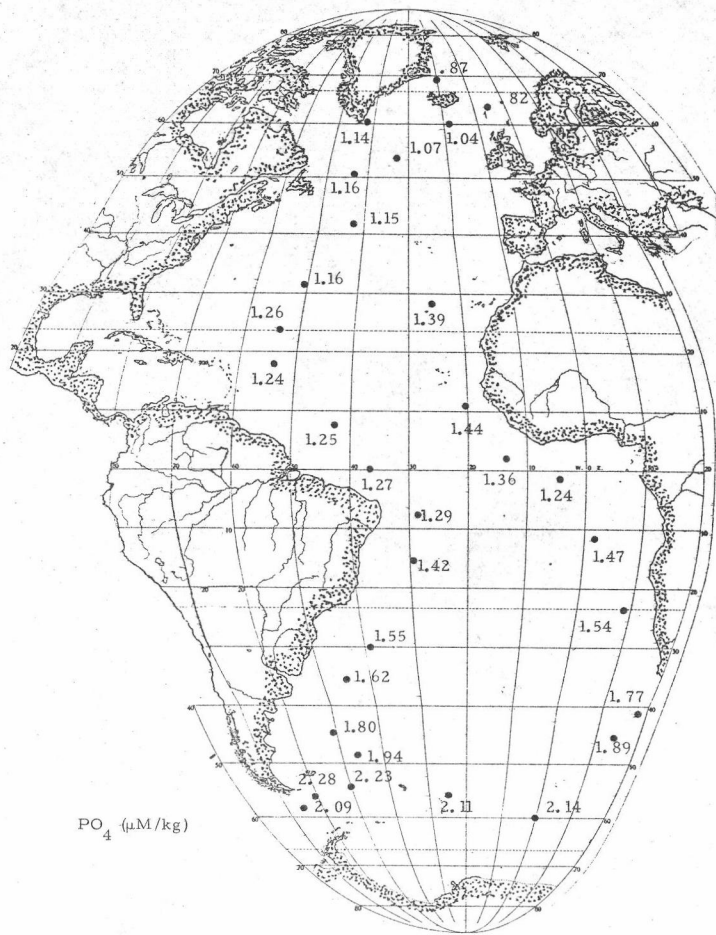


Figure III-27. Phosphate for the 27.82 potential density surface.

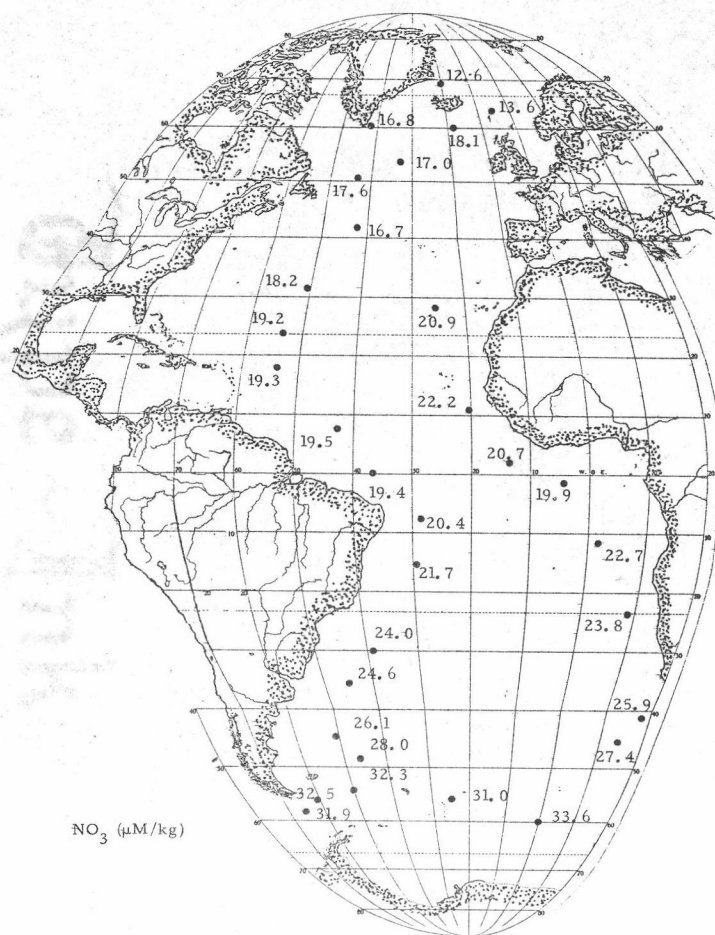


Figure III-28. Nitrate for the 27.82 potential density surface.

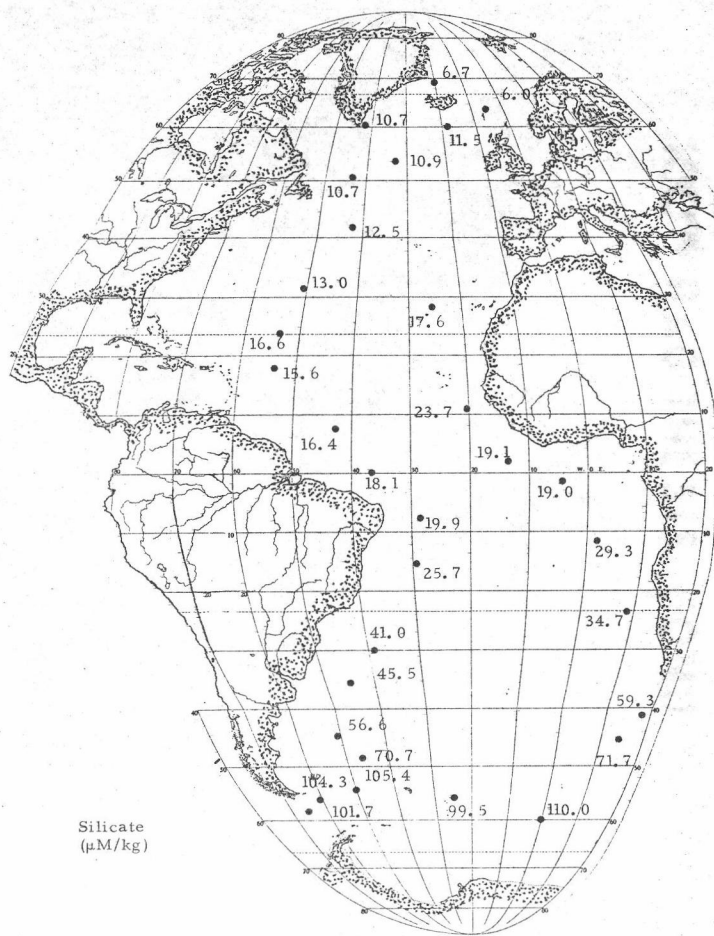


Figure III-29. Silicate for the 27.82 potential density surface.

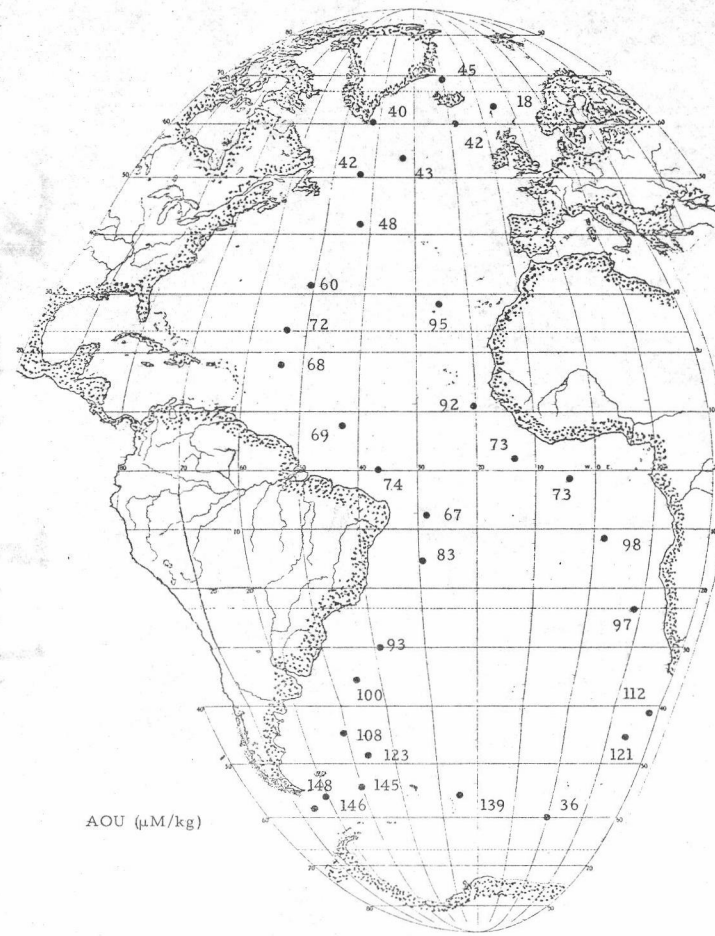


Figure III-30. AOU for the 27.82 potential density surface.

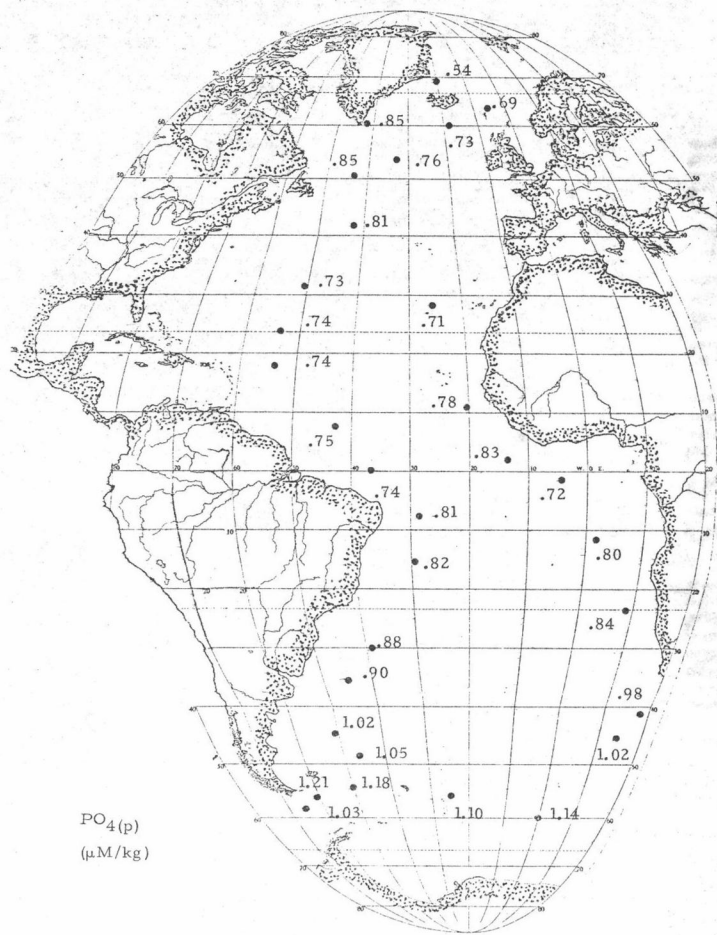


Figure III-31. Preformed phosphate for the 27.82 potential density surface.

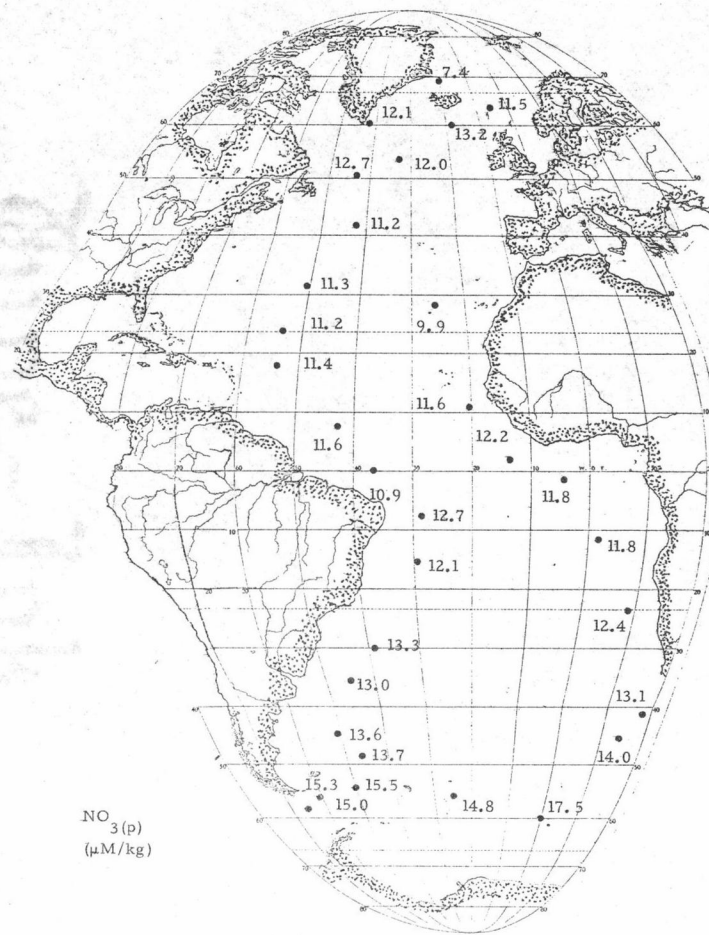


Figure III-32. Preformed nitrate for the 27.82 potential density surface.

this density surface due to the southward migration of the NADW. Assuming a source water level of 0.80 and 12.0  $\mu\text{M}/\text{kg}$  for the  $\text{PO}_{4(\text{p})}$  and  $\text{NO}_{3(\text{p})}$  in NADW, respectively, and values of 1.10 and 15.0  $\mu\text{M}/\text{kg}$  for water of Southern Ocean origin, 50% NADW influence would be at roughly 0.95 and 13.5  $\mu\text{M}/\text{kg}$ . From this rough calculation, a 50% character of NADW exists as far as  $40^\circ\text{S}$ . Similar observations can be inferred from the AOU,  $\text{PO}_4$ , and  $\text{NO}_3$  graphs.

By far the most marked extremes of concentration between NADW and deep Southern Ocean waters is in silicate (Fig. III-29). Silicate values at  $\sigma_\theta$  of 27.82 range clear from 6.0 to 110.0  $\mu\text{M}/\text{kg}$ . Applying the calculation for 50% NADW influence for silicate gives approximately 55  $\mu\text{M}/\text{kg}$  which falls near  $40^\circ\text{S}$ . At  $20^\circ\text{S}$  latitude in both the eastern and western basins, a similar calculation indicates over 75% water of North Atlantic origin. While salinity variations are on the order of .3‰ silicate varies nearly 100  $\mu\text{M}/\text{kg}$ . The potential for silicate as a tracer is indeed great in the Atlantic.

The TOC levels (Fig. III-33) on the  $\sigma_\theta$  of 27.82 again show no systematic variation greater than the error of the analysis. Values are very similar to the levels seen at  $\sigma_\theta$  of 27.34. The statements by Menzel (1970) and Menzel and Ryther (1968) indicating little decomposition of organic matter below the upper few hundred meters are substantiated in NADW.

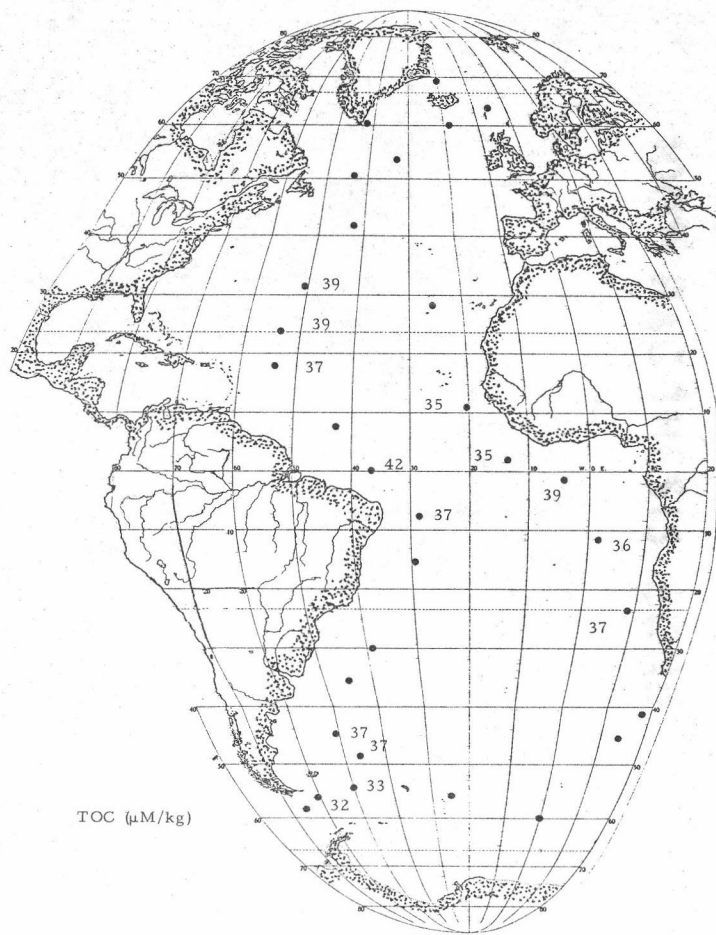


Figure III-33. TOC for the 27.82 potential density surface.

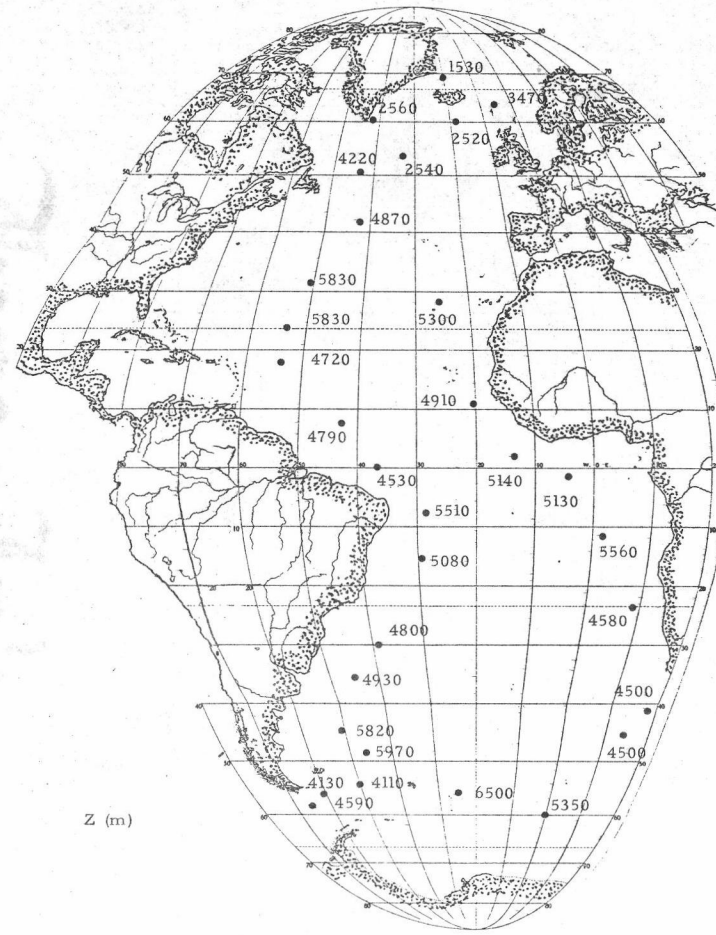


Figure III-34. Depth at the ocean bottom for the selected GEOSECS stations.

#### D. Bottom

The stations selected for this analysis are in most cases over 4 km in depth. Deep stations were preferentially chosen. A shallowing of the North Atlantic bottom necessitated the use of stations less than 4 km in this region. The depths at the bottom range from 1530 to 6500 meters (Fig. III-34).

Two quite different forms of bottom water are readily apparent from the  $\theta$ , S, and  $O_2$  graphs (Figs. III-35 to III-37). The AABW is colder ( $<0.0^\circ\text{C}$ ), poorer in oxygen ( $<230 \mu\text{M/kg}$ ), and fresher (34.67‰) than the North Atlantic counterpart ( $2.0^\circ\text{C}$ ,  $>270 \mu\text{M/kg}$ , and  $>34.90\text{‰}$  respectively). The North Atlantic Bottom Water is a mixture of Arctic Bottom Water, seen north of England, with low  $\theta$  and high  $O_2$  plus North Atlantic Waters of  $\theta$  near  $2^\circ\text{C}$ . The AABW is seen to move strongly northward along the western coast of South America with a good deal of mixing in the equatorial region. Neumann and Pierson (1966) describe an eastward branch of AABW through the Romanche fracture zone into the eastern basins. This is seen weakly in the  $\theta$  and S values near the equator in the eastern basins.

The nutrient distributions at the bottom mirror closely the  $\theta$  and S plots (Figs. III-38 to III-40). Strong nutrient maximum originate from the Southern Ocean and move northward. Relatively



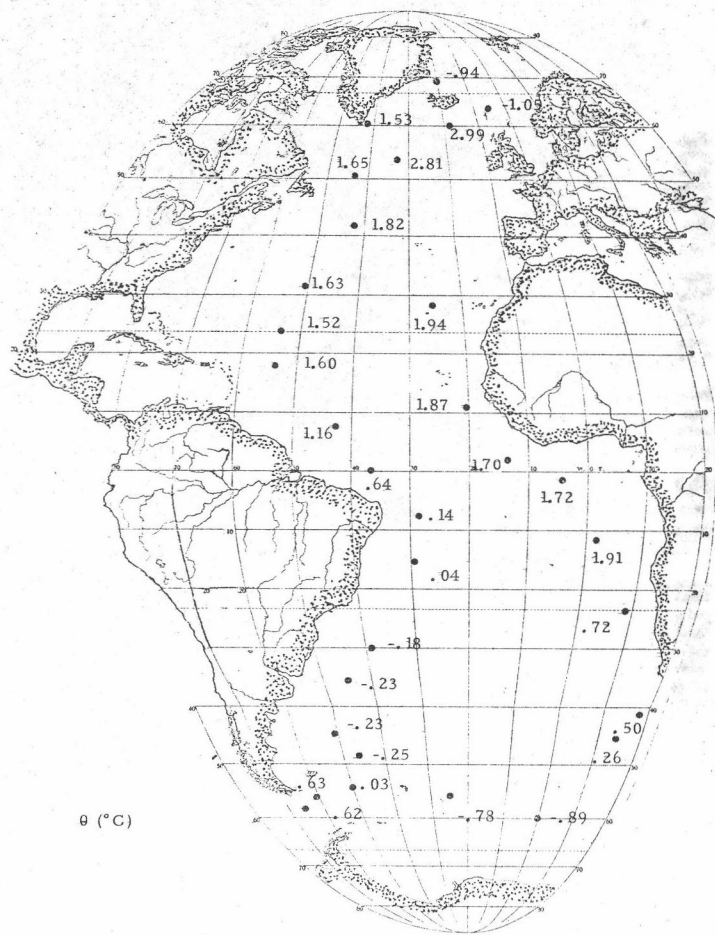


Figure III-35. Potential temperature near the ocean bottom for the selected GEOSECS stations.

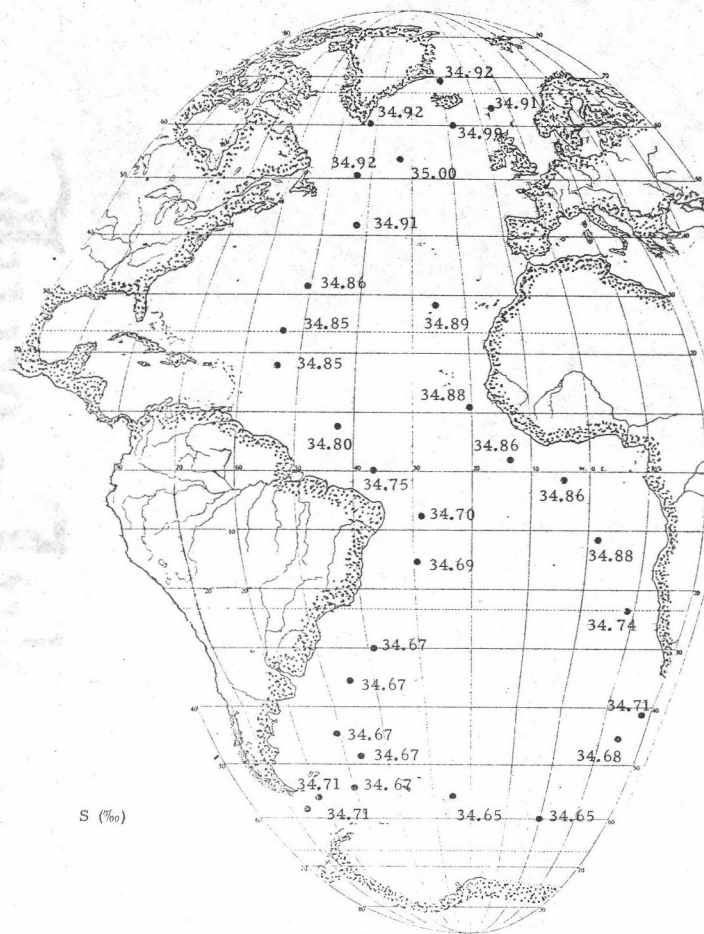


Figure III-36. Salinity near the ocean bottom for the selected GEOSECS stations.

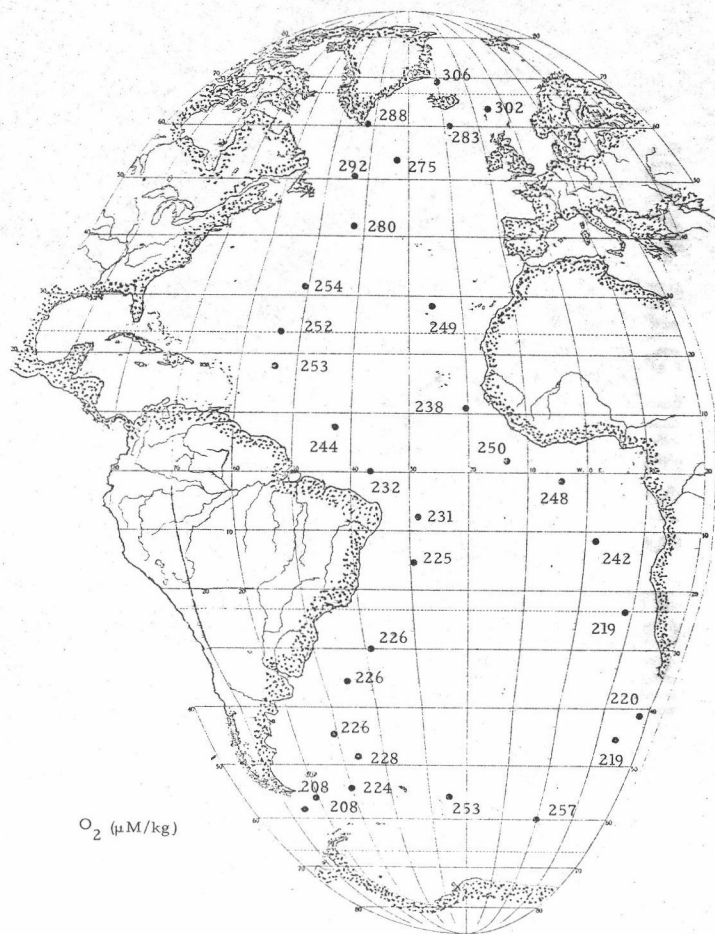


Figure III-37. Dissolved oxygen near the ocean bottom in the Atlantic.

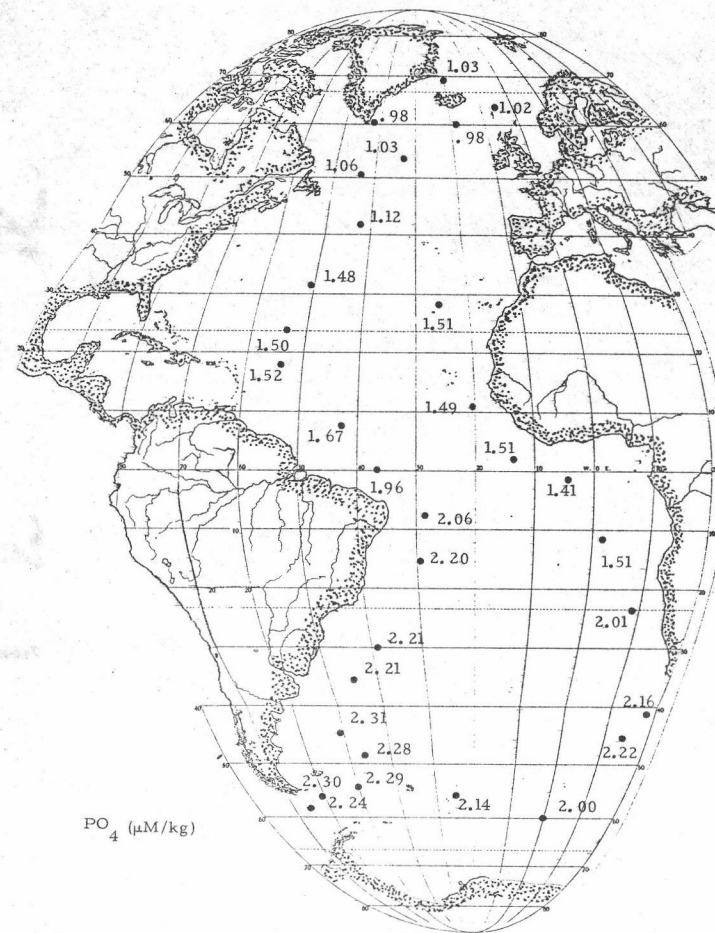


Figure III-38. Phosphate near the ocean bottom in the Atlantic.

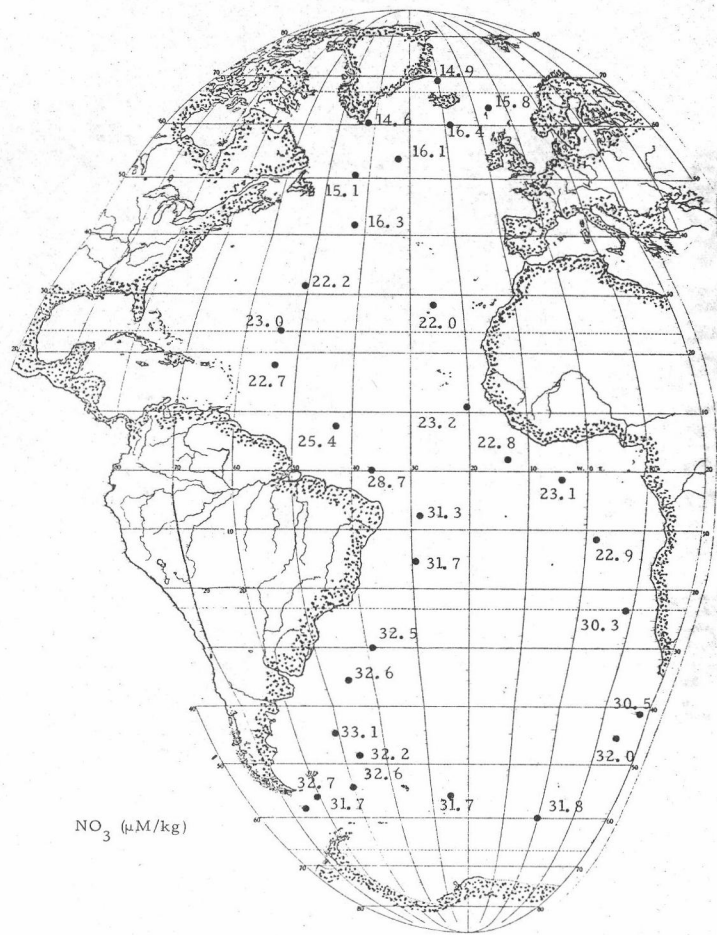


Figure III-39. Nitrate near the ocean bottom in the Atlantic.

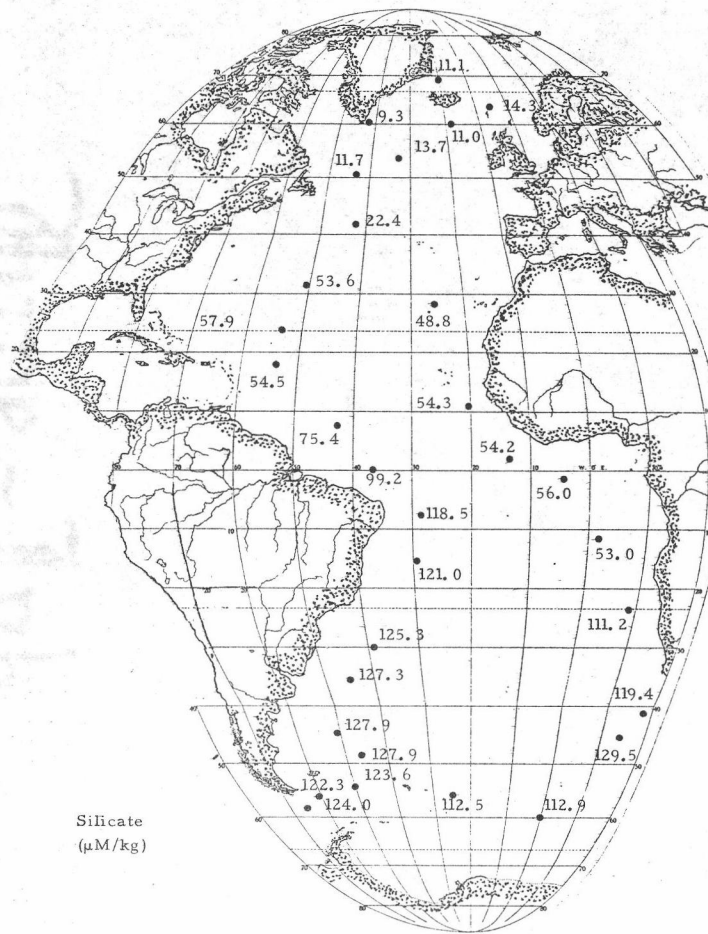


Figure III-40. Silicate near the ocean bottom in the Atlantic.

little dilution in concentration occurs until near the equator in the western basins. A slight enrichment in the eastern basin near the equator occurs from flow of AABW through the Romanche fracture zone. The conservative nature of the nutrients is striking and is discussed further later.

The plots of AOU,  $\text{PO}_{4(p)}$ , and  $\text{NO}_{3(p)}$  indicate similar patterns as earlier plots (Figs. III-41 to III-43). The consistency is an indication of the quality of the nutrient data that has been taken. Levels of  $\text{PO}_{4(p)}$  and  $\text{NO}_{3(p)}$  for AABW are approximately 1.40 and 18.0  $\mu\text{M}/\text{kg}$  respectively. The bottom waters of the North Atlantic have  $\text{PO}_{4(p)}$  and  $\text{NO}_{3(p)}$  values near 0.70 and 10.0  $\mu\text{M}/\text{kg}$ . Concentrations of 1.05 and 14.0  $\mu\text{M}/\text{kg}$  for  $\text{PO}_{4(p)}$  and  $\text{NO}_{3(p)}$  give rough approximation of equal northern and southern water influence. AABW exerts a 50% influence on the bottom water's character to between 0-10°N in the western basins of the Atlantic while North Atlantic Bottom Water shows a 50% influence as far as 20°S in the eastern basins.

The TOC values for the bottom waters do not change much horizontally (Fig. III-44). They do not vary significantly from those seen at  $\sigma_{\theta}$  surfaces of 27.34 and 27.82.

An additional perspective of the TOC data was made using the statistical analysis of two phase regression (Daly, 1974). When TOC is plotted against  $\theta$  (Fig. V-10) two distinct portions are extracted. One segment is the exponential decrease of TOC from the surface to

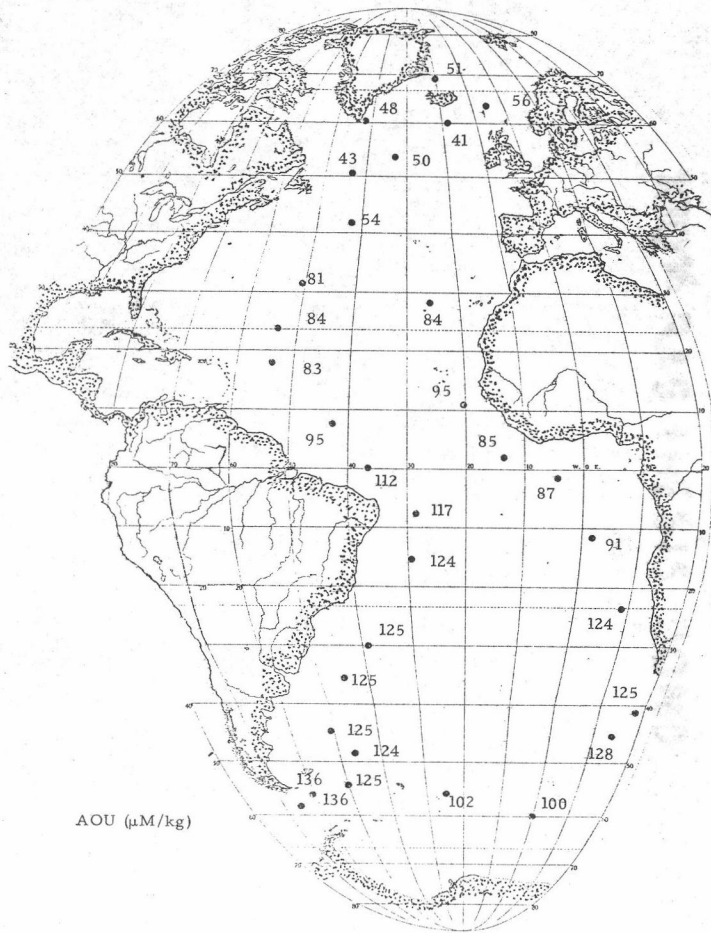


Figure III-41. AOU near the ocean bottom in the Atlantic.

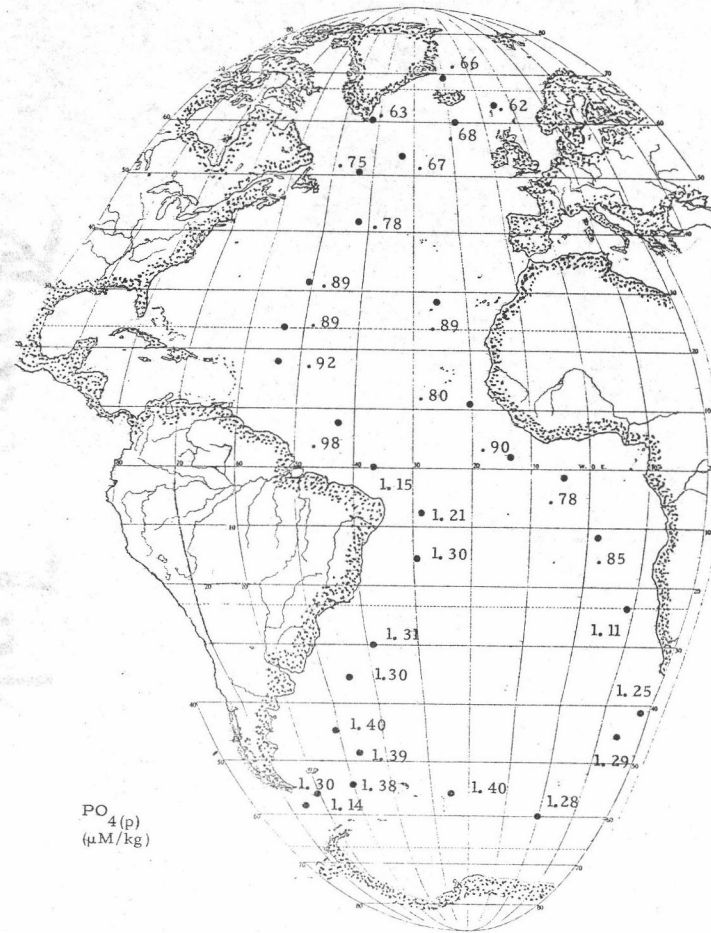


Figure III-42. Preformed phosphate near the ocean bottom in the Atlantic.

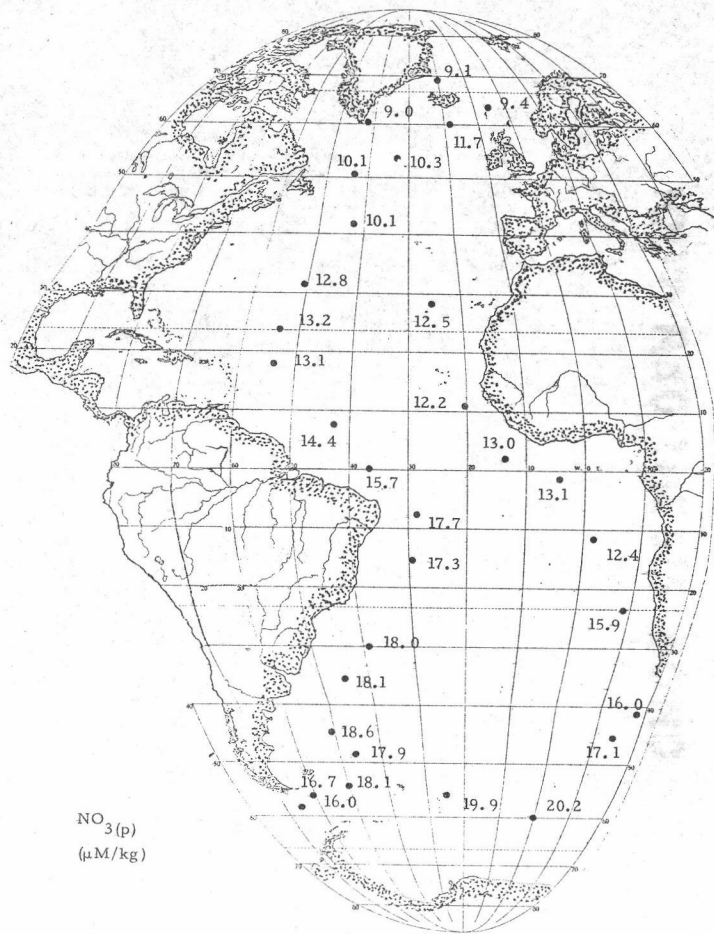


Figure III-43. Preformed nitrate near the ocean bottom in the Atlantic.

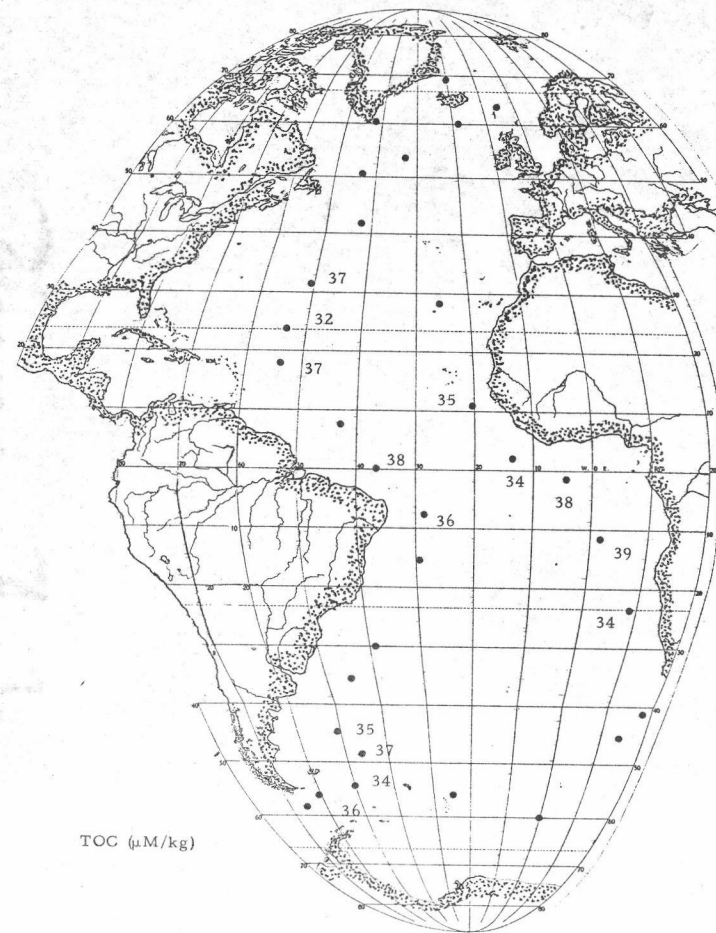


Figure III-44. TOC near the ocean bottom in the Atlantic.

a depth of a few hundred meters, while the second region is the segment showing minor variations within the error of the analysis. By attempting a varying series of data combinations, two lines can be fitted which statistically model the data most accurately. This method was applied to the GEOSECS TOC data and the various depths for the meeting point of the two lines were determined. The results are given in Table III-1.

Table III-1. Intersection depth and total organic carbon concentration for a best two line fit of  $\theta$ -TOC data.

| Station Number | Intersection Point<br>$\mu\text{M}/\text{kg}$ of Organic Carbon | Depth of Intersection<br>(m) |
|----------------|---|------------------------------|
| 30             | 45  | 333                          |
| 32             | 46  | 275                          |
| 34             | 37  | 450                          |
| 42             | 46  | 181                          |
| 49             | 38  | 252                          |
| 67             | 37  | 300                          |
| 68             | 37  | 129                          |
| 74             | 37  | 137                          |
| 75             | 37  | 555                          |
| 103            | 45  | 257                          |
| 107            | 45  | 272                          |
| 109            | 47  | 139                          |
| 111            | 38  | 250                          |
| 113            | 40  | 176                          |

In all cases, the lowest limit for the segment of decreasing organic carbon is above 600 m. The station with the deepest intersection, station 75, is also the southernmost station where organic carbon was measured. The depth of intersection shows no significant

geographical pattern, but the bulk of biochemical oxidation is completed in the upper portion of the water column. Since no TOC stations were taken in the Southern Ocean and high northern latitudes, source values of TOC for the deep and bottom waters are unknown.



#### IV. GRAPHICAL PRESENTATION OF NUTRIENT AND HYDROGRAPHIC DATA IN THE WESTERN BASINS OF THE ATLANTIC OCEAN

Redfield (1942) and Riley (1951) used the available nutrient data to graphically portray the Atlantic Ocean as a function of depth or  $\sigma_t$  versus latitude. Using their format, graphs for various hydrographic and nutrient parameters were plotted for the western basin of the Atlantic Ocean. The GEOSECS program completed a thorough transect of this area from 75°N to 60°S latitude (Fig. IV-1).

The diagrams of potential temperature and salinity are classic tools of the physical oceanographer (Figs. IV-2 and IV-3). The

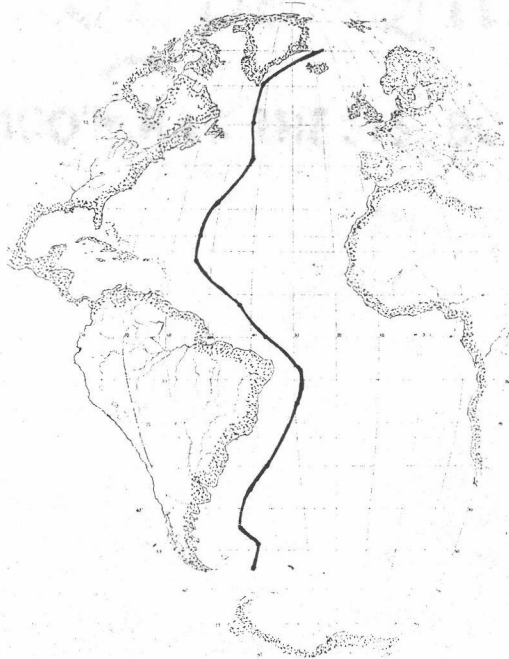


Figure IV-1. The cruise track for GEOSECS in the western basins of the Atlantic Ocean.

Figure IV-3. Salinity distribution in the western Atlantic.

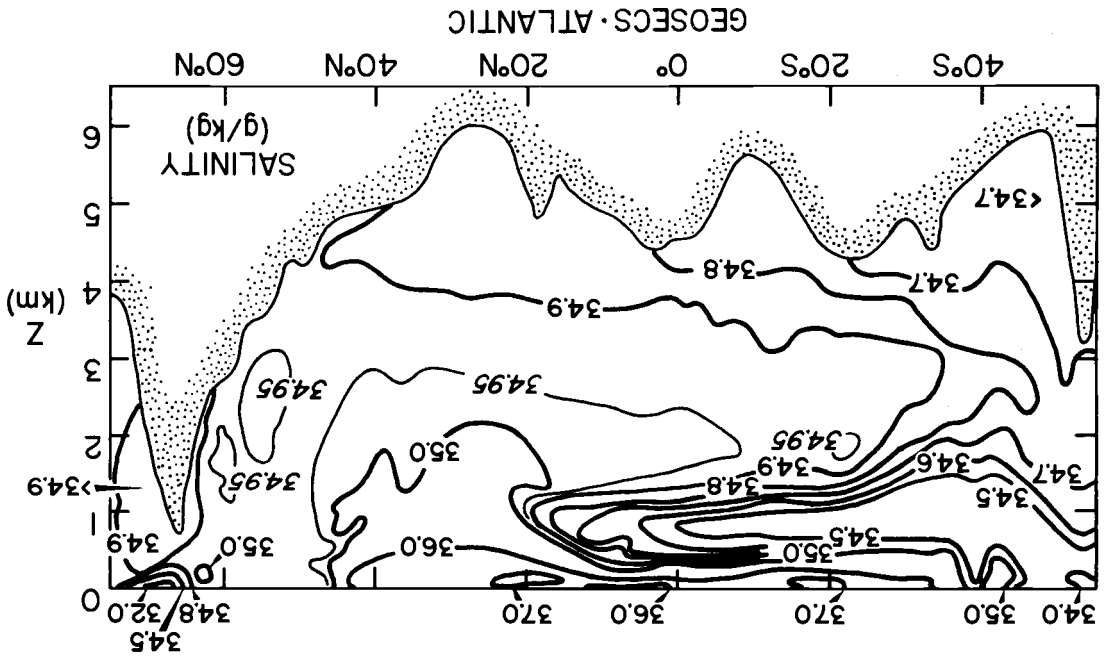
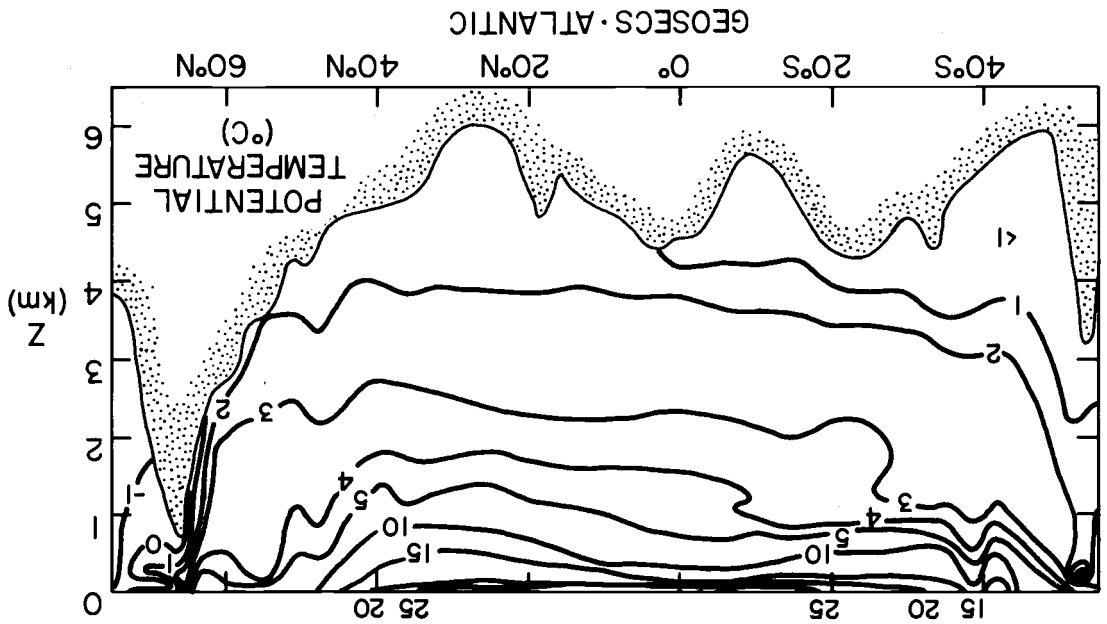


Figure IV-2. The potential temperature profile for the western Atlantic.



potential temperature plot shows the far northern and southern regions of deep water formation by the low surface temperatures and nearly vertical slope of the isotherms. Throughout the rest of the ocean, lateral motion appears to predominate. Salinity also demonstrates the strong lateral transport and is especially clear in demonstrating the northward movement of the low salinity AAIW to 20°N.

The use of  $\sigma_4$  has been suggested and utilized for tracing Atlantic water transport by Lynn and Reid (1968), Lynn (1971), and Buscaglia (1971). The definition of  $\sigma_4$  is the density of the water related to a pressure of 4000 decibars in contrast to  $\sigma_\theta$  which is the potential density at 0 decibars. Both parameters are useful in a descriptive analysis of deep water as  $\sigma_\theta$  can be used to determine water origin and  $\sigma_4$  may be utilized for deep ocean flow studies. Using  $\sigma_\theta$  for the deep ocean waters presents the appearance of North Atlantic Deep Water (NADW) being denser than Antarctic Bottom Water (AABW). Referred to zero decibar pressure this is true, but at the great pressure of the deep ocean the colder and hence more compressible AABW is more dense and moves beneath the NADW. This can be seen on the  $\sigma_4$  plot where the 46.0 isopycnal moves beneath the less dense NADW to a latitude of almost 20°N in the western basin (Fig. V-4).

The oxygen profile for the western basin of the Atlantic shows rather clearly the southward movement of the oxygen rich NADW as

Figure IV-5. Dissolved oxygen distribution in the western Atlantic.

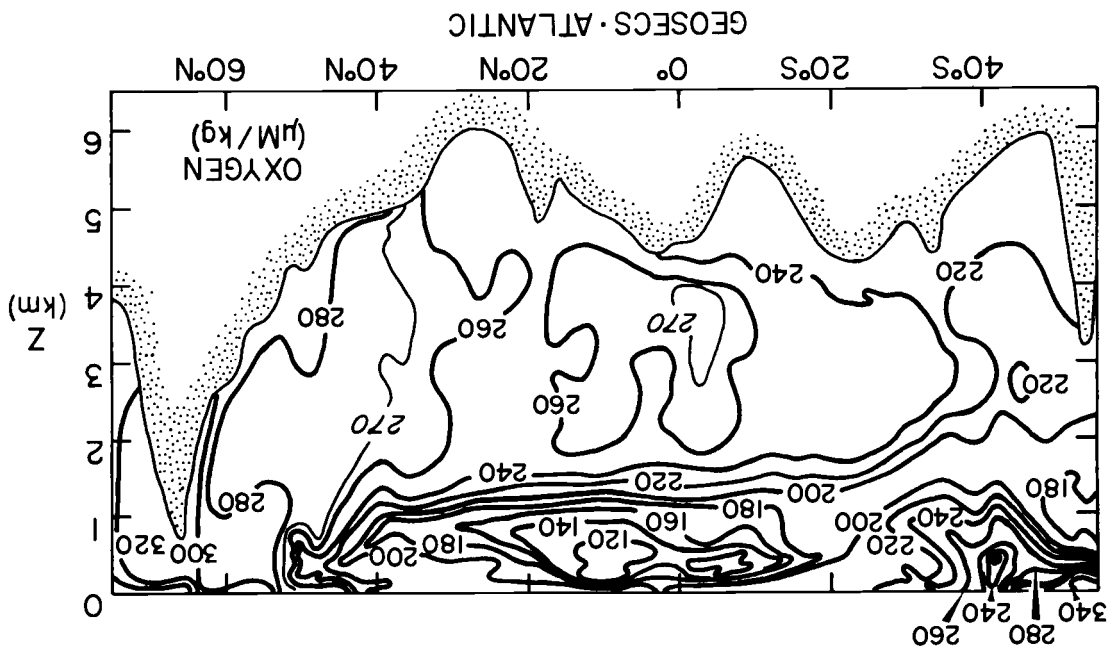
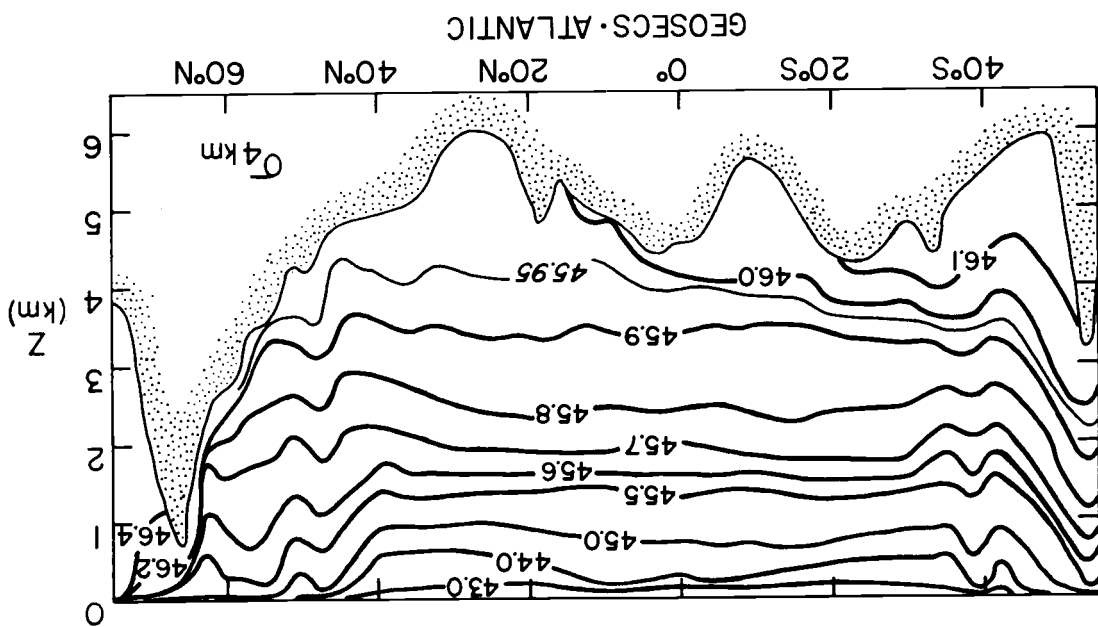


Figure IV-4.  $\sigma_t^4$  distribution in the western Atlantic.



far south as  $40^{\circ}\text{S}$  latitude (Fig. IV-5). In the equatorial region the deep water shows the influx of a high oxygen region greater than  $260\ \mu\text{M}/\text{kg}$  throughout a large portion of the deep water. This is shown by Neumann and Pierson (1966) as the influx of oxygen rich Middle North Atlantic Deep Water. At about 500 meters depth in the equatorial region is seen two separate areas with oxygen levels below  $120\ \mu\text{M}/\text{kg}$ . These are the minimum levels found in the western Atlantic Ocean. Sverdrup, Johnson, and Fleming (1942) do not present these clear minimum regions in their western Atlantic oxygen profile. The feature could be due either to in situ decomposition in these areas or transport of low oxygen water from the east. Observations on the rapidity of decomposition of organic material (Menzel and Ryther, 1968, and Menzel, 1970) support the conclusion of Skopintsev (1965) that isentropic mixing westward from the regions of lowest oxygen content along the coast of Africa are responsible for the minimum values near the equator in the western basins.

The precise nitrate and phosphate profiles (Figs. IV-6 and IV-7) taken along the western basins of the Atlantic Ocean distinctly illustrate the hydrographic control which produces the nutrient minima and maxima. The AAIW core near one kilometer remains distinctly evident to at least  $40^{\circ}\text{N}$  for both the  $\text{PO}_4$  and  $\text{NO}_3$  plots. In the case of the NADW, between 2 to 3 kilometers, a  $\text{PO}_4$  and  $\text{NO}_3$  minimum can be seen. Influence of the nutrient poor NADW extends

Figure IV-7. Nitrate in the western Atlantic.

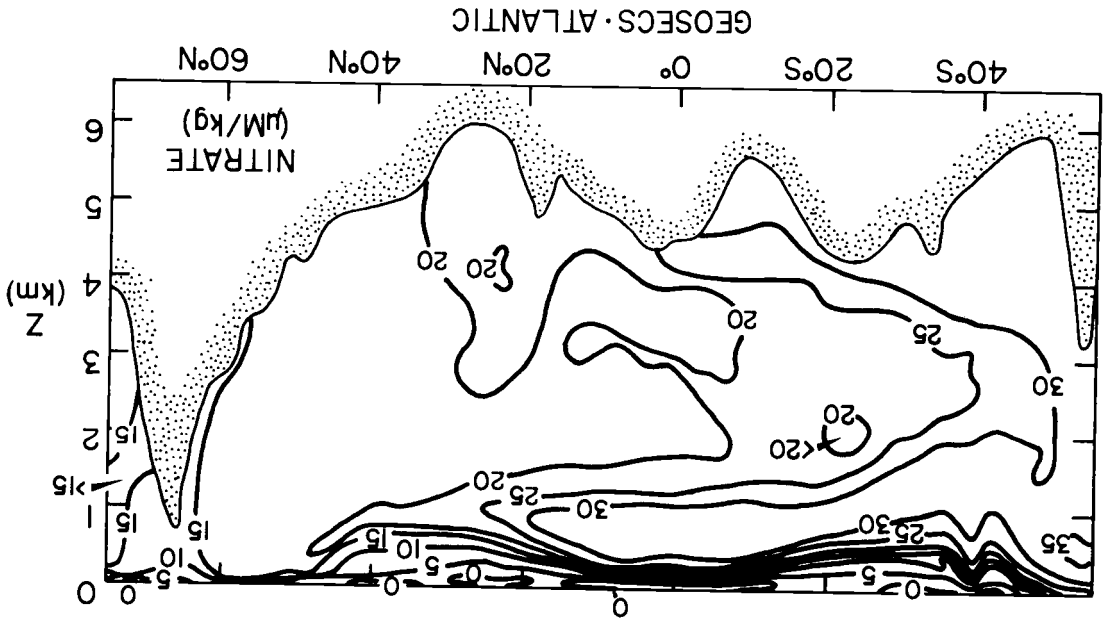
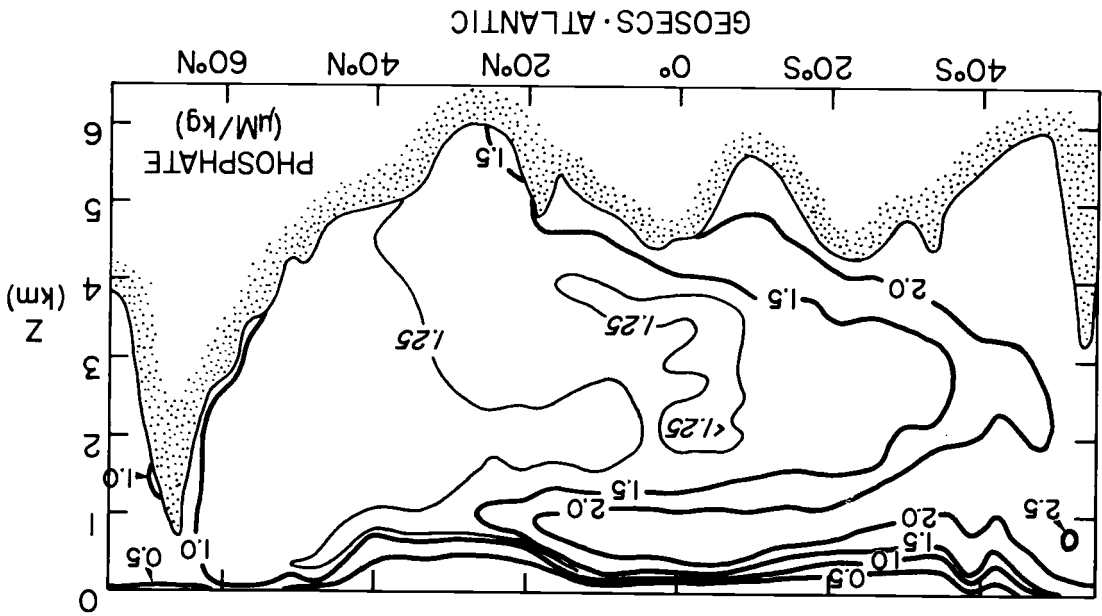


Figure IV-6. Phosphate in the western Atlantic.



well past  $40^{\circ}\text{S}$  as seen on the profiles. AABW corresponds to the nutrient maximum creeping northward along the ocean bottom. The  $\text{PO}_4$  graph shows the marked influence of AABW up beyond  $20^{\circ}\text{N}$  while  $\text{NO}_3$  values remain above  $25\ \mu\text{M}/\text{kg}$  to the north of the equator. There also appears in the equatorial region, immediately above the AABW, a section of low nutrient values. This agrees with the high oxygen region in this area (Fig. IV-5), where the influx of Middle North Atlantic Deep Water is seen. The correspondence of nutrient extrema and salinity extrema is also apparent from the comparison of the nutrient and salinity profiles (Fig. IV-6, IV-7 and IV-3). The readily identifiable cores of the various water masses far removed from their origin is indicative of the relative dominance of lateral transport over vertical mixing processes.

Metcalf (1969) and Richards (1958) hinted at the potential value of silicate as a water mass tracer. A sparsity of data coupled with a large percentage of questionable observations has limited the application of silicate as a tracer. The GEOSECS program, by the concurrent use of Oregon State University standards prepared by Professor Louis I. Gordon and the international nutrient standards prepared by Professor Ken Sugawara, now has an internally consistent silicate data file covering much of the Atlantic Ocean. The profile of silicate (Fig. IV-8) reinforces the earlier suggestions of the potential value of silicate for tracing water masses. A pronounced silico-cline

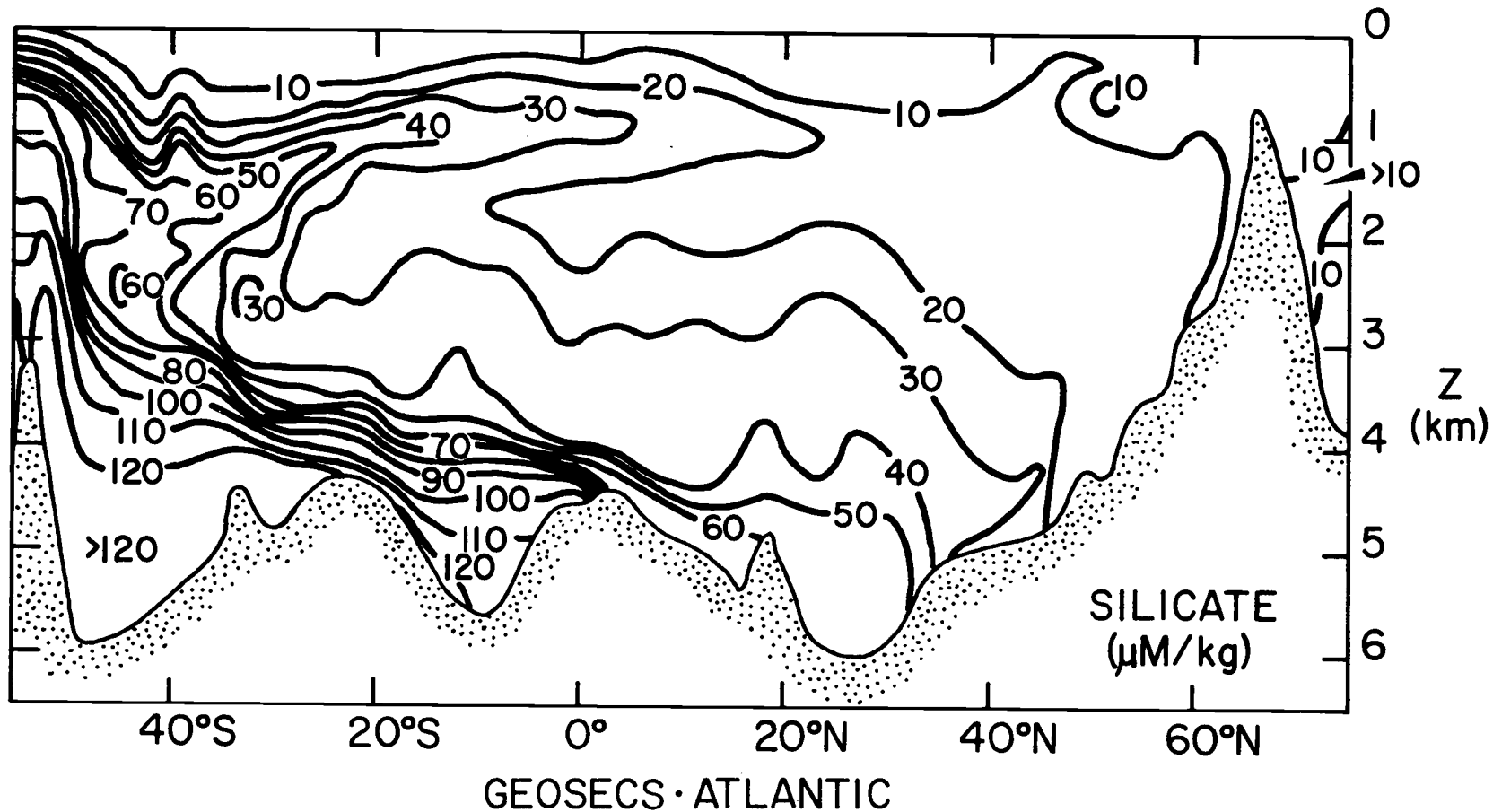


Figure IV-8. Silicate in the western Atlantic.



exists between the boundary of the NADW and AABW. Changes from 40 to 120  $\mu\text{M}/\text{kg}$  occur in regions of the South Atlantic where salinity varies only from 34.7 to 34.9‰. The AABW is very graphically apparent as it moves northward along the bottom. Strong AABW influence in the bottom waters is seen to the equator and a diminished influence is seen in the North Atlantic past 40°N. The NADW is distinguishable by the high level of silicate depletion. The core of the low silicate NADW is observable to below 40°S where it is entrained in the Circumpolar Deep Water of the Southern Ocean and loses its identity. The AAIW is a silicate maximum centered near 1 km depth that extends to 20°N. Spencer (1972) has shown that where  $\theta$ -S diagrams are linear at great depths, the silicate-S correlation is also linear. Therefore, silicate in this region may be treated as a conservative parameter for studying the hydrodynamics in the area of NADW and AABW.

An additional view of the silicate chemistry is seen in the three GEOSECS stations (76-78) taken in the Drake Passage. With only three available stations in the Drake Passage from the GEOSECS cruises, vertical profiling of a north-south transect of the passage was not attempted, but vertical profiles of the three stations (Fig. IV-9) hint at the potential for silicate chemistry studies in the Southern Ocean. The five water types in the Drake Passage are lettered A, B, C, D, E on the silicate versus depth plots. Two

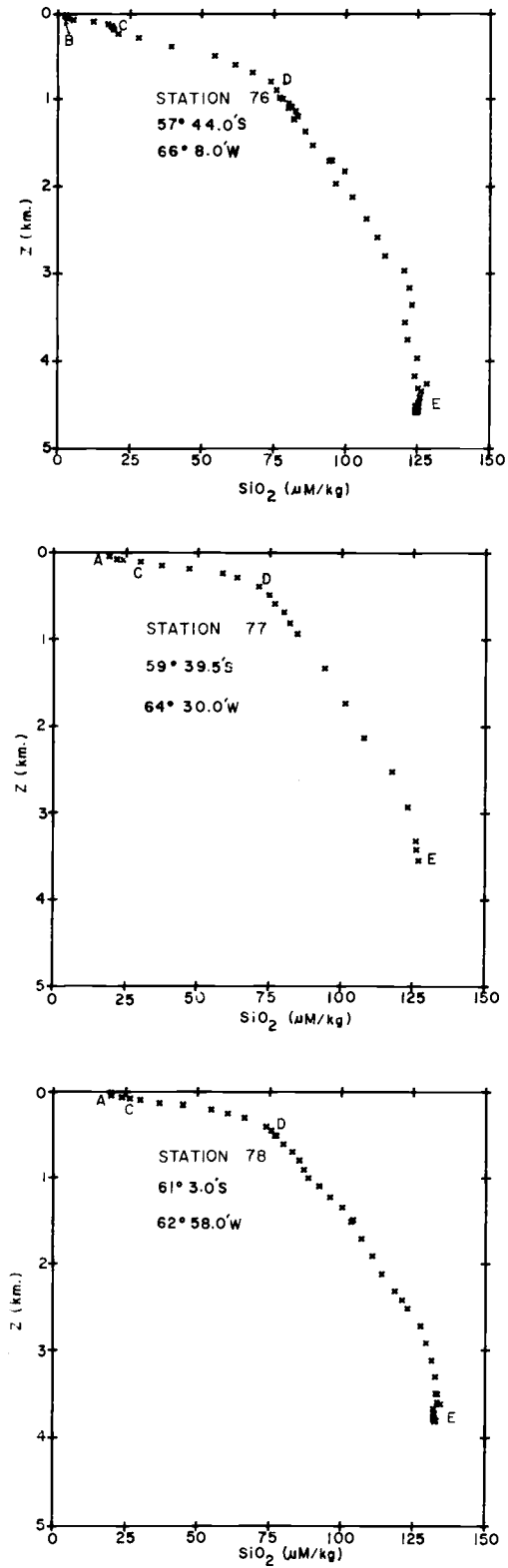


Figure IV-9. Silicate versus depth profiles for stations 76-78 in the Drake Passage with the cores of the various water masses lettered.

features, immediately apparent from the silicate data, are the increase in silicate with depth and the high surface depletion. The various water types correlate to widely varying silicate concentrations as seen in Table IV-1.

Table IV-1. Water type characterization in the Drake Passage for salinity, potential temperature, and silicate.

| Cumulative Water Type            | S<br>(‰)    | $\theta$<br>(°C) | Silicate<br>( $\mu\text{M}/\text{kg}$ ) |
|----------------------------------|-------------|------------------|---|
| A Antarctic Surface Water        | 33.75-33.85 | 1.0-2.0          | 10-20                                   |
| B Warmed Antarctic Surface Water | 33.90-34.00 | 4.0-5.0          | 0-5                                     |
| C Intermediate Antarctic Water   | 33.90-34.05 | -1.0-0.0         | 15-35                                   |
| D Transition Water               | 34.64-34.69 | 2.0              | 80-85                                   |
| E Bottom Water                   | 34.69-34.71 | 0-1.0            | 125-135                                 |

The wide variation in silicate concentrations between the water types suggests the potential for silicate to be a valuable tool to augment  $\theta$ , S, and  $\text{O}_2$  in examining subsurface circulation in the Southern Ocean.

Western basin data was also plotted as a function of  $\sigma_\theta$  in an attempt to update the classical work of Redfield (1942) using GEO-SECS data. By the use of  $\sigma_\theta$ , free movement by lateral mixing or flow is along horizontal lines and correlation of the distribution of any component of seawater with potential density is apparent. Plots of depth,  $\text{O}_2$ , AOU, silicate,  $\text{PO}_4$ ,  $\text{PO}_{4(\text{p})}$ ,  $\text{NO}_3$ , and  $\text{NO}_{3(\text{p})}$  were

constructed against  $\sigma_\theta$  for the western basins of the Atlantic (Figs. IV-10 to IV-17). In these diagrams, the AABW is centered near a  $\sigma_\theta$  of 27.88 and it is present immediately above the ocean bottom in the south. Silicate indicates some influence of AABW as far north as 45°N. AAIW can be seen as a tongue of high nutrient water between a  $\sigma_\theta$  of about 27.2-27.5 in the various nutrient diagrams. The NADW extends southward between the AAIW and AABW with  $\sigma_\theta$  from 27.8-27.9. At latitudes greater than 60°N a dense water of  $\sigma_\theta$  larger than 28.0 is shown. This is Lower North Atlantic Deep Water with high salinity and it is shown as being below AABW proceeding southward. Since AABW is actually denser in the environment of the high pressures of the ocean depths, the apparent distribution on the  $\sigma_\theta$  diagrams at great depths is inverted.

In addition to the nutrient, oxygen, and depth plots, the three derived values,  $\text{PO}_{4(p)}$ ,  $\text{NO}_{3(p)}$ , and AOU calculated from Redfield's ratio are plotted against  $\sigma_\theta$ . The AOU plots show a close inverse correlation to the  $\text{O}_2$ . Two cores of high AOU are seen on either side of the equator, due to the lateral transport of high AOU water from the regions of high productivity near the coast of Africa. These regions of highest biochemical oxidation occur near 7°N and 7°S at approximately 500 m depth. The lower levels of AOU are seen to correlate to the area of NADW influence while higher AOU is seen in waters of Southern Ocean origin.

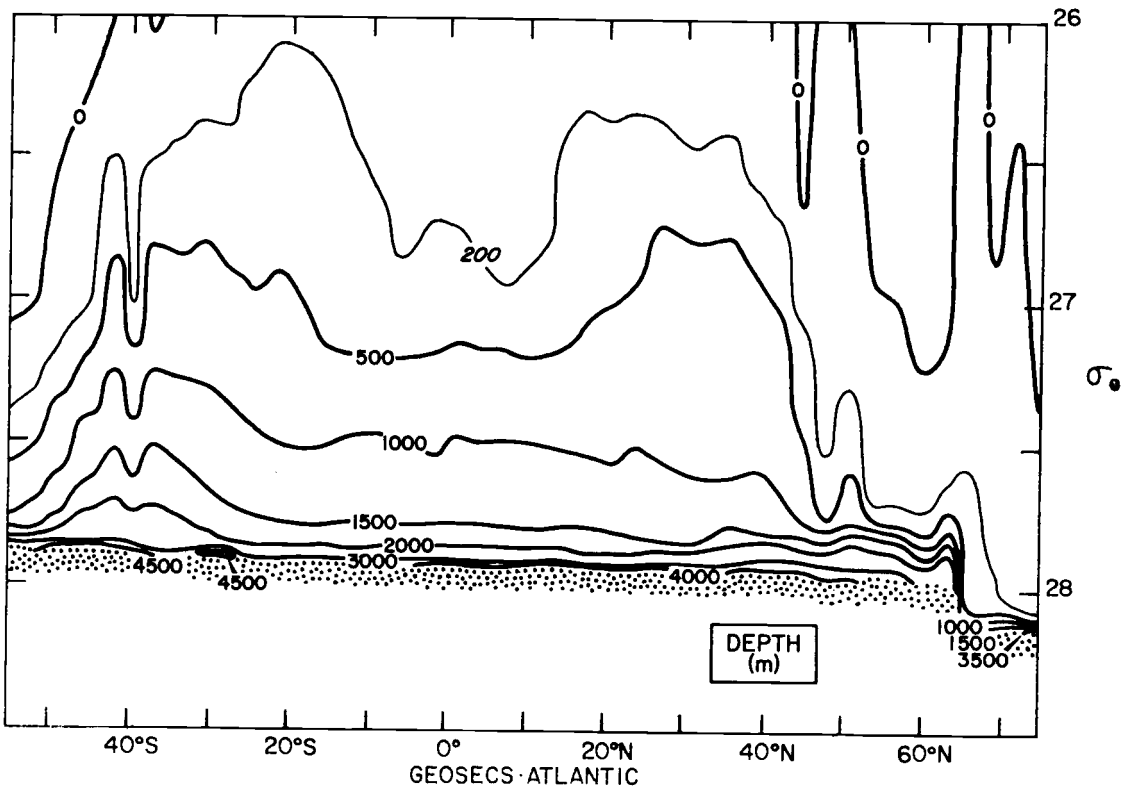


Figure IV-10. Depth to  $\sigma_\theta$  relationship in the western Atlantic.

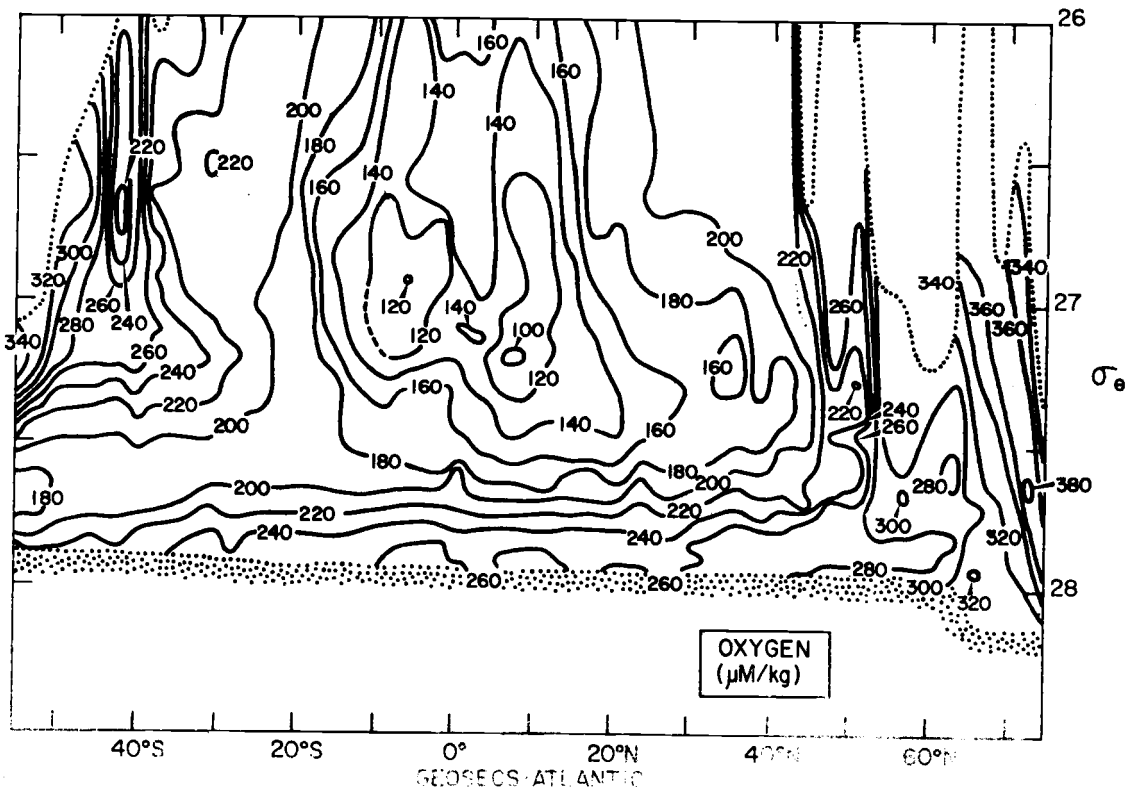


Figure IV-11. Oxygen to  $\sigma_\theta$  relationship in the western Atlantic.

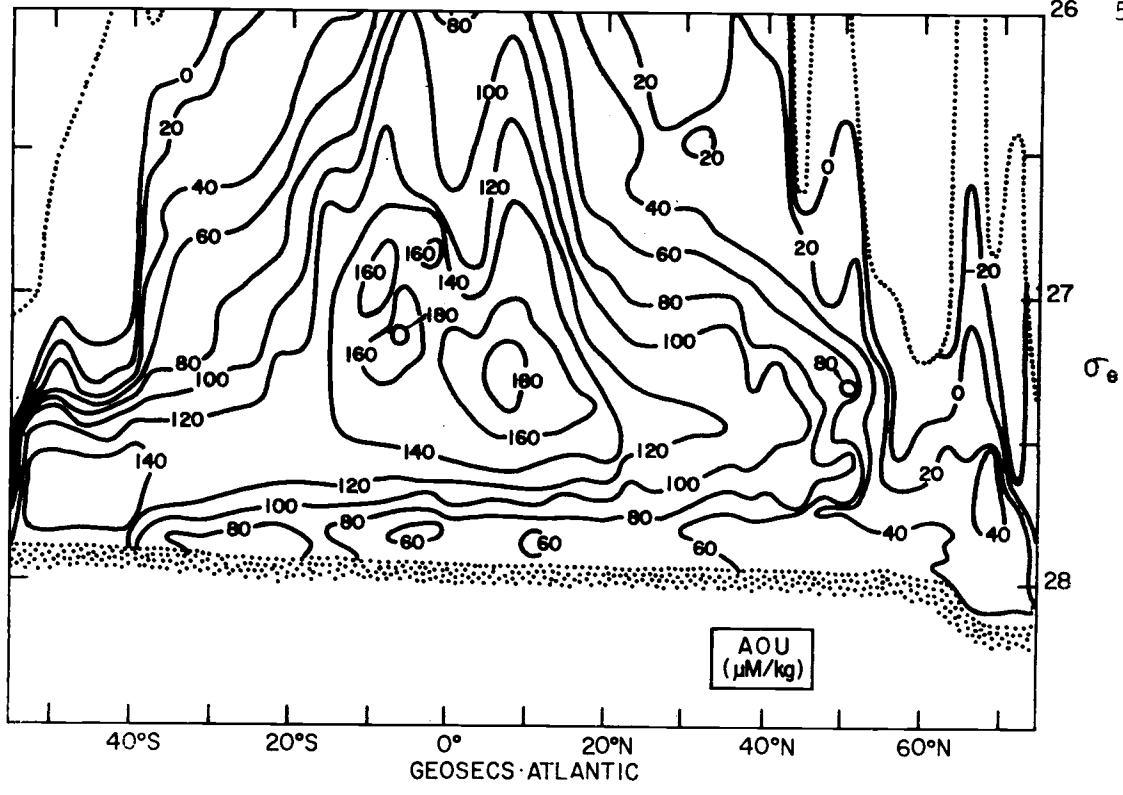


Figure IV-12. AOU to  $\sigma_\theta$  relationship in the western Atlantic.

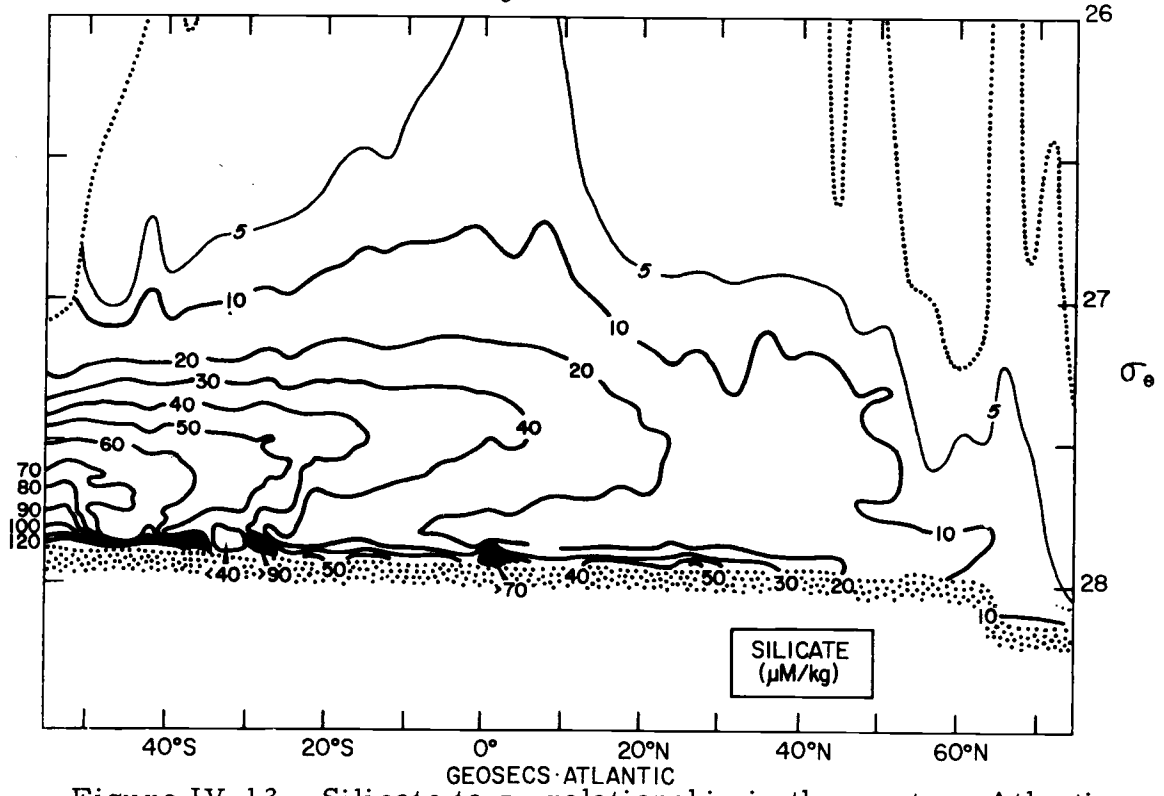


Figure IV-13. Silicate to  $\sigma_\theta$  relationship in the western Atlantic.

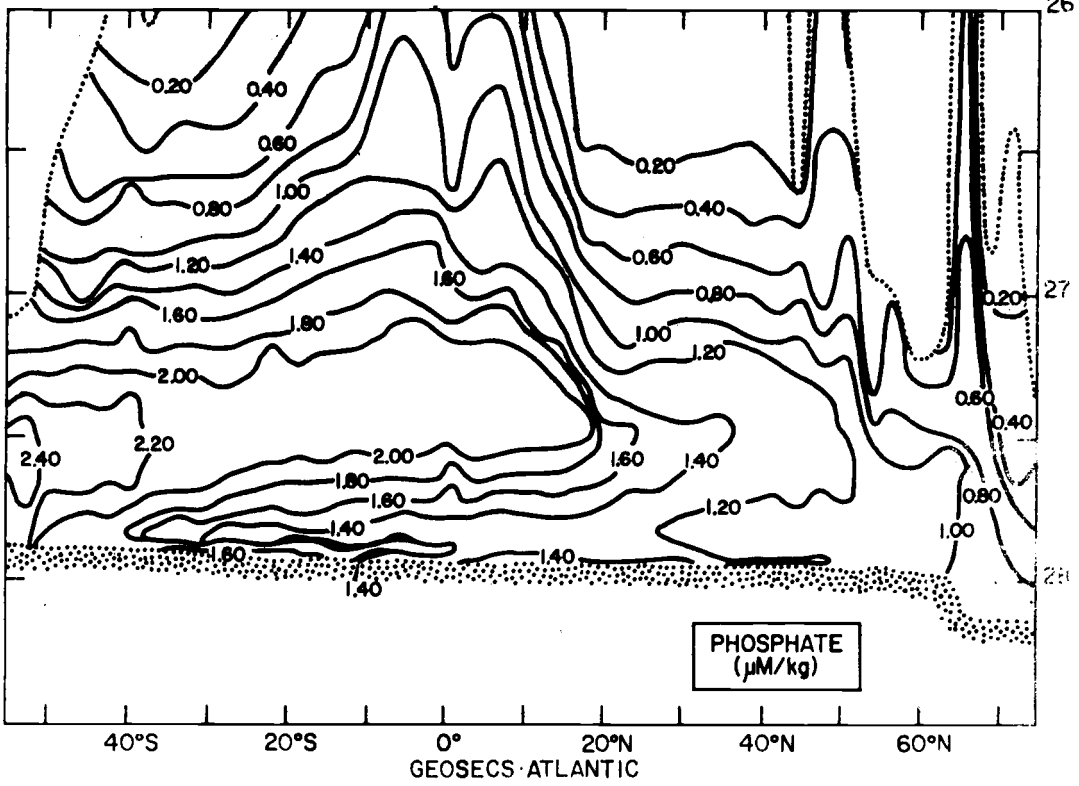


Figure IV-14. Phosphate to  $\sigma_\theta$  relationship in the western Atlantic.

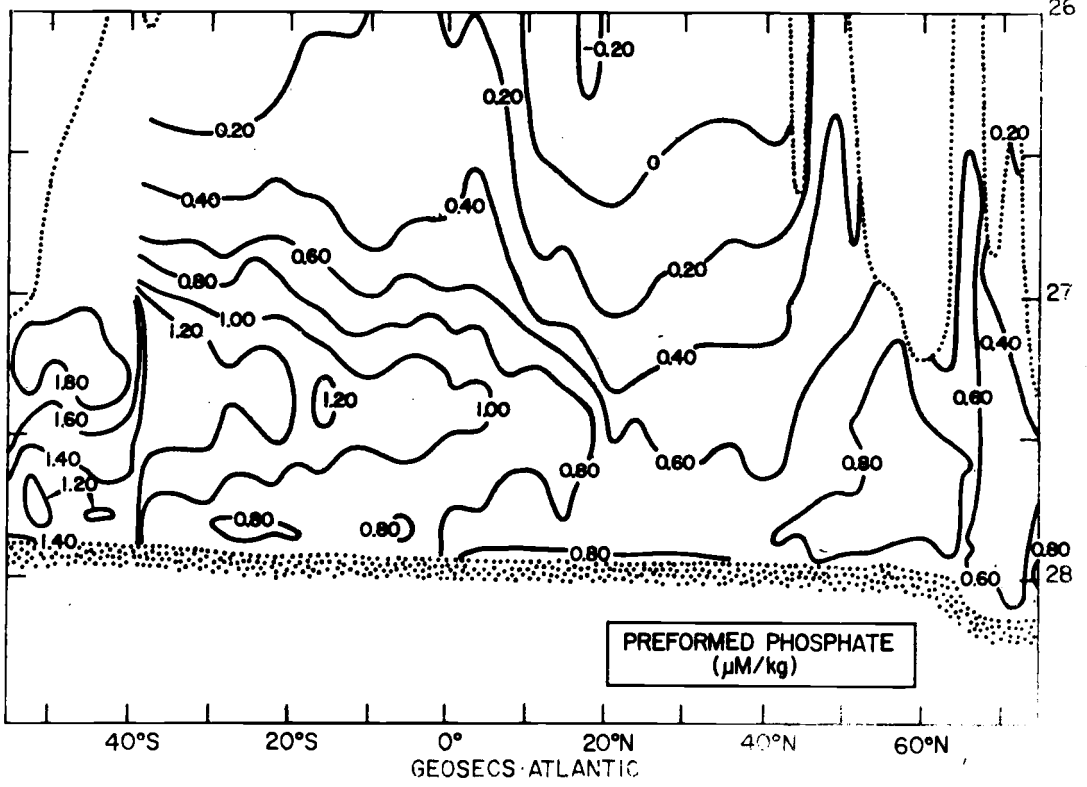


Figure IV-15. Preformed phosphate to  $\sigma_\theta$  relationship in the western Atlantic.

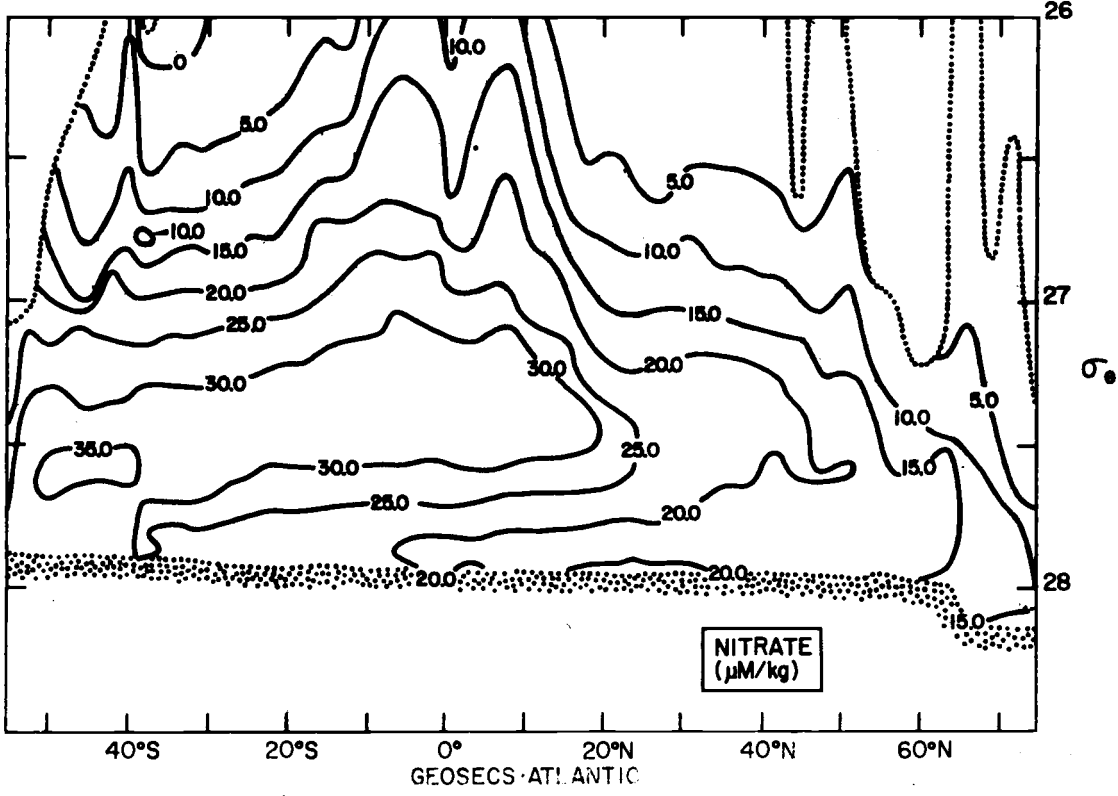


Figure IV-16. Nitrate to  $\sigma_\theta$  relationship in the western Atlantic.

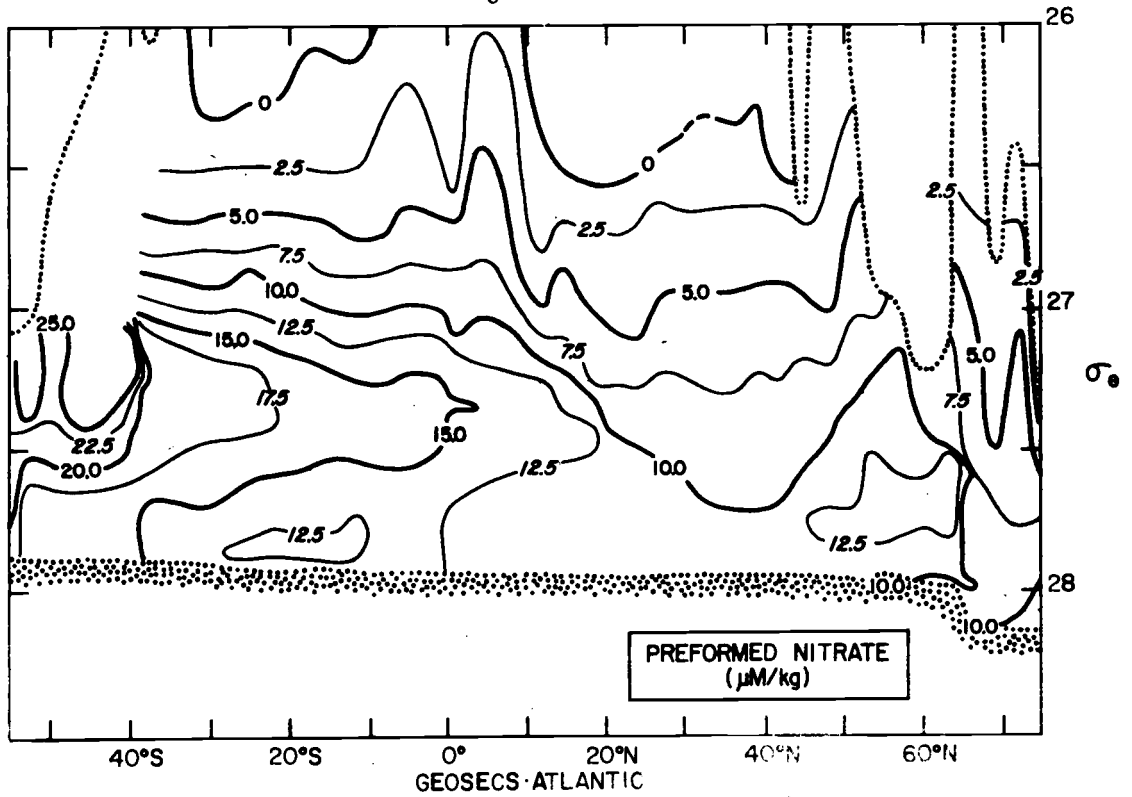


Figure IV-17. Preformed nitrate to  $\sigma_\theta$  relationship in the western Atlantic.



The preformed nutrient calculation shows NADW to be characterized by a core with about  $0.80 \mu\text{M}/\text{kg}$  for  $\text{PO}_{4(\text{p})}$  and  $12.5 \mu\text{M}/\text{kg}$  for  $\text{NO}_{3(\text{p})}$ . The AAIW at  $40^\circ\text{S}$  show levels of  $1.40$  and  $20.0 \mu\text{M}/\text{kg}$  for  $\text{PO}_{4(\text{p})}$  and  $\text{NO}_{3(\text{p})}$  respectively. This is attenuated northward reaching  $1.0$  and  $15.0 \mu\text{M}/\text{kg}$  for  $\text{PO}_{4(\text{p})}$  and  $\text{NO}_{3(\text{p})}$  near the equator. The AABW possesses a preformed nutrient maximum, but the use of  $\sigma_\theta$  is not clear in delineating this feature due to the density inversion for NADW and AABW. The degree of changes in preformed nutrient concentration suggests the extent of mixing between the various water masses due to the conservative nature of the preformed portion.

## V. NUTRIENT-OXYGEN RELATIONSHIPS IN THE ATLANTIC USING MULTIPLE LINEAR REGRESSION ANALYSIS

The water in the oceans of the world have routinely been classified into various water masses. The water masses have classically been defined by means of characteristic temperatures and salinities. Alternately, it is also possible to characterize these water masses by their varying chemical constituents. A method for differentiating water masses on the basis of their respective nutrient chemistry has been presented by Alvarez-Borrego (1973). The technique uses multiple linear regression to express  $O_2$  as a function of  $\theta$  or  $S$  and either  $PO_4$  or  $NO_3$ . The  $\theta$  or  $S$  variable represents the conservative portion of the  $O_2$  and nutrient, while the  $PO_4$  or  $NO_3$  term describes the non-conservative or biochemically altered fractions. When the differences between the actual  $O_2$  and that predicted by the model are plotted against a steadily increasing variable such as  $\theta$ , or  $S$  for Antarctic stations, a magnified picture of the variation in the preformed nutrient levels of the different water masses results.

The regression modeling also includes the added benefit of providing a means for examining the validity of the Redfield ratio for biochemical oxidation in the water masses in the water column. By applying the model to linear portions of the  $\theta$ - $S$  diagram or linear portions of the  $O_2$  residuals versus  $\theta$  or  $S$  diagram, a

confidence interval can be placed on the regression coefficients to check the consistency of the Redfield ratio for  $\Delta\text{O}_2:\Delta\text{PO}_4$  and  $\Delta\text{O}_2:\Delta\text{NO}_3$ .

This method is applied first to station 49 of GEOSECS Leg IV, off the coast of central Brazil, at  $7^\circ 12.6'S$ ,  $28^\circ 0.0'W$  (Figure V-1). This station was chosen as it shows the influence of seven distinct water types and is excellent for demonstrating the technique. Then stations 76-78 of Leg VIII, which make a north-south transect of the Drake Passage below South America, will be more intensively viewed with regression models. Station locations are  $57^\circ 44.0'S$ ,  $66^\circ 08.0'W$ ,  $59^\circ 39.5'S$ ,  $64^\circ 30.0'W$  and  $61^\circ 03.0'S$ ,  $62^\circ 58.0'W$  for stations 76-78 respectively (Figure V-2). These stations were occupied from December 31, 1972 to January 3, 1973.

Redfield (1934) proposed a biochemical oxidation ratio for the oceans of the world which relates the observed oxygen content to the extent of  $\text{O}_2$  consumption through oxidation. Redfield, Ketchum, and Richards (1963) altered this ratio slightly by considering more extensive planktonic data. The ratio of 276 atoms of oxygen consumed for each atom of phosphorus, 16 atoms of nitrogen, and 106 atoms of carbon regenerated is now generally accepted. Utilizing this ratio, the  $\text{PO}_4$  and  $\text{NO}_3$  concentrations can be divided into oxidative and preformed proportions. The preformed portion is conservative (Pytkowicz and Kester, 1966) and can be used to study physical

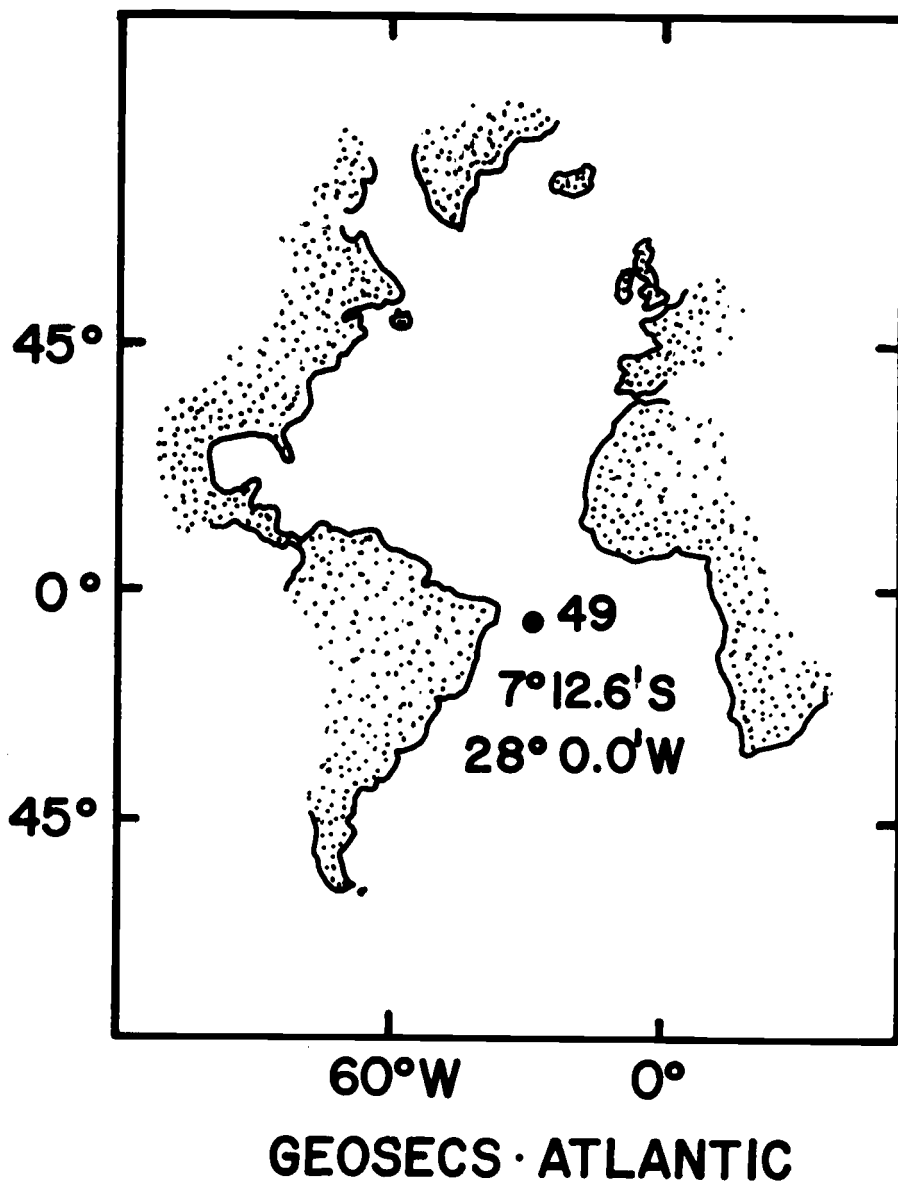


Figure V-1. GEOSECS station 49 location in the South Atlantic.

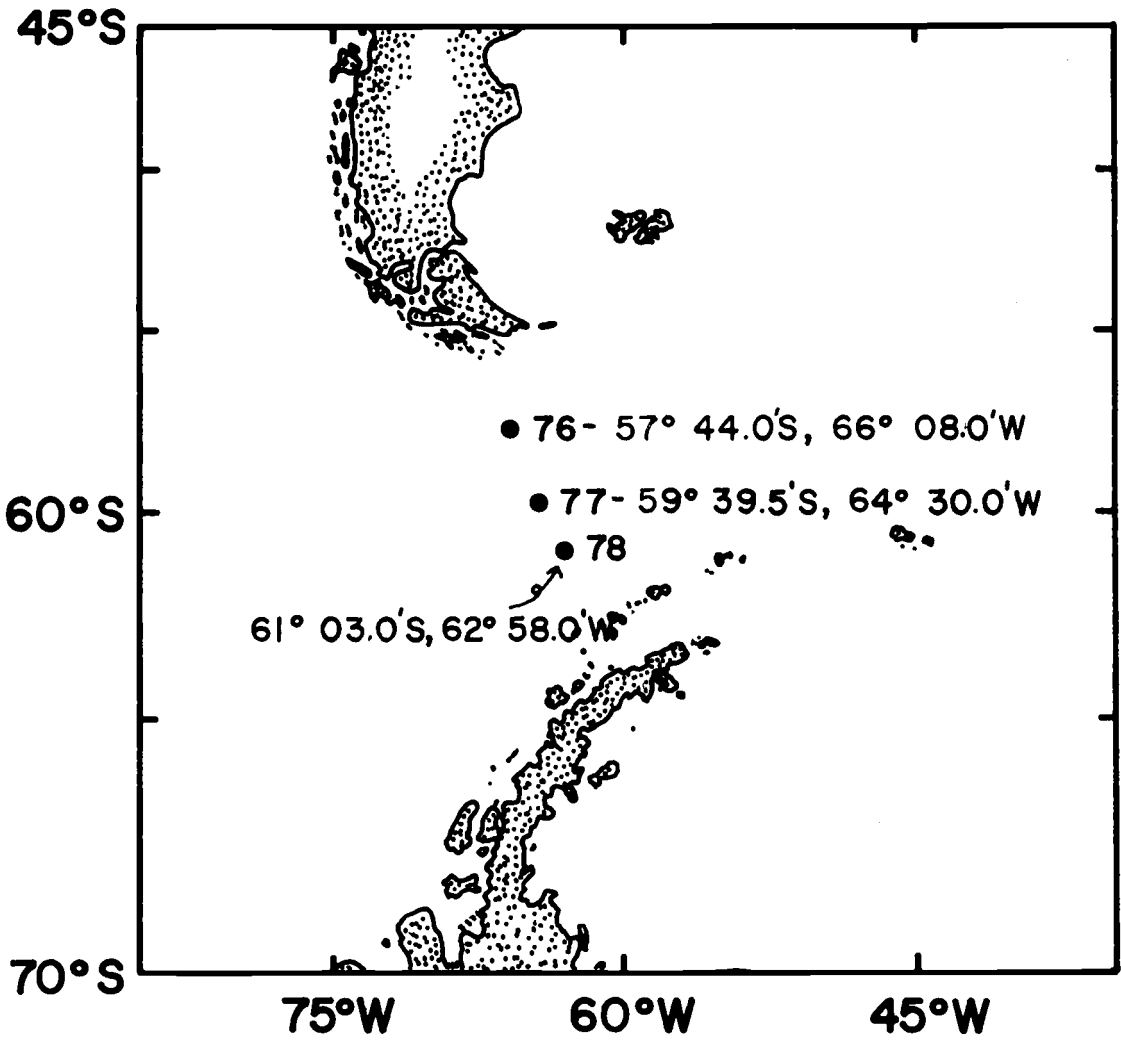


Figure V-2. GEOSECS station locations across the Drake Passage.

processes such as mixing and advection in the same manner as  $\theta$  and S. Redfield (1942) used this approach to describe and trace the various water masses throughout the Atlantic Ocean.

The theory behind the development of a statistical model of oxygen as a function of a conservative parameter, such as  $\theta$  or S, and  $\text{PO}_4$  or  $\text{NO}_3$  is derived from the Redfield ratio. Redfield (1934) and Redfield, Ketchum, and Richards (1963) defined the following concepts:

$$\text{AOU} = \text{O}_2' - \text{O}_2 \quad (\text{V-1})$$

$$\text{PO}_4 = \text{PO}_{4(\text{ox})} + \text{PO}_{4(\text{p})} \quad (\text{V-2})$$

$$138 \cdot \text{PO}_{4(\text{ox})} = \text{AOU} \quad (\text{V-3})$$

where AOU is the apparent oxygen utilization from biological oxidation,  $\text{O}_2'$  is the saturated dissolved oxygen level at the given  $\theta$  and S,  $\text{PO}_{4(\text{ox})}$  is the biologically oxidized portion of the phosphate concentration, and  $\text{PO}_{4(\text{p})}$  is the preformed  $\text{PO}_4$  defined as being entirely independent in origin from biological oxidation after the water type has left the surface. The constant 138 is from the Redfield ratio as a decrease of 138  $\mu\text{M}$  of  $\text{O}_2$  is predicted to correspond to an increase of 1  $\mu\text{M}$  of  $\text{PO}_4$ . Similar arguments can be used to develop a model for  $\text{NO}_3$ .

Manipulating algebraically, oxygen can be expressed as follows:

$$\text{O}_2 = -138 \cdot \text{PO}_4 + (\text{O}_2' + 138 \cdot \text{PO}_{4(\text{p})}) \quad (\text{V-4})$$

Since  $O_2'$  and  $PO_{4(p)}$  are not biologically altered and the variation of  $O_2'$  versus  $\theta$  is nearly linear, the  $(O_2' + 138 PO_{4(p)})$  segment can be approximated by

$$O_2' + a_1 \cdot PO_{4(p)} = a_0 + a_2 \cdot \theta^\circ C \quad (V-5)$$

For the GEOSECS stations in the Drake Passage, the presence of a near surface temperature minimum and a temperature maximum at a depth from 400-700 meters causes  $S$  to be a better parameter in the regression models. The  $O_2'$  is less dependent on  $S$  than  $\theta$ , but the steadily increasing nature of the  $S$  is better suited for graphical presentation. The high statistical correlation coefficient found with  $S$  in the model ( $> .90$ ) indicates that the use of  $S$  as the conservative parameter in the model is an acceptable alternative and does not introduce an undue degree of bias into the model. Therefore, substituting equation (5) with  $S$  instead of  $\theta$  into equation (4) and replacing  $-138$  by  $a_1$  yields the multiple linear regression model:

$$O_2 = a_0 + a_1 \cdot PO_4 + a_2 \cdot S\% \quad (V-6)$$

where  $O_2$  indicates a predicted oxygen value based on a salinity and phosphate value. This model can be fitted to the station data using a stepwise linear regression technique explained by Draper and Smith (1966, pp. 104-127) or with a computer program SIPS (Oregon State University, Department of Statistics, 1971).

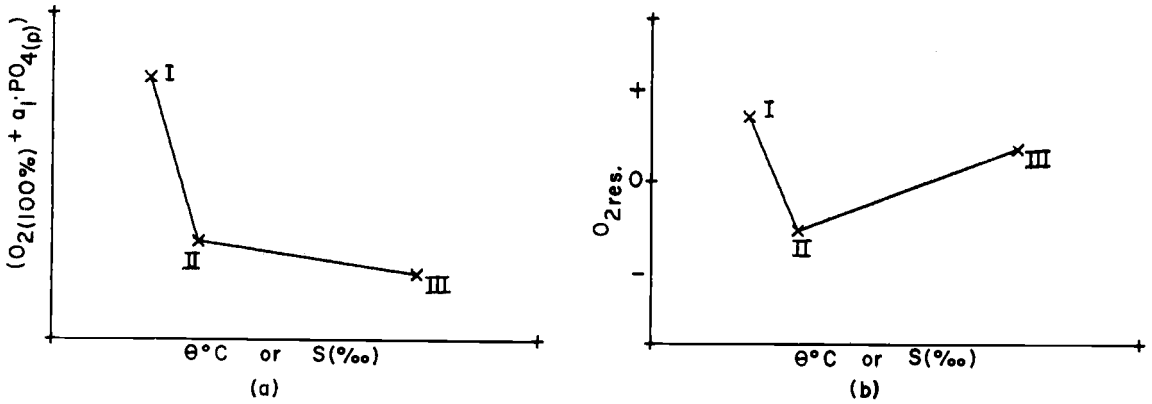


Figure V-3.  $(O_2(100\%) - a_1 \cdot PO_{4(p)})$  versus  $\theta^\circ C$  diagram (a) and  $O_{2 \text{ res}}$  versus  $\theta^\circ C$  diagram (b) of a hypothetical station.

When this model is applied to the field data, one assumption prohibits the predicted values of the model from being randomly scattered due only to analytical variation in the measurement of  $O_2$ ,  $PO_4$ , and  $S$ . This assumption is that  $(O_2' + PO_{4(p)})$  can be expressed linearly as a function of a conservative parameter such as  $\theta$  or  $S$ . Suppose that data from the whole water column at a particular station is composed of three water types I, II, and III displaying a nonlinear function of  $(O_2' + a_1 \cdot PO_{4(p)})$  versus  $\theta$  or  $S$  (Figure V-3a). A best linear fit of this data would generate an  $O_2$  residual plot (where  $O_2$  residual is defined as the observed  $O_2$  data minus the predicted  $O_2$  value of the model) versus  $\theta$  or  $S$  that accentuates this



nonlinear characteristic (Figure V-3b). If the preformed nutrient levels vary between different water types, this magnified pattern of the differences is seen on the  $O_2$  residual versus  $\theta$  or S diagrams. The water types present and their degree of influence at the station dictates the form of the residual plot. A plot of the  $O_2$  residuals versus  $\theta$  or S can then be used as a guide for identifying and tracing the water masses. For the stations in the Drake Passage, S is chosen for the conservative parameter when modeling the entire water column, while  $\theta$  is used for station 49.

An additional benefit of the derived model is present in the significance of the constant  $a_1$ . For the  $PO_4$  model,  $a_1$  corresponds to the  $\Delta O_2 : \Delta PO_4$  ratio. Similarly, a model with  $NO_3$  would correspond to the  $\Delta O_2 : \Delta NO_3$  ratio. Redfield's ratio predicts that 276 oxygen atoms are consumed to produce 16 atoms of nitrogen and 1 atom of phosphorus. This ratio was determined by analyzing a number of plankton species as to their relative proportions of carbon, nitrogen, and phosphorus. Redfield (1934) noted the variability of this ratio from species to species, but the averaged ratio appears to hold in the Northern Atlantic and Pacific Oceans where a statistical uniformity in composition is approximated (Alvarez-Borrego, 1973).

A statistical method can be used to test Redfield's ratio. The initial plot of the  $O_2$  res. versus S or  $\theta$  gives an indication of the water types present. Taking a linear portion from the  $O_2$  res. versus

S or  $\theta$  diagram and reapplying the model (equation V-6) should yield a random  $O_2$  residual distribution attributable only to random errors in the  $O_2$ ,  $PO_4$  or  $NO_3$ , and  $\theta^\circ C$  or S measurements. The random distribution indicates the model is statistically correct in modeling the data and 95% confidence intervals may be applied to the constants. The interval on the constant  $a_1$  will include -138 for  $PO_4$  and -138/16 (-8.63) for  $NO_3$  if Redfield's ratio holds.

For station 49, the results of the regression of  $\theta$  with  $PO_4$  or  $NO_3$  on the dependent variable  $O_2$  are:

$$O_2 = 452.97 - 9.84 \cdot \theta - 120.51 \cdot (PO_4) \quad (V-7)$$

$$O_2 = 449.79 - 10.22 \cdot \theta - 7.56 \cdot (NO_3) \quad (V-8)$$

where  $O_2$  is a predicted value from the model based on the independent variables  $\theta$  and  $PO_4$  or  $NO_3$ . The  $O_2$  residuals ( $O_{2 \text{ res}}$ ) range from -50 to +30  $\mu M/kg$  at station 49.

The plots of  $O_{2 \text{ res}}$  versus  $\theta$  show a clear dependency of the residuals on  $\theta$  (Figs. V-4 and V-5). Statistically this indicates that the model is not adequately describing the data. A statistically correct regression model would show only random scatter in the residual plots. The explanation for the nonrandom distribution of the residuals lies in the variable preformed nutrient proportions characteristic of the individual water masses. This orderly variation produces a

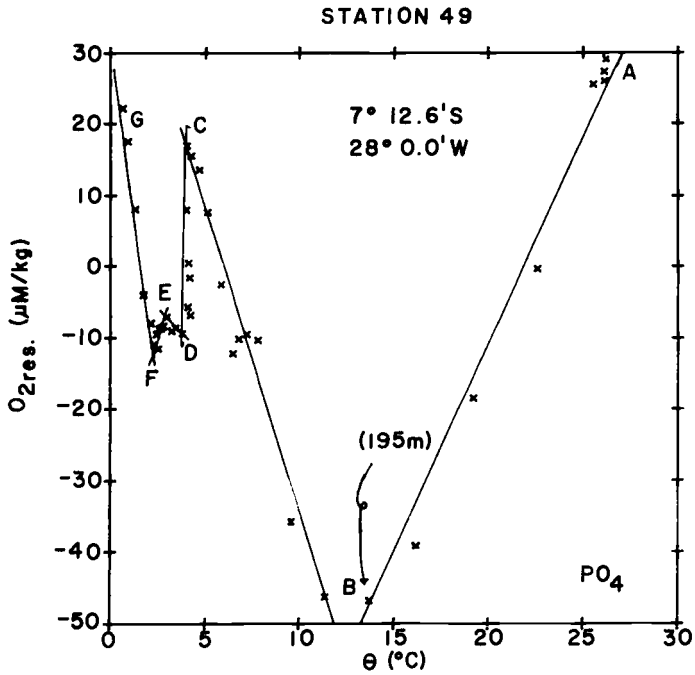


Figure V-4. Oxygen residuals versus potential temperature at station 49. PO<sub>4</sub> is the nutrient parameter.

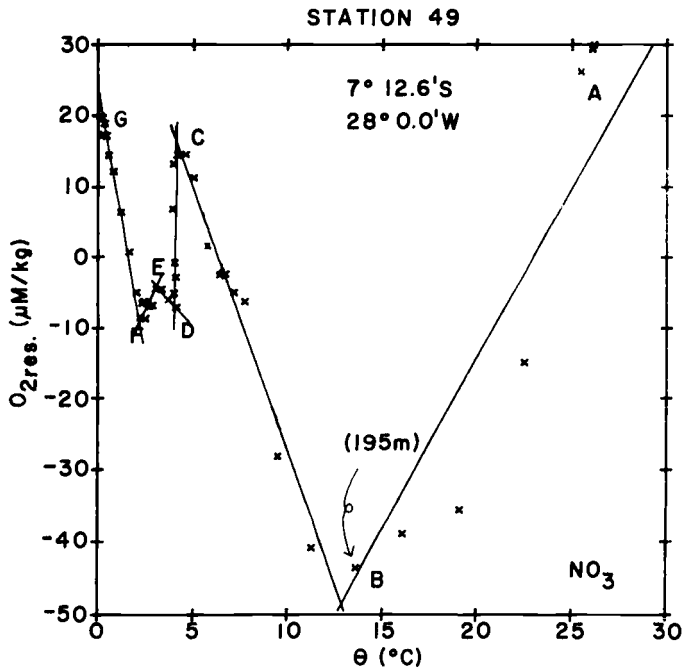


Figure V-5. Oxygen residuals versus potential temperature at station 49. NO<sub>3</sub> is the nutrient parameter.

pattern indicating the influence of seven water types in the water column marked A, B, C, D, E, F, and G in the  $O_2$  res versus  $\theta$  diagrams.

The  $\theta$ -S diagram for station 49 is shown in Figure V-6. In Figure V-7, an expansion of the bottom section of the  $\theta$ -S diagram below  $5^\circ\text{C}$  and between 34.5-35.0‰ S is shown to more clearly show water masses D, E, and F. The  $\theta$ -S diagrams are consistent with the residual plots in showing the various water masses except for water type B which is not as readily apparent in the  $\theta$ -S diagram. This water type will be discussed later.

As an additional tool for studying the water masses at station 49, preformed nutrient versus potential temperature plots were constructed (Figures V-8 and V-9). Again, the influence of the seven water types seen in the  $O_2$  res versus  $\theta$  diagrams are suggested in preformed nutrients versus potential temperature plots, although not always as clearly as in the  $O_2$  res versus  $\theta$  diagrams.

Having used three different methods to picture the water masses in the water column at station 49, consistent results are seen, except that the influence of water type B is not seen in the  $\theta$ -S diagram. The water masses encountered at station 49 can be identified by the  $\theta$ -S relationships in the manner of Sverdrup, Johnson and Fleming (1942) and Neumann and Pierson (1966). In addition, these same water masses can be described in terms of their preformed nutrient content as seen in Table V-1.

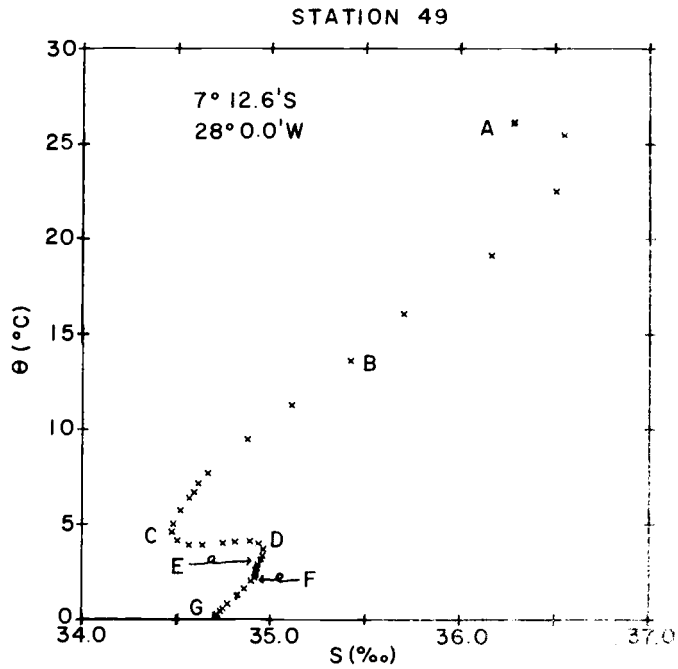


Figure V-6.  $\theta$ -S diagram for station 49.

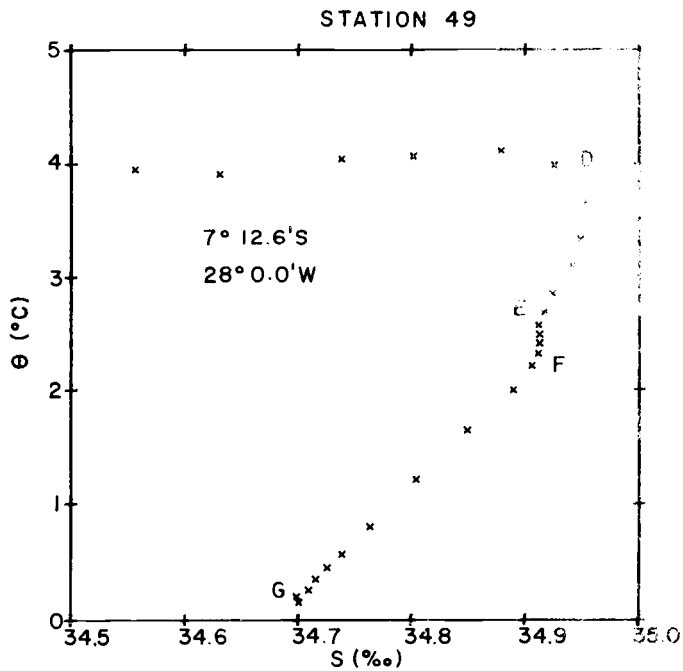


Figure V-7. Expanded  $\theta$ -S diagram for  $\theta = 0$ - $5^{\circ}$ C and  $S = 34.5$ - $35.0$ ‰ region of station 49.

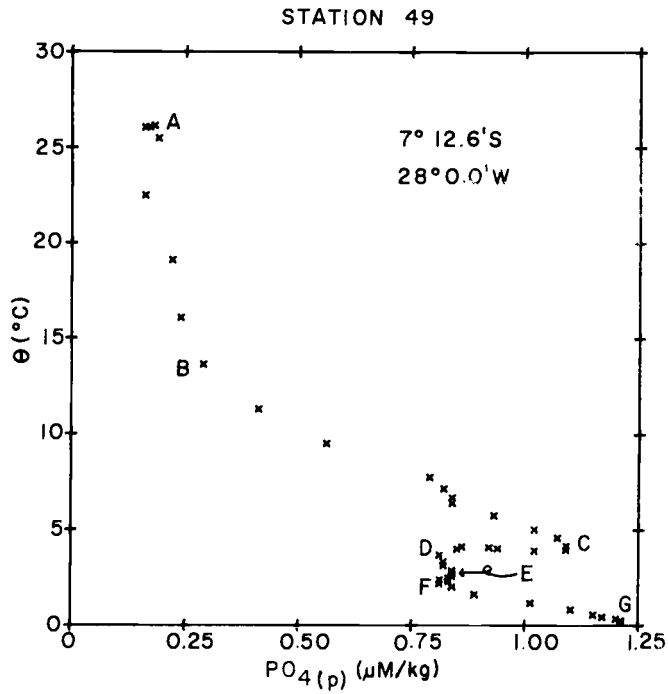


Figure V-8.  $\theta$ - $\text{PO}_4(\text{p})$  diagram at station 49.

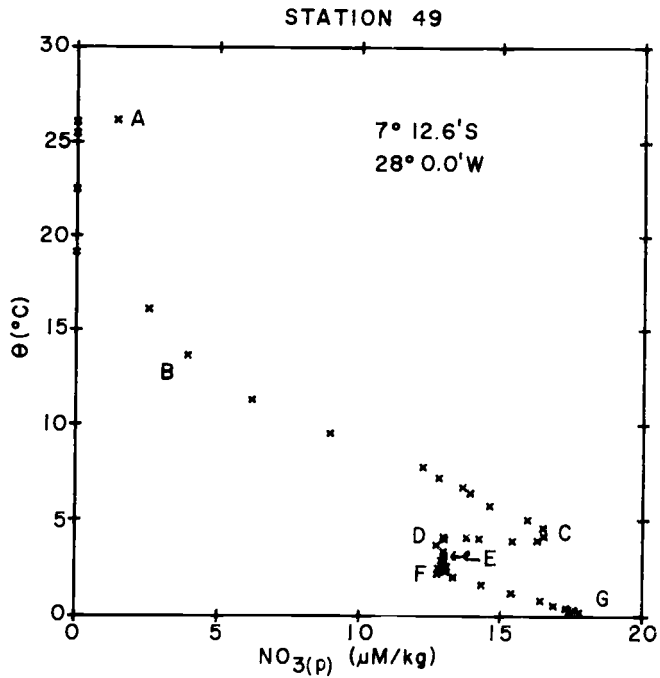


Figure V-9.  $\theta$ - $\text{NO}_3(\text{p})$  diagram at station 49.

Table V-1. Characterization of water masses at station 49 by  $\theta$ , S,  $\text{PO}_{4(p)}$  and  $\text{NO}_{3(p)}$ .

| Water Mass | Name                             | $\theta$ | S     | $\text{PO}_{4(p)}$ | $\text{NO}_{3(p)}$ |
|------------|----------------------------------|----------|-------|--------------------|--------------------|
| A          | Surface Water                    | 26.1     | 36.20 | 0.1                | 0.0                |
| B          | Subsurface Water                 | 13.6     | 35.41 | 0.3                | 3.9                |
| C          | Antarctic Intermediate Water     | 4.5      | 34.47 | 1.09               | 16.5               |
| D          | Upper North Atlantic Deep Water  | 3.7      | 34.95 | 0.81               | 12.7               |
| E          | Middle North Atlantic Deep Water | 2.7      | 34.92 | 0.84               | 13.0               |
| F          | Lower North Atlantic Deep Water  | 2.3      | 34.91 | 0.82               | 12.8               |
| G          | Antarctic Bottom Water           | 0.2      | 34.70 | 1.21               | 17.7               |

The variation in the preformed nutrient levels for the three types of North Atlantic Deep Water are quite small, but  $\theta$ -S diagrams substantiates their presence. The Upper North Atlantic Deep Water shows the influence of the Mediterranean waters causing the higher temperature and salinity and decreased preformed nutrients. The Middle North Atlantic Deep Water is thought to originate near Greenland while the Lower North Atlantic Deep Water may better be called a Subarctic Bottom Water merged with Arctic Bottom Water (Neumann and Pierson, 1966). The fact that these various water types of only minimal variations can be separated thousands of kilometers from their origin indicates the strong predominance of lateral transport over those of vertical mixing in the Atlantic.

In addition to the water masses apparent by both multiple linear regression residual plots and the  $\theta$ -S diagram, there is seen the influence of a water type B not apparent in the  $\theta$ -S relationship. This water type is distinguished by large negative  $O_2$  residual values. This means that the predicted  $O_2$  value, based on  $\theta$  and either  $PO_4$  or  $NO_3$  data, is considerably higher than the observed value. Therefore, this water type has shown a higher  $O_2$  depletion than predicted by the regression model. The likely source for this oxygen depletion is biochemical oxidation.

At station 49 in the South Atlantic, total organic carbon (TOC) was also measured. The distribution of TOC in the water column appears to be divided into two segments. The first portion shows a rapid decrease with depth from the maximum values ( $72 \mu\text{M}/\text{kg}$ ) found at the surface. The second segment, comprising the majority of the water column, maintains a small range of constant TOC values ( $35\text{-}41 \mu\text{M}/\text{kg}$ ) with depth. Since the precision of the analysis is  $4 \mu\text{M}/\text{kg}$ , this bottom portion can be considered as unvarying. Barber (1968) has demonstrated that the organic carbon present in the deep waters of the oceans is composed of refractory compounds that are very slowly oxidized. Plotting  $\theta$  versus TOC in Figure V-10 shows the two segments clearly. A two phase linear regression (Daly, 1974) was calculated for the two segments with intersection at approximately  $11.5^\circ\text{C}$ . This temperature correlates very well with the location of



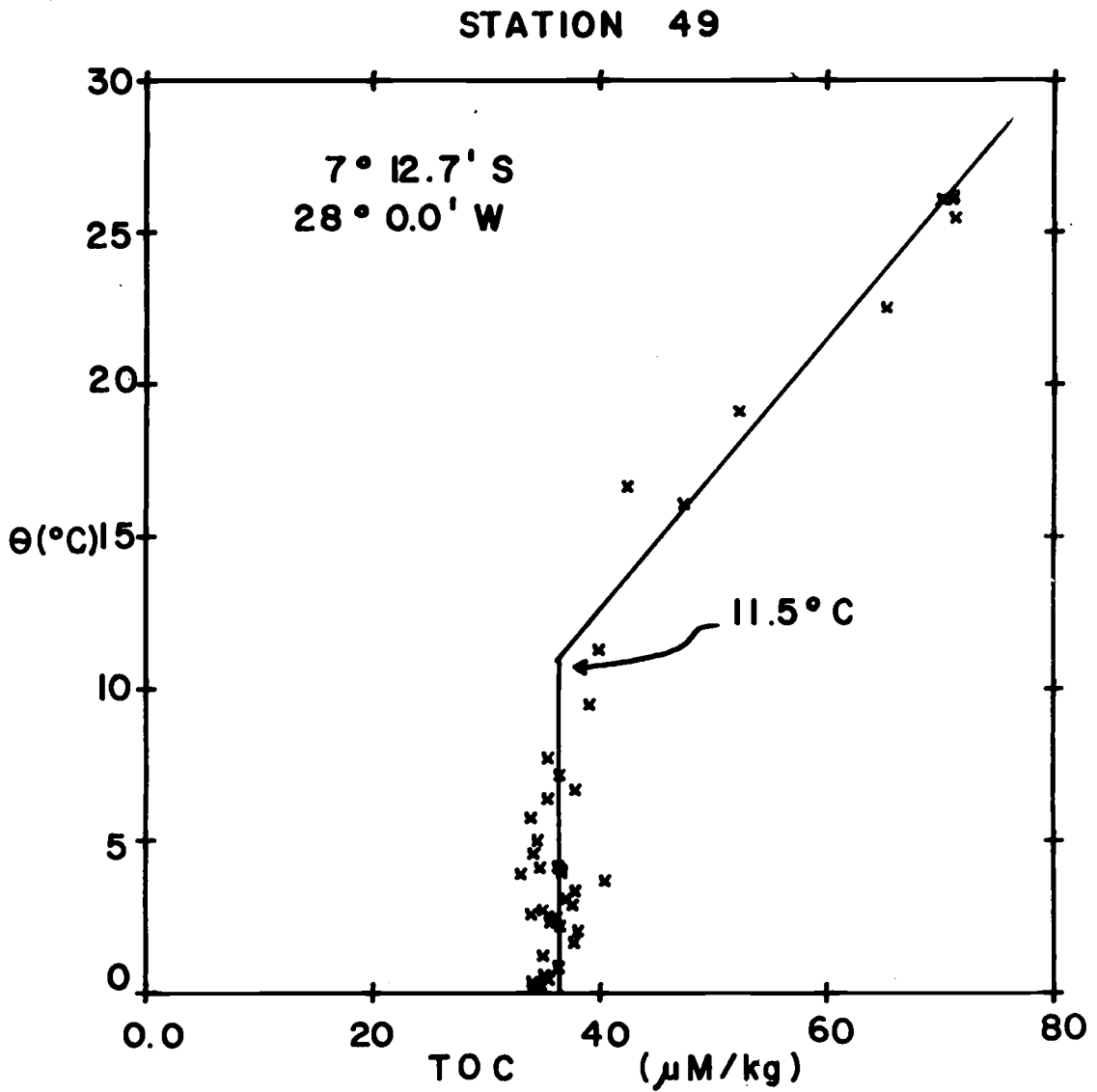


Figure V-10. TOC as a function of  $\theta$  with the best fit two phase regression and intersection point.

water type B in the  $O_2$  <sub>res</sub> versus  $\theta$  diagrams in Figures V-4 and V-5.

Menzel and Ryther (1968) indicate that appreciable decomposition of organic matter occurs at depths no greater than 400 meters. The subsurface water type B is centered at approximately 200 meters. Also, the TOC data suggests that at near 200 meters the more easily oxidizable portion of the organic carbon has been decomposed. This water type is probably the lower limit of the region in the water column where the majority of the biochemical oxidation takes place. This would result in a water type relatively high in  $PO_4$  and  $\theta$ , but low in  $PO_{4(p)}$ , which would yield large negative values for the  $O_2$  residuals in the multiple linear regression model.

To test Redfield's ratio for  $\Delta O_2 : \Delta PO_4$  and  $\Delta O_2 : \Delta NO_3$ , linear portions of the  $O_2$  <sub>res</sub> vs.  $\theta$  plots were chosen. The model was then calculated again. Residual plots showed a random distribution indicating the model was statistically describing the data. Scatter was due only to analytical deviations in the measurement of  $O_2$ ,  $\theta$ ,  $PO_4$ , and  $NO_3$ . The three portions of North Atlantic Deep Water were included as one segment as insufficient data points existed for analysis of each portion. The results of the regression with 95% confidence levels for station 49 are given along with the depth, the coefficient of determination  $R^2$ , and the residual degrees of freedom (n-p-1) (Table V-2).

Table V-2. Regression equations of O<sub>2</sub> on PO<sub>4</sub> and θ°C and on NO<sub>3</sub> and θ°C for linear segments of the O<sub>2</sub> res -θ plot for station 49.

| Depth Range<br>(m) | Regression Equations (with 95% confidence intervals)                            | R <sup>2</sup> | n-p-1 |
|--------------------|---|----------------|-------|
| 0-195              | O <sub>2</sub> = (254.04±114.74) - (1.23±4.32)θ - (96.09±45.02)PO <sub>4</sub>  | .995           | 5     |
|                    | O <sub>2</sub> = (120.76±78.45) + (3.57±3.12)θ - (2.83±1.96)NO <sub>3</sub>     | .979           | 5     |
| 256-909            | O <sub>2</sub> = (634.33±74.80) - (23.17±2.75)θ - (169.92±28.15)PO <sub>4</sub> | .989           | 7     |
|                    | O <sub>2</sub> = (533.45±64.79) - (19.34±2.40)θ - (8.36±1.54)NO <sub>3</sub>    | .986           | 7     |
| 1009-3478          | O <sub>2</sub> = (410.74±7.78) - (10.89±2.78)θ - (93.53±6.98)PO <sub>4</sub>    | .995           | 13    |
|                    | O <sub>2</sub> = (417.91±8.75) - (11.24±2.99)θ - (6.22±.50)NO <sub>3</sub>      | .994           | 13    |
| 3690-5513          | O <sub>2</sub> = (297.43±61.05) + (5.14±11.63)θ - (32.64±28.50)PO <sub>4</sub>  | .999           | 7     |
|                    | O <sub>2</sub> = (315.59±74.63) + (3.37±12.78)θ - (2.72±2.31)NO <sub>3</sub>    | .999           | 7     |

For the first kilometer, the Redfield ratio holds at a 95% confidence interval or is extremely close with the exception of the  $\text{NO}_3$  coefficient for 0-195 m. The apparent lack of inorganic nitrate oxidation can be satisfactorily explained due to the limiting nature of  $\text{NO}_3$ . No  $\text{NO}_3$  or  $\text{NO}_2$  is seen in the upper 100 meters and unoxidized nitrogen compounds such as ammonia and urea decrease the coefficient of oxygen change due to nitrate regeneration near the surface. The inconsistency of the Redfield proportion below one kilometer is much harder to justify. The segment from 1009-3478 m did include grouping the different North Atlantic Deep Water types which might bias the model enough to yield the slightly lower ratios of -94:1 for  $\Delta\text{O}_2:\Delta\text{PO}_4$  and -6.22:1 for  $\Delta\text{O}_2:\Delta\text{NO}_3$ . No such justifications exist for the bottom segment which would explain the very low ratios found by the regression equation. Possible explanations for this variation in the Redfield ratio are discussed later for the Drake Passage stations.

Multiple linear regression analysis on station 49 accurately distinguishes the water types present at the station plus indicates an additional near surface water type associated with the lower limit of rapid oxidation of organic material. The separation of the water types influencing station 49 is due to variations in  $\text{PO}_{4(p)}$  and  $\text{NO}_{3(p)}$  in the various water types (Figure V-11). A test on the Redfield ratio at station 49 indicates that while the ratio holds for surface and intermediate waters, deep and bottom waters appear to break down.

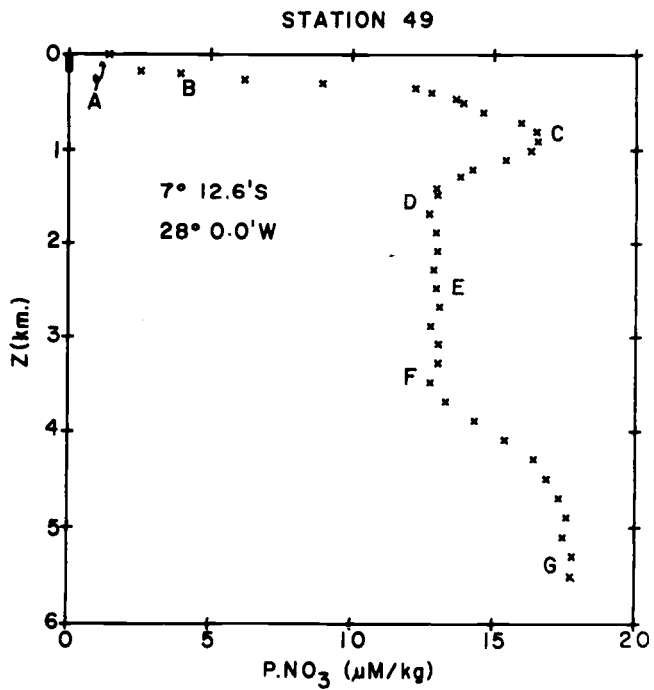
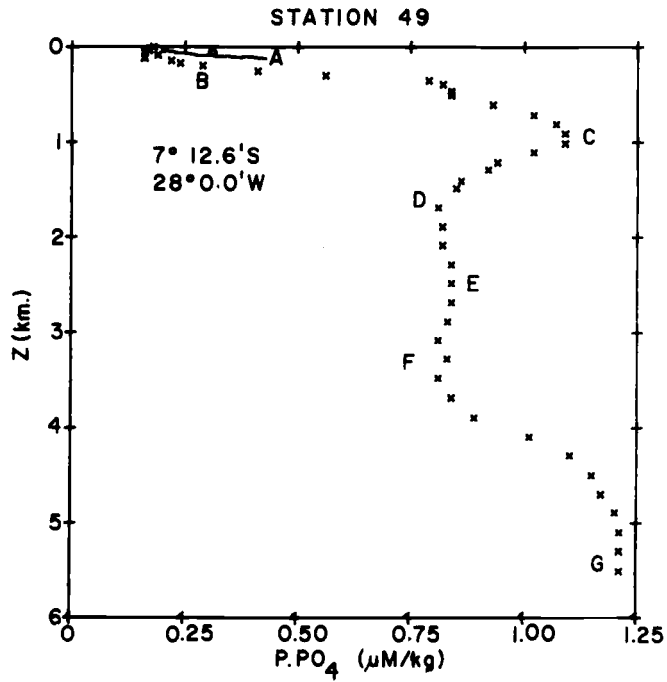


Figure V-11. Preformed nutrients versus depth at station 49.

As the GEOSECS nutrient and oxygen data has been demonstrated to be of the quality necessary for multiple linear regression analysis, a further study involving a series of stations in the Atlantic can be considered. Three stations (76-78) in the Drake Passage will be viewed with the regression modeling technique.

The multiple linear regression model was applied to the three stations in the Drake Passage with the dependent variable  $O_2$  being expressed as a function of  $PO_4$  or  $NO_3$  and S. The results for each station and for a regression applied to all the data from the three stations combined are:

Station 76 ( $57^\circ 44.0'S$ ,  $66^\circ 08.9'W$ )

$$O_2 = 5003.50 - 134.27 \cdot (S) - 71.67 (PO_4) \quad (V-9)$$

$$O_2 = 4039.40 - 103.06 \cdot (S) - 8.35 (NO_3) \quad (V-10)$$

Station 77 ( $59^\circ 39.5'S$ ,  $64^\circ 30.0'W$ )

$$O_2 = 4724.80 - 121.60 \cdot (S) - 144.53 \cdot (PO_4) \quad (V-11)$$

$$O_2 = 4458.60 - 112.96 \cdot (S) - 10.73 \cdot (NO_3) \quad (V-12)$$

Station 78 ( $61^\circ 3.0'S$ ,  $62^\circ 58.0'W$ )

$$O_2 = 4457.20 - 113.94(S) - 140.83(PO_4) \quad (V-13)$$

$$O_2 = 4278.60 - 107.84(S) - 10.44(NO_3) \quad (V-14)$$

All three stations together

$$O_2 = 4940.00 - 131.35(S) - 87.34(PO_4) \quad (V-15)$$

$$O_2 = 4277.40 - 109.38(S) - 8.86(NO_3) \quad (V-16)$$

The  $O_2$  residuals range from  $-45 \mu\text{M}/\text{kg}$  at station 76 to  $+30 \mu\text{M}/\text{kg}$  at station 78.

The  $O_2$  res versus S plots for the stations in the Drake Passage show the influence of five water types. These are labeled A, B, C, D, and E on the  $O_2$  res -S plots (Figure V-12). This is consistent with the observed  $\theta$ -S diagrams for these stations (Figure V-13). The variations exhibited in the  $O_2$  res -S plots are due to variations in the preformed nutrient levels of the various water types influencing each station. The preformed nutrient distribution,  $\theta$ , and S (Table V-3) show the variation found in these water types which produce the systematic residual pattern, although again not as clearly apparent as in the  $O_2$  res -S diagram.

Table V-3. Characteristic S,  $\theta$ ,  $\text{PO}_4(\text{p})$  and  $\text{NO}_3(\text{p})$  for the water types present in the Drake Passage.

| Cumulative Water Type            | S<br>(‰)    | $\theta$<br>(°C) | $\text{PO}_4(\text{p})$<br>( $\mu\text{M}/\text{kg}$ ) | $\text{NO}_3(\text{p})$<br>( $\mu\text{M}/\text{kg}$ ) |
|----------------------------------|-------------|------------------|--|--|
| A Antarctic Surface Water        | 33.75-33.85 | 1.0-2.0          | 1.6-1.7  | 25-26  |
| B Warmed Antarctic Surface Water | 33.90-34.00 | 4.0-5.0          | 1.35   | 23.5   |
| C Intermediate Antarctic Water   | 33.90-34.05 | -1.0-0.0         | 1.8  | 26-27  |
| D Transition Water               | 34.64-34.69 | 2.0              | 1.0  | 15   |
| E Bottom Water                   | 34.69-34.71 | 0.0-1.0          | 1.15-1.20  | 16-17  |

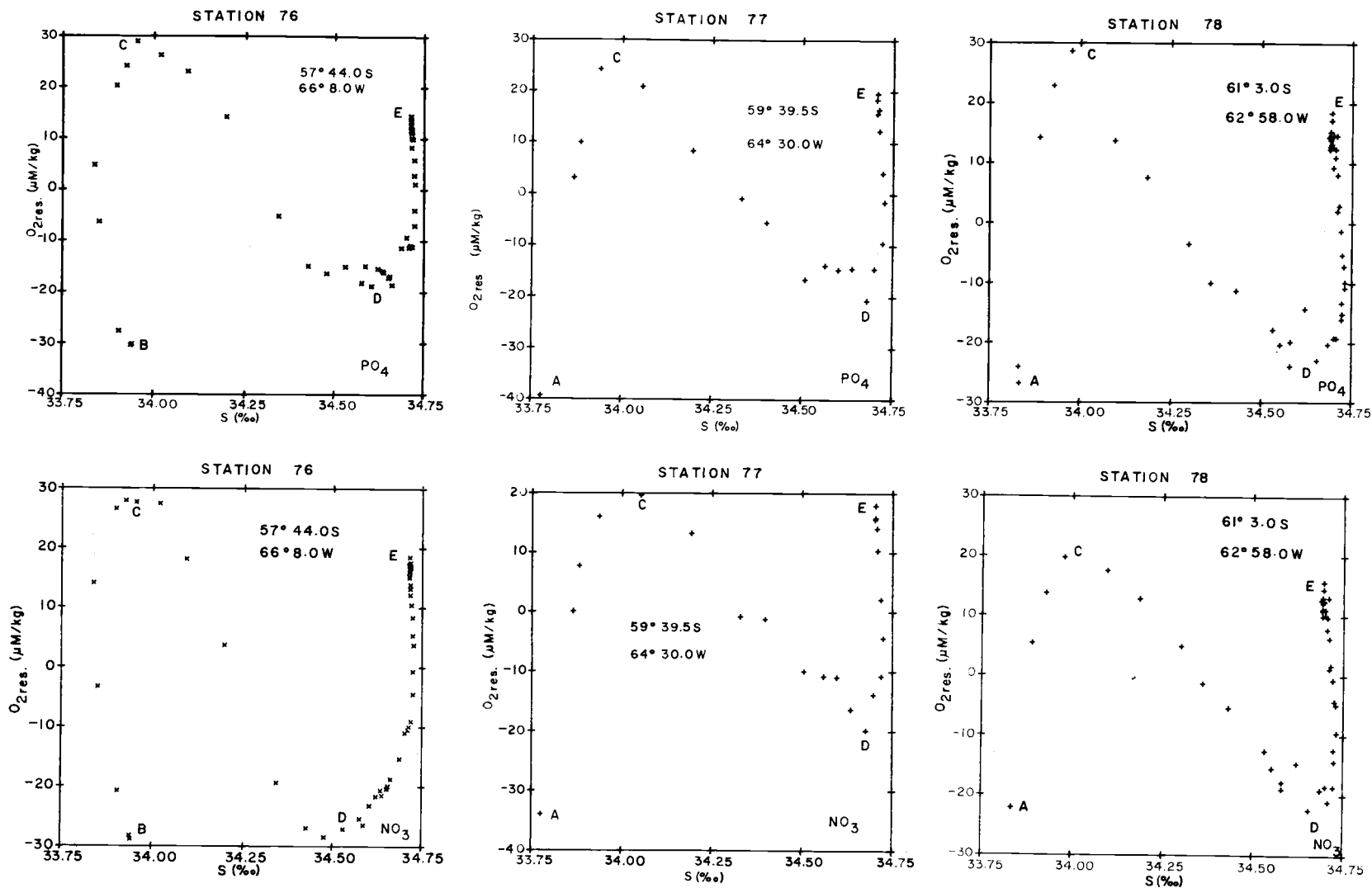


Figure V-12. Oxygen residuals versus salinity from the regression model using S and  $PO_4$  or  $NO_3$  as independent variables for stations 76-78 in the Drake Passage.



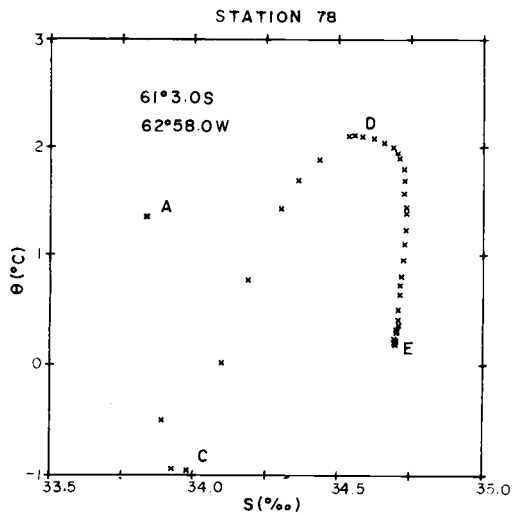
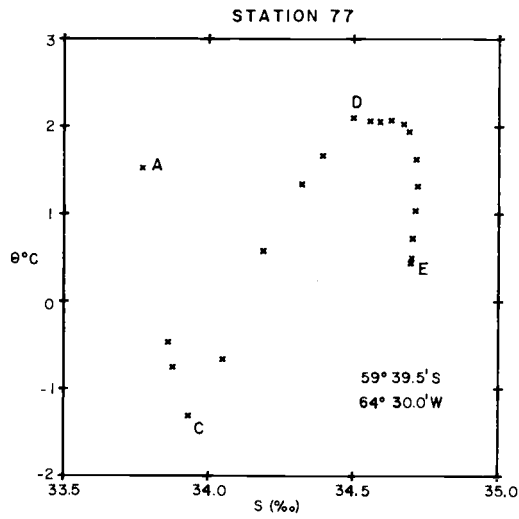
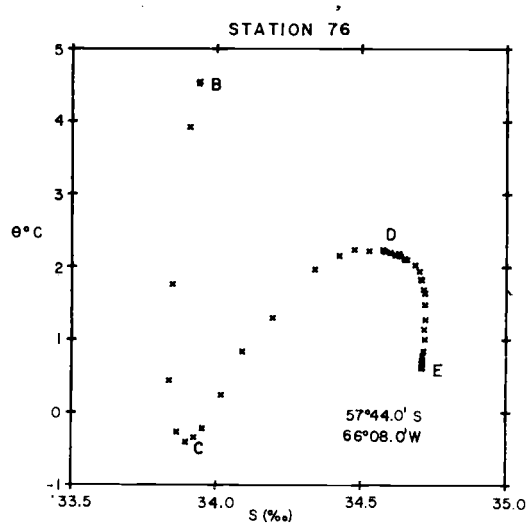


Figure V-13.  $\theta$ -S diagrams for stations 76-78 in the Drake Passage.

The surface waters in this region display the influence of melting sea ice which lowers the salinity. The Transition Water is discussed by Gordon (1971). A number of water types from the deep waters of the various oceans are mixing here with Antarctic surface waters and the deep waters of the Southern Ocean. The scatter seen in the residual plots in this region of the water column is a result of this complex intermingling of water types in the Transition Water.

Additional regression models were calculated from the combined data of GEOSECS stations 76-78. Best least square fits were calculated for the linear segments of each station from the combined regression residual values. These lines were then plotted on a  $O_2$  res-S plot (Figure V-14) with  $PO_4$  as the nutrient parameter. Using  $NO_3$  in the model results in a similar diagram. The influence of the various water types are clearly shown by the plot. For the near surface data, station 76, the northernmost station, shows high negative  $O_2$  residual values with progressively less negative values proceeding southward. Since

$$O_{2 \text{ res}} = O_2 - \hat{O}_2 \quad (V-17)$$

where  $\hat{O}_2$  is the value predicted by the model and  $O_2$  is the observed field data, the actual  $O_2$  value is lower than predicted by the model. The increased biological depletion of  $PO_4$  moving northward causes the increasingly negative character of the residuals from south

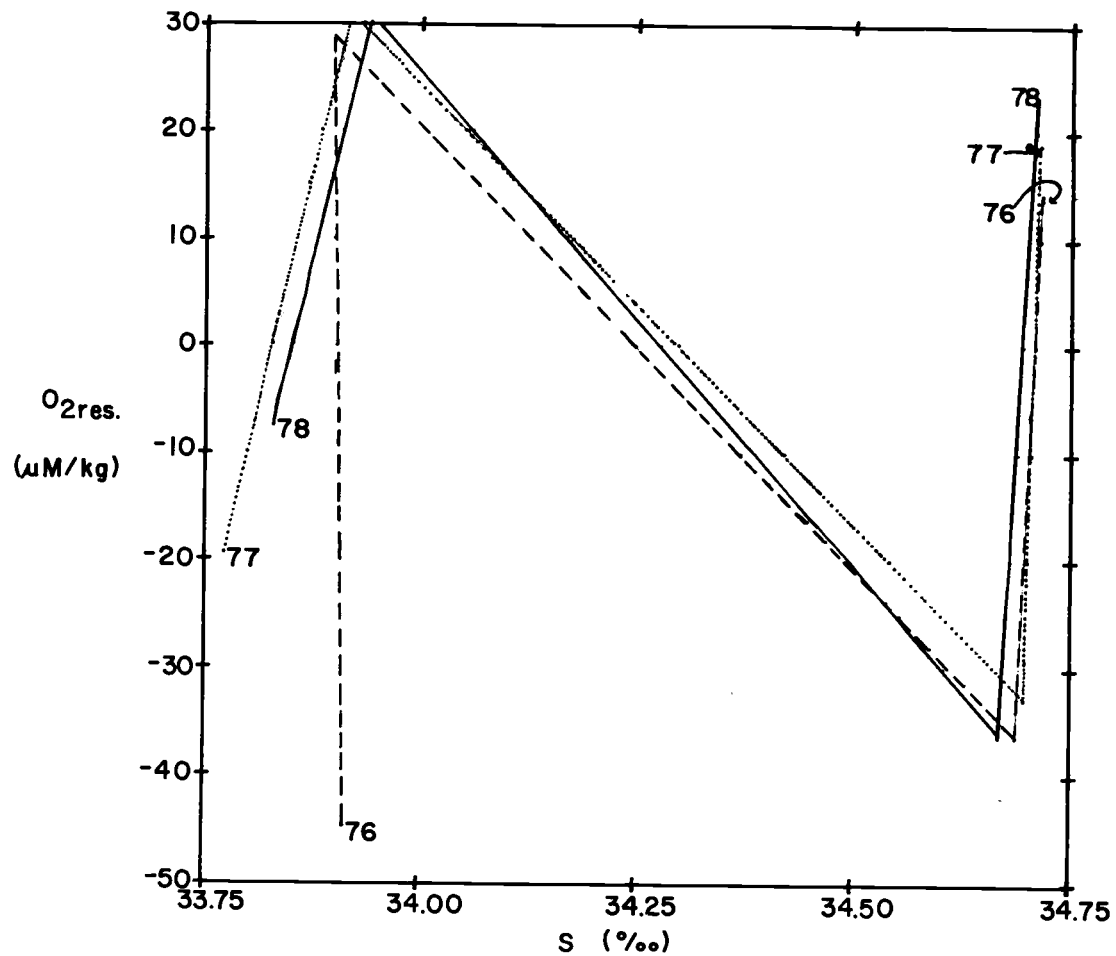


Figure V-14. Best fit lines of the  $O_2$  res versus  $S$  data for stations 76-78 in Drake Passage after a combined regression model using  $PO_4$  as the nutrient variable.

to north.

A second observation on the combined model occurs for the deep water at salinities near 34.7‰ (Figure V-14). Positive O<sub>2</sub> residuals result from the model proceeding southward. Since the data density in this region is high, this phenomena is statistically significant. The bottom water to the south is showing the influence of a richer oxygen source, as the PO<sub>4</sub> and S levels at the three stations vary only slightly. Reid and Nowlin (1971) describe this cold oxygen rich intrusion into the southeastern Drake Passage and conclude from current measurements that a weakening of eastward flow may cause an exchange by mixing due to the strong gradients of temperature, salinity, and oxygen between the bottom water of the Drake Passage and bottom water from the Scotia Sea.

C. R. Mann (personal communication) obtained data in the Drake Passage during the Hudson 70 expedition from twelve current meters which indicates an actual westwardly component in the bottom water flow. This is in contrast to the measurements of Reid and Nowlin (1971). The westernly flow in the south of the Passage supports the conclusion of Gordon (1966) of a bottom water flow from the Scotia Sea into this region. The combined residual plot also supports this occurrence of a westward flow in the southern portion of the Drake Passage during the period of the GEOSECS sampling. The effects of this current are observed on the combined multiple linear regression

analysis as increasingly high positive residuals southward. From the conflicting data available, variable and intermittent currents in the deep and bottom waters of the Drake Passage are not inconsistent with the distribution of properties in and around the Drake Passage.

To check the consistency of the Redfield ratio for Antarctic waters, the southernmost station was selected for analysis. The water column was broken into three linear proportions as seen in the  $O_2$  res-S diagrams (Figure V-12). The results of the regressions with 95% confidence intervals are shown in Table V-4.

Potential temperature is chosen as the conservative parameter for the first and third segment while salinity is utilized for the second segment. This is done as the relatively unchanging temperature passing through a maximum around 500 meters produces slopes approaching infinity which expands any error in the model for the second segment. Using S improves the coefficient of determination  $R^2$  and removes the temperature problem.

The region from the surface to 96 meters approximates the predicted Redfield ratio. From 96-998 m the confidence intervals are slightly higher than predicted. As the  $O_2$  saturation is more dependent on  $\theta$  than S, the use of S is somewhat less accurate in removing the conservative portion of the oxygen dependency and may be the cause of these slightly high ratios. Such an explanation cannot be considered for the region from 1346 to 3811 meters. As for station

Table V-4. Regression equations of O<sub>2</sub> on PO<sub>4</sub> and θ°C, NO<sub>3</sub> and θ°C, PO<sub>4</sub> and S, and NO<sub>3</sub> and S for station 78 in the Drake Passage.

| Depth Range<br>(m) | Regression equations (showing 95% confidence intervals)                            | R <sup>2</sup> | n-p-1 |
|--------------------|--|----------------|-------|
| 0-96               | O <sub>2</sub> = (624.42±194.53) - (18.37±13.60)θ - (154.54±108.10)PO <sub>4</sub> | .950           | 2     |
|                    | O <sub>2</sub> = (624.29±31.25) - (11.47±1.46)θ - (10.47±1.81)NO <sub>3</sub>      | .999           | 2     |
| 96-998             | O <sub>2</sub> = (6274.10±314.70) - (164.32±9.38)S - (182.44±23.35)PO <sub>4</sub> | .995           | 11    |
|                    | O <sub>2</sub> = (6532.60±254.44) - (172.42±7.45)S - (11.50±1.19)NO <sub>3</sub>   | .997           | 11    |
| 1346-3811          | O <sub>2</sub> = (264.35±55.25) - (17.88±1.70)θ - (21.05±25.44)PO <sub>4</sub>     | .990           | 20    |
|                    | O <sub>2</sub> = (301.93±75.88) - (17.96±1.43)θ - (2.59±2.36)NO <sub>3</sub>       | .990           | 20    |

49, the bottom water predicts a  $\Delta O_2:\Delta PO_4$  and  $\Delta O_2:\Delta NO_3$  far below those commonly hypothesized.

An initial reaction to explain this deviation is that the material being oxidized deviates from the assumed ratio. Examination of diatom chemical compositions given in Strickland (1965) and Platt and Irwin (1973) shows approximately the predicted ratios of Redfield. As the deviating region is the lower portion of the water column including the bottom, the possible oxidation or dissolution of heavier detrital material is suggested. Vinogradov (1953) examines such materials as skeletal matter which are high in phosphate, but the oxidation or dissolution of such material does not explain the reduced  $\Delta O_2:\Delta NO_3$  ratio. In addition, the volume of water which significant bottom oxidation or dissolution must affect to deviate the ratio so greatly would require tremendous amounts of dissolution or oxidation.

As the probability of biological or geochemical changes producing such a variation in the proposed model is slight, examination of the model for statistical breakdowns was made. Assumptions, such as approximating  $O_2^i + a_1 \cdot PO_{4(p)}$  by a linear equation for temperature and such as a completely random residual distribution resulting from the model, all proved correct.

The appropriate clue for the observed deviation was finally realized through examination of the 95% confidence intervals on the variables  $PO_4$  and  $NO_3$ . At station 49, the lower limit of this interval

is 4.14 for  $\text{PO}_4$  and 0.41 for  $\text{NO}_3$ . For station 78, the lower limits are -4.39 and 0.23 for  $\text{PO}_4$  and  $\text{NO}_3$  respectively. In all cases, the variation explained by the nutrient term is approaching zero or includes zero for the model at a 95% confidence level.

A regression was then run for the two strongly deviating segments at stations 49 and 78 using the following model:

$$\text{O}_2 = a_0 + a_1 \cdot \theta \quad (\text{V-18})$$

The results were:

Station 49 (3690-5513 m)

$$\text{O}_2 = 227.53 + 18.44 \cdot \theta \quad (\text{V-19})$$

Station 78 (1346-3811 m)

$$\text{O}_2 = 218.64 - 16.64 \cdot \theta \quad (\text{V-20})$$

The coefficients of determination were .997 for V-19 and .988 for V-20. The entering F value of the incoming variable,  $\theta$ , was 2891 for V-19 and 1727 for V-20. Subsequent addition of a  $\text{PO}_4$  or  $\text{NO}_3$  term to the models yielded entering F values in all four cases that were insignificant in removing any added variation at a 99 percent confidence level. The oxygen for the bottom water segment at stations 49 and 78 can be modeled exclusively as a function of the conservative variable  $\theta$ .

In terms other than statistical, there is not enough oxidation



occurring in the bottom water such that a test of Redfield's ratio can be made. Purely physical processes of mixing and advection control the  $O_2$  distribution. The  $O_2$  and subsequently the nutrients can be viewed as conservative in the bottom waters at these two stations for the level of analytical precision attained by GEOSECS for the measurement of  $O_2$ ,  $PO_4$ , and  $NO_3$ . From the formation of the bottom water through the movement northward to station 49 off Brazil, an insignificant  $O_2$  depletion occurred at the sensitivity of analytical techniques to be statistically significant in modeling oxygen as a function of  $\theta$  plus a nutrient term. The TOC data hinted at this fact for deep waters, but the statistical modeling approach elucidated this more clearly at a much greater level of precision.

## VI. CONCLUDING REMARKS

The GEOSECS program has collected such an enormous amount of data, nine complete notebooks for the Atlantic alone, that out of necessity the first view of the nutrient data I have described in this thesis was quite general. The further possible avenues to pursue in analyzing this data are almost limitless, but a few suggestions are appropriate:

1. There has never been such a thorough and complete set of silicate data available for one ocean. The potential use of silicate as a tracer, for box model studies, and biological uptake studies in the Southern Ocean is immense. Profitable time could be spent digging deeper into this body of data.
2. The conservative nature of the bottom water seen in the South Atlantic and Drake Passage should be analyzed more completely. Time scales for the very slow oxidation rates at great depths might be estimated by a more thorough consideration of the bottom waters in the Atlantic through  $O_2$ -nutrient relationships.
3. To a large extent, the eastern basins of the Atlantic have been ignored. It is in this region that the greatest  $O_2$  depletion occurs and high productivity is found along the coast of Africa. A much more detailed study such as given to the western basins should be executed. A greater knowledge of the nutrient chemistry of the eastern basins could be of value to the emerging nations along western Africa.

## BIBLIOGRAPHY

- Alvarez-Borrego, S. 1973. Oxygen-carbon dioxide-nutrients relationships in the northeastern Pacific Ocean and southeastern Bering Sea. Ph. D. Thesis. Corvallis, Oregon State University. 171 numb. leaves.
- Alvarez-Borrego, S. and K. Park. 1971. AOU as indicator of water-flow direction in the central North Pacific. *Journal of the Oceanographical Society of Japan*. 27: 142-151.
- Alvarez-Borrego, S. and K. Park. 1973. Oxygen-total inorganic carbon dioxide relationship in the Pacific Ocean. *J. Oceanographical Society of Japan*. 29:193-202.
- Alvarez-Borrego, S., L. I. Gordon, L. B. Jones, P. K. Park, and R. M. Pytkowicz. 1972. Oxygen-carbon dioxide- nutrients relationships in the southeastern region of the Bering Sea. *J. Oceanographical Society of Japan*. 28: 71-93.
- Arons, A. B. and H. Stommel. 1967. On the abyssal circulation of the world ocean - III. An advection-lateral mixing model of the distribution of a tracer property in an ocean basin. *Deep-Sea Res.* 14:441-457.
- Atlas, E. L., L. I. Gordon, S. W. Hager, and P. K. Park. 1971. A practical manual for use of the Technicon AutoAnalyzer® in seawater nutrient analyses. Technical Report 215. School of Oceanog., Oregon State Univ.
- Barber, R. T. 1968. Deepwater dissolved organic carbon resists microbial oxidation. *Nature, Lond.* 220:274-275.
- Bubnov, V. A. 1966. The distribution pattern of minimum oxygen concentrations in the Atlantic. *Oceanology*. 6: 193-201.
- Buscaglia, J. L. 1971. On the circulation of the intermediate water in the southwestern Atlantic Ocean. *J. Mar. Res.* 29:245-255.
- Callaway, J. C., R. D. Tomlinson, L. I. Gordon and P. K. Park. 1973. An instruction manual for use of the Technicon Auto-Analyzer® in precision seawater nutrient analyses. Manual for instruction of GEOSECS technicians. In preparation. School of Oceanog., Oregon State Univ.

- Carpenter, J. H. 1965. The Chesapeake Bay Institute technique for the Winkler dissolved oxygen. *Limnol. Oceanogr.* 10: 141-143.
- Craig, H. 1971. The deep metabolism: oxygen consumption in abyssal ocean water. *J. Geophys. Res.* 76:5078-5086.
- Dahm, C. N., S. Alvarez-Borrego, L. I. Gordon and P. K. Park. 1973. Atlantic water mass characterization by multiple linear regression analysis. Winter AGU. Vol. 54:1113.
- Daly, C. 1974. A Bayesian approach to two-phase regression. Ph. D. Thesis. Corvallis, Oregon State University. 77 numb. leaves.
- Draper, N. R. and S. Smith. 1966. Applied regression analysis. John Wiley, New York. 407 p.
- Duedall, I. W. and A. R. Coote. 1972. Oxygen distribution in the South Atlantic. *J. Geophys. Res.* 77:496-498.
- Duursma, E. K. 1961. Dissolved organic carbon, nitrogen, and phosphorus in the sea. *Neth. J. Sea Res.* 1:1-148.
- Duursma, E. K. 1965. The dissolved organic constituents of sea water. In: Chemical oceanography, J. P. Riley and G. Skirrow, editors. Academic Press, London, I, 712 p.
- Fleming, R. H. 1941. The composition of plankton and units for reporting population and production. *Proceedings of the Sixth Pacific Science Congress California, 1939.* 3:535-540.
- Gilbert, W., W. Pawley, and K. Park. 1968. Carpenter's oxygen solubility tables and nomograph for seawater as a function of temperature and salinity. Corvallis, Oregon State University, Department of Oceanography. 139 p. (Data Report No. 29).
- Gordon, A. L. 1971. Oceanography of Antarctic water. *Am. Geophys. Un. Antarctic Res. Ser.* 15:169-203.
- Hager S. W., E. L. Atlas, L. I. Gordon, A. W. Mantyla, and P. K. Park. 1972. A comparison at sea of manual and Auto-analyzer<sup>®</sup> analyses of phosphate, nitrate, and silicate. *Limnol. Oceanogr.* 17(16):931-937.

- Hart, T. J. and R. I. Currie. 1960. The Benguela Current. Discovery Rept. Cambridge Univ. Press., London. 31:123-298.
- Harvey, H. W. 1955. The chemistry and fertility of sea waters. Cambridge, Cambridge University. 240 p.
- Kester, D. R., and R. M. Pytkowicz. 1968. Oxygen saturation in the surface waters of the Northeast Pacific Ocean. J. Geophys. Res. 73:5421-5424.
- Lynn, R. J. 1971. On potential density in the deep South Atlantic Ocean. J. Mar. Res. 29:171-177.
- Lynn, R. J. and J. L. Reid. 1968. Characteristics and circulation of deep and abyssal waters. Deep-Sea Res. 15:577-598.
- Menzel, D. W. 1964. Distribution of dissolved organic carbon in the deep sea. Deep-Sea Res. 14:229-238.
- Menzel, D. W., and J. H. Ryther. 1968. Organic carbon and the oxygen minimum in the South Atlantic Ocean. Deep-Sea Res. 15:327-337.
- Menzel, D. W. and R. F. Vaccaro. 1964. The measurement of dissolved organic and particulate carbon in sea water. Limnol. Oceanogr. 10:354-363.
- Metcalf, W. G. 1969. Dissolved silicate in the deep North Atlantic. Deep-Sea Res. 16 (Supplement):139-145.
- Montgomery, R. B. 1938. Circulation in upper layers of Southern North Atlantic deduced with use of isentropic analysis. Papers in Physical Oceanography and Meteorology. Vol. 6, No. 2, 55 p.
- Neumann, G. and W. J. Pierson. 1966. Principles of physical oceanography. Englewood Cliffs, N. J., Prentice-Hall. 545 p.
- Oregon State University, Department of Statistics. 1971. Statistics Instruction Programming System (SIPS). Preliminary User's Guide. Corvallis, Oregon. Unpublished manuscript. 25 p.
- Park, K. 1967. Nutrient regeneration and preformed nutrients off Oregon. Limnol. Oceanogr. 12(2):353-357.

- Platt, T., and B. Irwin. 1973. Caloric content of phytoplankton. *Limnol. Oceanogr.* 18:306-310.
- Pytkowicz, R. M. 1968. Water masses and their properties at 160°W in the Southern Ocean. *Journal of the Oceanographical Society of Japan.* 24:21-31.
- Pytkowicz, R. M. 1971. On the apparent oxygen utilization and the preformed phosphate in the oceans. *Limnol. Oceanogr.* 16: 39-43.
- Pytkowicz, R. M. and D. R. Kester. 1966. Oxygen and phosphate as indicators for the deep intermediate waters in the Northeast Pacific Ocean. *Deep-Sea Research.* 13:373-379.
- Redfield, A. C. 1934. On the proportions of organic derivatives in sea water and their relation to the composition of plankton. James Johnstone Memorial Volume, Liverpool, p. 176-192.
- Redfield, A. C. 1942. The processes determining the concentration of oxygen, phosphate and other organic derivatives within the depths of the Atlantic Ocean. *Papers in Physical Oceanography and Meteorology.* Vol. 9, No. 2, 22 p.
- Redfield, A. C., B. H. Ketchum, and F. A. Richards. 1963. The influence of organisms on the composition of seawater. In: *The Sea*, ed. by M. N. Hill. Vol. 2, New York, Interscience, p. 26-77.
- Reid, J. L., and W. D. Nowlin, Jr. 1971. Transport of water through the Drake Passage. *Deep-Sea Res.* 18(1):51-64.
- Richards, F. A. 1957. Oxygen in the ocean. In: *Treatise on Marine Ecology and Paleoecology*, J. Hedgpeth, editor, *Mem. Geol. Soc. Am.* 67:185-238.
- Richards, F. A. 1958. Dissolved silicate and related properties of some western North Atlantic and Caribbean waters. *J. Mar. Res.* 17:449-465.
- Richards, F. A. and A. C. Redfield. 1955. Oxygen-density relationships in the western North Atlantic. *Deep-Sea Res.* 2:182-199.
- Riley, G. 1951. Oxygen, phosphate and nitrate in the Atlantic Ocean. *Bingham Oceanographic College Bulletin* 13.

- Riley, G. A. 1970. Particulate organic matter in sea water. *Adv. Mar. Biol.* 8:1-118.
- Seiwell, H. R. 1937. The minimum oxygen concentration in the western basin of the North Atlantic. *Papers in Physical Oceanography and Meteorology*. Vol. 5, No. 3, 24 p.
- Skopintsev, B. A. 1960. Organic matter in sea water. *Oceanology*. 19:1-14.
- Skopintsev, B. A. 1965. Investigation of water layer with oxygen minimum in the North Atlantic Ocean in the autumn of 1959. *Okeanologicheskkiye Issledovaniya*. 13:108-114. Translated by M. Slessers, U. S. Naval Oceanographic Office. *Trans.* 296.
- Spencer, D. W. 1972. Geosecs II, the 1970 North Atlantic station: hydrographic features, oxygen, and nutrients. *Earth Planet. Sci. Lett.* 16:91-102.
- Strickland, J. D. H. 1965. Production of organic matter in the primary stages of the marine food chain. *In: Chemical oceanography*, J. P. Riley and G. Skirrow, editors, Academic Press, London, I, 712 p.
- Sugiura, V. 1965. Distribution of reserved (preformed) phosphate in the Subarctic Pacific Region. *Papers in Meteorology and Geophysics*. 15: 208-215.
- Sverdrup, H. U., M. W. Johnson, and R. H. Fleming. 1942. *The oceans, their physics, chemistry, and general biology*. New York, Prentice-Hall. 1087 p.
- Taft, B. A. 1963. Distribution of Salinity and Dissolved Oxygen on Surfaces of Uniform Potential Specific Volume in the South Atlantic, South Pacific, and Indian Oceans. *J. Mar. Res.* 20:129-146.
- Vinogradov, A. P. 1953. The elementary chemical composition of marine organisms. *Sears Foundation for Marine Research, Memoir II*. Albert Parr, editor. 647 p.
- von Arx, W. S. 1962. *An introduction to physical oceanography*. Palo Alto, Addison-Wesley. 422 p.